12-2010

Characterization and Evaluation of a Novel Tissue Engineered Aortic Heart Valve Construct

Mary Tedder
Clemson University, mtedder@clemson.edu

Recommended Citation

Characterization and Evaluation of a Novel Tissue Engineered
Aortic Heart Valve Construct

A Dissertation
Presented to
the Graduate School of
Clemson University

In Partial Fulfillment
of the Requirements for the Degree
Doctor of Philosophy
Bioengineering

by
Mary Elizabeth (Betsy) Tedder
December 2010

Accepted by:
Dan Simionescu, Ph.D., Committee Chair
Jake Isenburg, Ph.D.
Martine LaBerge, Ph.D.
Jiro Nagatomi, Ph.D.
Timothy Williams, MD

ABSTRACT

Tissue engineering holds great promise for treatment of valvular diseases. Scaffolds for engineered heart valves must function immediately after implantation, but must also permit repopulation with autologous host cells and facilitate gradual remodeling.

Native aortic heart valves are composed of three layers, i.e. two strong external fibrous layers (*ventricularis* and *fibrosa*) separated by a central, highly hydrated *spongiosa*. The fibrous layers provide strength and resilience while the *spongiosa* layer facilitates shearing of the external layers. Our working hypothesis is that partially cross-linked collagen scaffolds that closely mimic the layered histo-architecture of the native valve would fulfill these requirements. To test this hypothesis we have developed heart valve-shaped tri-layered constructs based on collagen, the major structural component in natural heart valves. We describe here the development and characterization of two types of scaffolds, namely the fibrous scaffolds prepared from decellularized porcine pericardium and *spongiosa* scaffolds from elastase-treated decellularized pulmonary arteries. Fibrous scaffolds were cross-linked with penta galloyl glucose (PGG) to control remodeling. In order to assemble the scaffolds into a 3D valve structure and form the tri-layered leaflets, we developed a bio-adhesive consisting of mixtures of bovine serum albumin and glutaraldehyde (BTglue) and an efficient method to reduce aldehyde toxicity. Glued fibrous scaffolds were tested *in vitro* for biocompatibility (cell culture) and degradation (collagenase and proteinase K digestion). Tri-layered constructs were also tested for *in vivo* biocompatibility, cell repopulation and calcification.

In current studies, we have confirmed that scaffolds glued with BTglue were non-cytotoxic, with living cells spread across the entire surface of the BT-glue test area and cells growing directly on to the glued surfaces. With the long term aim of our studies being to create anatomically correct scaffolds to be used as personalized constructs for heart valve tissue engineering, we created silicone molds from porcine aortic heart valves and then modeled decellularized porcine pericardium into anatomically correct scaffolds. After drying them in their molds, the scaffolds have acquired the shape of the aortic valve which could then be preserved by exposure to PGG. After inserting decellularized pulmonary artery between the fibrous scaffolds to mimic the *spongiosa* layer, functionality testing of the heart valve-shaped scaffolds in a custom-made bioreactor showed good leaflet coaptation upon closure and good opening characteristics. Stem cell-seeded scaffolds also showed cellular differentiation into valvular interstitial-like cells (VICs) in similar bioreactor studies.

Future studies are needed to perfect the assembly process of the tri-layered construct. Additionally, further evaluation of stem cell differentiation is needed to confirm the presence of VICs in the aortic valve. If successful, there is potential that this approach of layering collagenous scaffolds into tri-layered constructs that mimic the native structure of the native aortic heart valve holds promise for the future of heart valve tissue engineering.

DEDICATION

This work is dedicated to my parents, Terry and Mary Beth - words can't capture what your love and support has meant to me my entire life. Thank you for being not only great teachers but my best friends. I would not have been able to get to this point without you. To my brother Ed, my grandmother (Mamma) and the rest of my family – I can't imagine there is a more encouraging family in the world. Without you all I wouldn't be ready to start the next adventures in my life.

ACKNOWLEDGMENTS

First, I would like to thank my advisor, Dr. Dan Simionescu, for his indispensable knowledge, experience, guidance and support the past few years. The opportunities he has presented to me during my time at Clemson University have been both enjoyable and valuable in regards to not only my professional development, but growth as a person. Through our relationship, he taught me how to be a better scientist, as well as a better person. I would also like to thank Dr. Aggie Simionescu, who has been not only like a second advisor, but a second mother. I have learned so much from you and Dan and could not have been blessed with better people to work with. Thanks also to my other committee members, Dr. Martine LaBerge, Dr. Jiro Nagatomi, and Dr. Jake Isenburg, for their expertise and making my learning experience even more valuable, and Dr. Tim Williams, whose medical expertise and constant encouragement was always appreciated (and Karen Thomason, who always kept me in contact with Dr. Williams).

In addition, I would like to thank all of the past and present members of the Biocompatibility and Tissue Regeneration Laboratory. It started with Dan, Tom and I a little over 4 years ago and has grown to over 30 that have worked in our lab. Their knowledge and friendship have been the driving forces behind my great time here at Clemson. I would particularly like to thank Tom Chung, Lee Sierad, and Jeremy Mercuri- it was just us for a while, and you three will always be like brothers to me. Other members of the Clemson community have also given me their assistance throughout the

course of my graduate education including Mrs. Cassie Gregory, Mrs. Maria Martin, and Mrs. Linda Jenkins.

I would also like to acknowledge: Dr. Jun Liao at Mississippi State University, for help with mechanical characterization of the scaffolds.

TABLE OF CONTENTS

Table of Contents (Continued)

Table of Contents (Continued)

Table of Contents (Continued)

Table of Contents (Continued)

LIST OF TABLES

LIST OF FIGURES

List of Figures (Continued)

List of Figures (Continued)

List of Figures (Continued)

List of Figures (Continued)

CHAPTER 1

INTRODUCTION

Replacement or regeneration of aortic heart valves, exquisite examples of durability, design and adaptability, has challenged engineers and surgeons for the last 50 years. Current treatment of valvular pathology is surgical replacement with mechanical valves, valves made from biological tissues or human allografts, but these devices have functional limitations, such as the need for life-long anticoagulation, risks of developing endocarditis and propensity to degenerate and calcify [1].

Native aortic valve leaflets are complex structures composed of external layers, the *fibrosa* (composed of collagen) on the arterial aspect and the *ventricularis* (collagen and elastin) on the ventricular aspect. The fibrous layers are sustained internally by a highly hydrated central *spongiosa* layer (rich in proteoglycans) that serves as a cushion material to mediate deformations of the fibrous layers, allows shearing between the outer layers and absorbs compressive forces during valve function [2-4]. Lack of a buffering layer results in large shear stress and tissue buckling when subjected to bending [5].

The predominant cell populations in heart valves are valvular interstitial cells (VICs) which continuously secrete matrix components as well as matrix degrading enzymes that mediate remodeling [6-8]. VICs exhibit a dynamic phenotypic spectrum ranging from quiescent fibroblast-like cells (characterized by expression of vimentin and low expression of alpha-smooth muscle cell actin), to activated VICs, assimilated as

myofibroblasts (characterized by proliferation, migration and high expression of alpha-smooth muscle cell actin) [1, 9-12].

Tissue engineering, the science of combining scaffolds, cells and specific signals to create living tissues is feasible and holds great promise for treatment of heart valve disease [13]. Two main strategies have been developed in recent years. The first is based on use of decellularized porcine valves followed by *in vitro* or *in vivo* repopulation with cells of interest. Despite their excellent mechanics, acellular valves are very dense and thus difficult to repopulate with desired cells. The second approach employs cell seeded polymeric biodegradable matrices [14] or scaffolds built from fibrin [15]. While polymeric and fibrin-based scaffolds have shown very promising results, these degradable matrices have insufficient strength to withstand arterial pressures immediately after implantation.

Our novel strategy relies on use of stabilized collagen scaffolds that mimic the natural valve fibrous layers, based on decellularized porcine pericardium [16] and delicate, highly hydrated porous collagen scaffolds to be used as the middle *spongiosa* layer. Chemically stabilized pericardium has outstanding mechanical properties, a good record of implantation in humans as valves, and as reconstructive surgery biomaterial patches in other organs [17-23]. To reduce scaffold biodegradation, we have also investigated the use of penta-galloyl glucose (PGG), a naturally derived collagen-binding polyphenol [16, 24]. No reports to date have documented the use of PGG-stabilized acellular pericardium for construction of tissue engineered heart valves. Since the xenoantigen Galα1-3Gal (Galα), is responsible for rejection of vascularized organ

transplants we are also paying special attention to Galα detection in decellularized scaffolds [25-29].

Recognizing the outstanding mechanical performance of natural valve homografts, the vital importance of the three leaflet layers [30], and the need for reconstruction of the physiologic valve design, we developed five building blocks for this new approach: a) partially stabilized collagenous scaffolds which degrade slowly with time, b) anatomically analogous 3-D heart valve shapes made from solid molds, c) tri-layered constructs that mimic the native heart valve histo-architecture, d) autologous multipotent mesenchymal stem cells for repopulation and remodeling and e) mechanical cues to induce stem cell differentiation into valvular cells capable of maintaining matrix homeostasis.

Cell sourcing for seeding heart valve scaffolds includes differentiated cells (smooth muscle cells, fibroblasts) and mesenchymal or embryonic stem cells [31, 32]. Other cell sources include peripheral blood and human umbilical cord blood [33]. Upon biochemical and/or mechanical stimulation, most of these cells express markers of quiescent VICs such as vimentin, among others [34]. We have chosen to investigate bone marrow-derived stem cells as a possible source for stem cells.

To assemble the 3D heart valve structures we developed and implemented the use of biological adhesives for tissue engineering purposes. At a minimum, these adhesives need to exhibit adequate bond strength and elasticity, long term stability and biocompatibility. We chose to implement a modified albumin/glutaraldehyde adhesive for the construction of living heart valves. We describe the development and extensive

characteristics of novel scaffolds to be used as the acellular fibrous pericardial scaffolds used to mimic the *fibrosa* and *ventricularis,* the amorphous pulmonary artery scaffolds to be used as the *spongiosa* layer, and utilization of a biological glue to assemble the tri-layered constructs. We also show that bioreactor conditioning of stem cell-seeded tri-layered valves induced differentiation into VIC-like cells.

References

1.   Mendelson, K. and F.J. Schoen, *Heart valve tissue engineering: concepts, approaches, progress, and challenges.* Ann Biomed Eng, 2006. **34**(12): p. 1799-819.

2.   Talman, E.A. and D.R. Boughner, *Glutaraldehyde fixation alters the internal shear properties of porcine aortic heart valve tissue.* Ann Thorac Surg, 1995. **60**(2 Suppl): p. S369-73.

3.   Talman, E.A. and D.R. Boughner, *Internal shear properties of fresh porcine aortic valve cusps: implications for normal valve function.* J Heart Valve Dis, 1996. **5**(2): p. 152-9.

4.   Schoen, F.J. and R.J. Levy, *Tissue heart valves: current challenges and future research perspectives.* J Biomed Mater Res, 1999. **47**(4): p. 439-65.

5.   Vesely, I., D. Boughner, and T. Song, *Tissue buckling as a mechanism of bioprosthetic valve failure.* Ann Thorac Surg, 1988. **46**(3): p. 302-8.

6.   Simionescu, D.T., J.J. Lovekamp, and N.R. Vyavahare, *Degeneration of bioprosthetic heart valve cusp and wall tissues is initiated during tissue preparation: an ultrastructural study.* J Heart Valve Dis, 2003. **12**(2): p. 226-34.

7.   Simionescu, D.T., J.J. Lovekamp, and N.R. Vyavahare, *Glycosaminoglycan-degrading enzymes in porcine aortic heart valves: implications for bioprosthetic heart valve degeneration.* J Heart Valve Dis, 2003. **12**(2): p. 217-25.

8.   Simionescu, D.T., J.J. Lovekamp, and N.R. Vyavahare, *Extracellular matrix degrading enzymes are active in porcine stentless aortic bioprosthetic heart valves.* J Biomed Mater Res, 2003. **66A**(4): p. 755-63.

9.   Latif, N., et al., *Characterization of structural and signaling molecules by human valve interstitial cells and comparison to human mesenchymal stem cells.* J Heart Valve Dis, 2007. **16**(1): p. 56-66.

10. Ku, C.H., et al., *Collagen synthesis by mesenchymal stem cells and aortic valve interstitial cells in response to mechanical stretch.* Cardiovasc Res, 2006. **71**(3): p. 548-56.

11. Taylor, P.M., et al., *The cardiac valve interstitial cell.* Int J Biochem Cell Biol, 2003. **35**(2): p. 113-8.

12. Liu, A.C., V.R. Joag, and A.I. Gotlieb, *The emerging role of valve interstitial cell phenotypes in regulating heart valve pathobiology.* Am J Pathol, 2007. **171**(5): p. 1407-18.

13. Yacoub, M., *Viewpoint: Heart valve engineering. Interview by James Butcher.* Circulation, 2007. **116**(8): p. f44-6.

14. Sutherland, F.W., et al., *From stem cells to viable autologous semilunar heart valve.* Circulation, 2005. **111**(21): p. 2783-91.

15. Robinson, P.S., et al., *Functional tissue-engineered valves from cell-remodeled fibrin with commissural alignment of cell-produced collagen.* Tissue Eng Part A, 2008. **14**(1): p. 83-95.

16. Tedder, M.E., et al., *Stabilized collagen scaffolds for heart valve tissue engineering.* Tissue Eng Part A, 2009. **15**(6): p. 1257-68.

17. Liao, J., et al., *Molecular orientation of collagen in intact planar connective tissues under biaxial stretch.* Acta Biomater, 2005. **1**(1): p. 45-54.

18. Obermiller, J.F., et al., *A comparison of suture retention strengths for three biomaterials.* Med Sci Monit, 2004. **10**(1): p. PI1-5.

19. Oswal, D., et al., *Biomechanical characterization of decellularized and cross-linked bovine pericardium.* J Heart Valve Dis, 2007. **16**(2): p. 165-74.

20. Simionescu, D., A. Simionescu, and R. Deac, *Mapping of glutaraldehyde-treated bovine pericardium and tissue selection for bioprosthetic heart valves.* J Biomed Mater Res, 1993. **27**(6): p. 697-704.

21. Simionescu, D., R.V. Iozzo, and N.A. Kefalides, *Bovine pericardial proteoglycan: biochemical, immunochemical and ultrastructural studies.* Matrix, 1989. **9**(4): p. 301-10.

22. Simionescu, D.T. and N.A. Kefalides, *The biosynthesis of proteoglycans and interstitial collagens by bovine pericardial fibroblasts.* Exp Cell Res, 1991. **195**(1): p. 171-6.

23. Deac, R.F., D. Simionescu, and D. Deac, *New evolution in mitral physiology and surgery: mitral stentless pericardial valve.* Ann Thorac Surg, 1995. **60**(2 Suppl): p. S433-8.

24. Isenburg, J.C., et al., *Structural requirements for stabilization of vascular elastin by polyphenolic tannins.* Biomaterials, 2006. **27**(19): p. 3645-51.

25. Azimzadeh, A., et al., *Comparative study of target antigens for primate xenoreactive natural antibodies in pig and rat endothelial cells.* Transplantation, 1997. **64**(8): p. 1166-74.

26. Strokan, V., et al., *Heterogeneous expression of Gal alpha1-3Gal xenoantigen in pig kidney: a lectin and immunogold electron microscopic study.* Transplantation, 1998. **66**(11): p. 1495-503.

27. Daly, K.A., et al., *Effect of the alphaGal epitope on the response to small intestinal submucosa extracellular matrix in a nonhuman primate model.* Tissue Eng Part A, 2009. **15**(12): p. 3877-88.

28. McPherson, T.B., et al., *Galalpha(1,3)Gal epitope in porcine small intestinal submucosa.* Tissue Eng, 2000. **6**(3): p. 233-9.

29. Raeder, R.H., et al., *Natural anti-galactose alpha1,3 galactose antibodies delay, but do not prevent the acceptance of extracellular matrix xenografts.* Transpl Immunol, 2002. **10**(1): p. 15-24.

30. Schoen, F.J., *Cardiac valves and valvular pathology - Update on function, disease, repair, and replacement.* Cardiovascular Pathology, 2005. **14**(4): p. 189-194.

31. Fang, N.T., et al., *Construction of tissue-engineered heart valves by using decellularized scaffolds and endothelial progenitor cells.* Chin Med J (Engl), 2007. **120**(8): p. 696-702.

32. Visconti, R.P., et al., *An in vivo analysis of hematopoietic stem cell potential: hematopoietic origin of cardiac valve interstitial cells.* Circ Res, 2006. **98**(5): p. 690-6.

33.   Schmidt, D., et al., *Engineering of biologically active living heart valve leaflets using human umbilical cord-derived progenitor cells.* Tissue Eng, 2006. **12**(11): p. 3223-32.

34.   Fraser, J.K., et al., *Fat tissue: an underappreciated source of stem cells for biotechnology.* Trends Biotechnol, 2006. **24**(4): p. 150-4.

CHAPTER 2

LITERATURE REVIEW

2.1   Physiology of Native Heart Valves

The heart provides unidirectional flow of blood through the body's circulatory system (**Figure 2.1**). This is due to the superb structure of natural heart valves. The four valves of the heart are excellent examples of optimum durability, design, and adaptability.
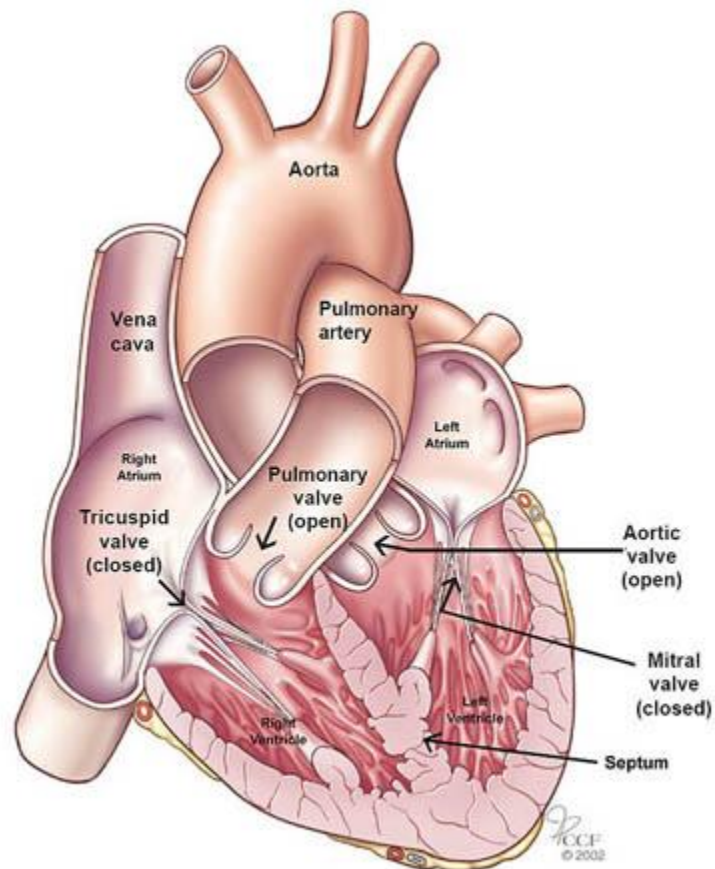
Figure 2.1: The four valves of the heart in systole [1]

The right side of the heart consists of the right atrium, which collects deoxygenated blood from the circulatory system, and the right ventricle, which pumps this blood to the lungs to be oxygenated. Between these two chambers is the tricuspid valve. anchored in its insertions into the annulus by thread-like chordae tendinae [2]. It functions to ensure that the blood within the right ventricle is pumped to the lungs rather than back into the right atrium during systole. The blood then moves through the pulmonary valve, or semilunar valve, which prevents flow of blood from the pulmonary trunk back into the right ventricle while the ventricle fills during diastole.

The left side of the heart has a similar structure to the right. Oxygenated blood from the lungs arrives at the left atrium from the pulmonary vein. During diastole, blood flows through the mitral valve, into the left ventricle. The mitral valve is unique in that it is composed of only two cusps, one anterior and one posterior [2]. Like the tricuspid valves, it is associated with an extensive support system anchoring the cusps in place to the base of the left ventricle via chordae tendinae [2]. As systole begins, intraventricular pressure rises, closing the mitral valve and opening the aortic valve [3]. Like the pulmonary and tricuspid valves, the aortic valve also has three cusps, lying at the origin of the aorta. Blood flows out the aorta to feed the systemic circulation. As the ventricle again begins to relax, the pressure increases to about 120 mmHg, and the aortic valve snaps shut and the ventricle begins to fill. By the time the pressure in the aorta drops to about 80 mmHg, the left ventricle has begun its contraction to pump another bolus of blood and return the pressure to 120 mmHg [4].

The left side of the heart must develop higher pressures than those on the right side (**Figure 2.2**). This possibly contributes to the fact that heart valves on the left side of the heart are most often affected by disease. **Therefore, further discussion will focus on the anatomy and physiology of the aortic valve, which is the most frequently diseased and also most commonly replaced of the valves** [5].
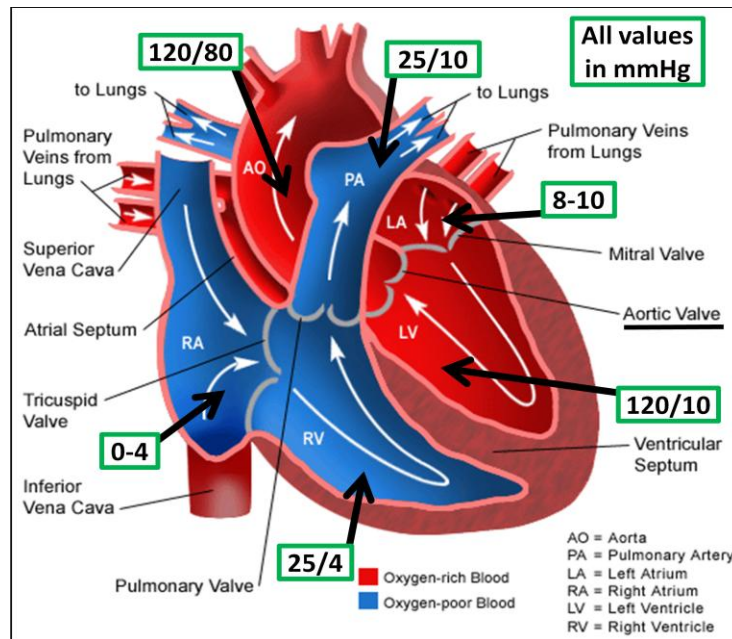
Figure 2.2: Blood flow through the heart and pressures in various segments [4]

2.1.1 Native Aortic Heart Valve Structure and Function

The aortic valve opens and closes approximately 103,000 times each day and about 3.7 billion times in a lifetime [6]. In order to create an aortic valve replacement it is essential to understand its function, anatomy and morphology of this valve.

The aortic valve is composed of three semilunar cusps (leaflets) attached to the aortic valve ring, referred to as the annulus, at the commisures (**Figure 2.3**). Valve

leaflets have few and only focal blood vessels, likely because valves cusps and leaflets are thin enough to be nourished predominately by diffusion from blood [4]. The cusps are cup-like, passive soft tissue structures attached to the wall of the aorta, in a region called the aortic root. Because of its passive mechanism, the structure of the aortic valve must open with minimal pressure differences between the ventricle and aorta [4]. During closing, this same mechanism must prevent backflow by perfectly aligning the cusps, which must have enough structural integrity to withstand systemic pressures. These leaflets open during systole and press against the aortic root wall. When they snap close at the start of diastole they meet to create a seal that can prevent backflow even with the 40 mmHg transvalvular pressure difference [4]. At this point, when the aortic valve is closed, the aorta must distort to better comply with the increased pressures, thereby decreasing the amount of stress on any one of the cusps.

In the aortic root, the cusps themselves are attached within the aortic sinuses, with each cusp lying in direct apposition to three shallow indentations, known as the sinuses of Valsalva [2] (**Figure 2.3**). These indentations in the aortic root change the fluid dynamics of the valve significantly [7]. It is believed that the sinuses cause the formation of vortices that aid in valve closure during retrograde blood flow [7]. Because two of these sinuses give rise to coronary arteries, they have been conventionally named as the right coronary, left coronary and noncoronary sinuses.
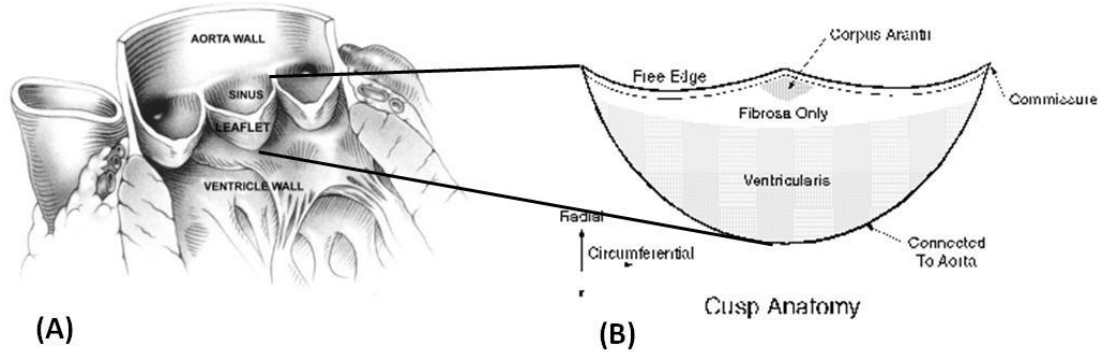
Figure 2.3: (A) The three leaflets of the aortic valve [8] and (B) a depiction of an individual leaflet and key landmarks [9].

2.1.2   Native Aortic Heart Valve Ultra-structure

Native heart valves maintain unidirectional blood flow via a dynamic structure with several key characteristics: viability, sufficient strength to withstand repetitive and substantial mechanical stress, and the ability to adapt and repair injury by connective tissue remodeling [10]. The extreme amounts of cyclic fatigue that these tissues must withstand in order to ensure optimum cardiac performance requires a highly organized ultra-structure refined for these tasks. The four cardiac valves have microstructural similarities, however the aortic valve best illustrates the central features and has served as a standard by which to characterize the microstructural and cellular components of the valves and how they relate to functional requirements [11]. Microscopically, the aortic valve is composed of three distinct layers that adapt to mechanical changes and aid in optimum opening and closing during the cardiac cycle: the *fibrosa*, the *spongiosa*, and the *ventricularis* (**Figure 2.4**).
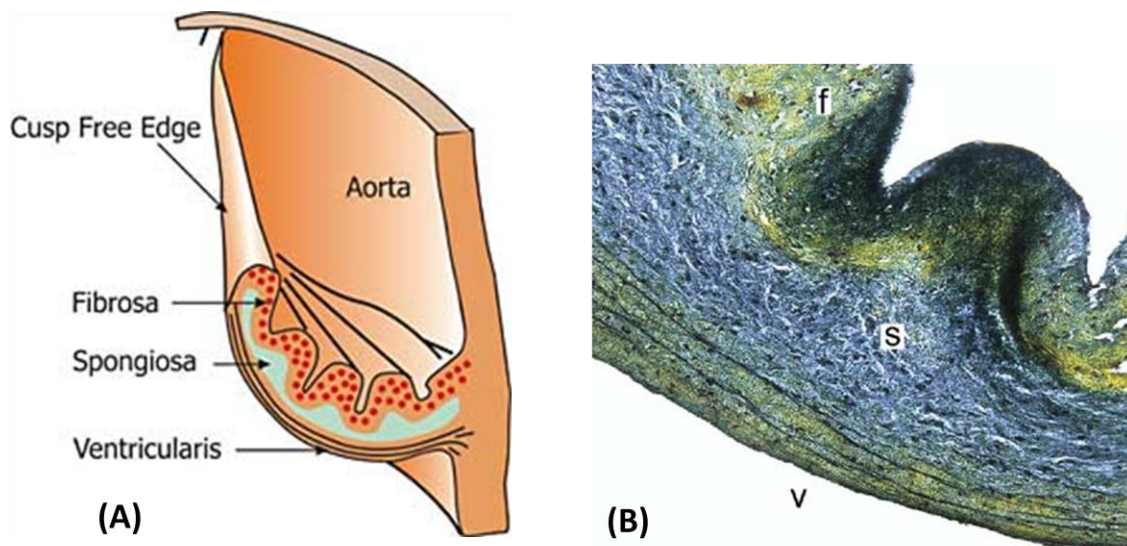
Figure 2.4: (A) Cross-sectional view of the aortic valve representing the tri-layered architecture of the native aortic valve [12]. (B) shows the normal interstitial cellularity (cell nuclei: dark magenta) and the expected layered structure of the leaflet with the *ventricularis* (v) as inflow side, *spongiosa* (s) as inner layer, followed by *fibrosa* (f) as the outflow side (Movat-pentachrome stain for visualization of the major matrix proteins: collagen, yellow; glycosaminoglycans, green-blue; elastin, black.) [10, 13].

The cuspal layer nearest the outflow surface (closest to the aorta) is known as the *fibrosa*. It is composed primarily of densely packed, circumferentially aligned collagen fibers that span the cusp from one commisure to another [11] (**Figure 4, 5(A)**). The collagen fibers provide strength and stiffness to maintain coaptation during diastole, when the cusp has maximal area. Thus, the collagen fibers carry the load that the cusps are exposed to when the valve is closed and transfer this load to the aortic wall.

The middle layer, located between the *fibrosa* and the *ventricularis*, is the *spongiosa*. It is composed mostly of glycosaminoglycans (GAGs) and collagen. The collagen within this layer is crimped and densely packed with parallel arrangement to the free edge of the cusp [14] (**Figure 2.5**). GAGs are high molecular weight linear

polysaccharides composed of a series of repeating, negatively charged, hydrophilic disaccharides [15]. The *spongiosa* has a gelatinous consistency, due in large part to the hydrophilicity of the GAG molecules [15, 16]. It is thus easily deformed in the presence of shear forces and cushions shock during the valve cycle and is not readily compressed. This resistance to compression during bending aids in cuspal mechanics by preventing buckling during flexion (systole), which could result in overall cuspal damage [17].

The final layer of the cusp is the *ventricularis*. It is located nearest the inflow surface, adjacent to the left ventricle. The layer consists primarily of radially aligned elastin fibers which, when relaxed, pull the collagen fibers of the *fibrosa* together, forming the corrugations on the surface of the leaflet (**Figure 2.4(B), 2.5(A)**) [17]. In general, the elastin in the valve forms an inter-connected matrix that binds the collagen bundles, forming an elastin-collagen hybrid within a larger network of interconnected collagen fibers [14]. The elastin extends during diastole and contracts in systole to minimize cusp area, the net effect being to provide a dampening effect as the valve closes and the cusp is stretched to coapt with its two neighboring leaflets [18].

Hence, it can be summarized that the structural layers within the valve are arranged such that they are anisotropically oriented, resulting in greater compliance of the valve in the radial direction as opposed to the circumferential (**Figure 2.5**) [17]. As such, the valve has unequal mechanical properties in different directions. This allows the cusp thickness to vary from 300-700 μm throughout the course of the entire cardiac cycle [19], and thus decreases the chance of impeded blood flow. Furthermore, the different structural components and their specific functions within each of the layers of the cusps

work to transfer stresses that allow for coaptation of the valve. As visualized in the stress-strain curve in the **Figure 2.5**, during opening, elastin extends at minimal load during the extension of the collagen crimp and corrugations. The collagen in the fibrous layer is arranged and fold in a lengthwise manner, and is oriented towards the commisures such that this reduces sagging in the cusp centers and conserves maximal coaptation, thereby preventing regurgitation [17]. Then, near full closure of the cusp, and thus complete collagen unfolding (diastole), the load-bearing element shifts from elastin to collagen [17]. Stress rises progressively while coaptation is maintained. Returning to systole, the elastin restores the contracted configuration of the cusp and the cycle can begin again. Thus, both the macroscopic valve geometry of collagen and elastin and the fibrous components within the valve work to transfer stresses caused by the diastolic force to the aortic wall and the annulus, minimizing the stresses the cusp itself must continuously experience [20]. **This is an important concept to consider for tissue engineering of heart valves**.

In studies on normal and pathological valves, it has been observed that the main determinant of valve stability and durability is the valvular extracellular matrix (ECM), comprised of the collagen, GAGs, and elastin [21]. Most of the mechanical strength of the valve is provided by collagen, which is comprised primarily of type I, III, and V collagen [22]. The quantities of each of these components is conversely determined by the valvular interstitial cells (VICs) [10, 23] (**Figure 4, (B)**). As touched upon earlier, heart valve leaflets experience states of mechanical stress during every cardiac cycle, such as

15
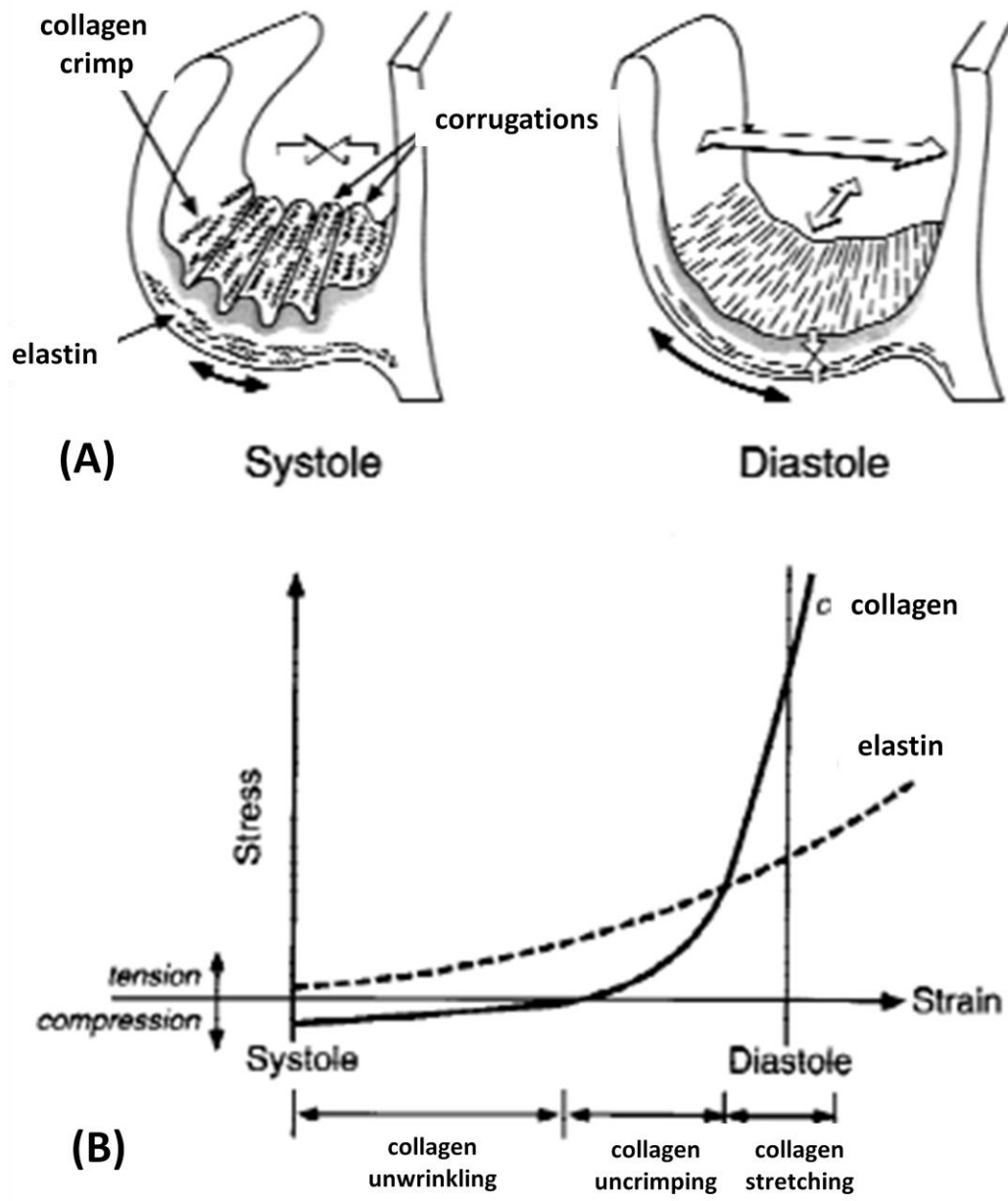
Figure 2.5: (A) Cuspal configuration during and ultra-structural arrangement of collagen and elastin during systole and diastole for an aortic heart valve and the complementary biomechanical effects of each of these ultra-structural components elucidated in the stress-strain plot (B) [20]

shear stress due to blood blow and when the valve opens, flexure during opening and closing, and tension when the valve closes [10]. The forces act on the valve at a microscopic level, translating the forces into biomechanical responses, which are then transduced into biochemical responses by VICs that, at a cellular level, induce up or down regulation of ECM synthesis [24].

Another important cell type present in the aortic valve is the valvular endothelial cell (VEC). It covers the surface of the valve, maintaining a nonthrombogenic blood-tissue interface [25]. The next section will provide more information on the valvular cells.

2.1.3   Cells of the Native Aortic Heart Valve

There are two main types of cells present in the heart valve: a layer of cells that cover the valve leaflets known as VECs and the inner cells, VICs. Among the VICs, some researchers have identified three cellular phenotypes: smooth muscle cells, arranged in bundles or just as single cells [26, 27], fibroblasts maintaining the extracellular matrix, and cells that have phenotypic features of both fibroblasts and smooth muscle cells, referred to as myofibroblasts [28-30]. The unique characteristics of the myofibroblasts, expressing both skeletal and cardiac contractile proteins, may be central to the lifelong durability of the valve [29]. In adult valve leaflets, the more quiescent fibroblast phenotype predominates among the VICs, characterized by the expression of vimentin and low expression of α-smooth muscle actin (α-SMA) [24]. During development and adaptation due to diseases, the phenotype of the cells is shifted

17

towards a more activated myofibroblast phenotype, characterized by vimentin and α-SMA coexpression and secretion of proteolytic enzymes that are capable of degrading the matrix, mediating matrix remodeling [31]. This is important when considering tissue engineering applications because these can be helpful markers to assess (vimentin and α-SMA) as indicators of an engineered tissue's potential to remodel. Various types of these proteolytic enzymes (MMPs) and their tissue inhibitors (TIMPs) are present in normal valve leaflets in a specific profile and on specific locations [32] (see section Valvular Repair and Remodeling for further details).

Professor Avrum I. Gotlieb recently proposed to categorize five phenotypes that represent VICs: embryonic progenitor endothelial/mesenchymal cells, quiescent VICs (qVICs), activated VICs (aVICs), progenitor VICs (pVICs), and osteoblastic VICs (obVICs), as shown in **Table 2.1** [33]. Based on this data, VICs seem to express a variety of defined phenotypes associated with remodeling and repair, in balance within a functioning valve; changes in this balance can lead to valve pathology.

When the cells change their phenotype (such as during development and adaptation to higher loads), this balance will be shifted towards one enabling matrix remodeling. The distribution of the various phenotypes among the valvular interstitial cells in the aortic valve leaflet depend on the biological and mechanical microenvironment [24]. In the normal adult aortic valve leaflet, fibroblasts are mainly found in the *ventricularis*, while myofibroblasts and smooth muscle cells are usually segregated in the fibrosa [34]. A comparable distribution pattern can be found in the vascular wall with myofibroblasts and smooth muscle cells in the medial layer and

fibroblasts in the adventitial layer. In the case of hypertension, fibroblasts of the adventitia convert into myofibroblasts to adapt to the higher mechanical loads [35].

Classification of VIC Markers and Functions into Five Phenotypes		
Cell type	**Location**	**Function**
Embryonic progenitor endothelial/mesenchymal cells	Embryonic cardiac cushions	Give rise to resident qVICs, possibly through an activated stage. EMT can be detected by the loss of endothelial and the gain of mesenchymal markers
qVICs	Heart valve leaflet	Maintain physiologic valve structure and function and inhibit angiogenesis in the leaflets
pVICs	Bone marrow, circulation, and/or heart valve leaflet	Enter valve or are resident in valve to provide aVICs to repair the heart valve, may be CD34-, CD133-, and/or S100-positive
aVICs	Heart valve leaflet	α-SMA-containing VICs with activated cellular repair processes including proliferation, migration, and matrix remodeling. Respond to valve injury attributable to pathological conditions and abnormal hemodynamic/ mechanical forces
obVICs	Heart valve leaflet	Calcification, chondrogenesis, and osteogenesis in the heart valve. Secrete alkaline phosphatase, osteocalcin, osteopontin, bone sialoprotein

Table 2.1: VIC markers and Classification into Five Phenotypes [37]

This same adaptation process might explain the distribution pattern of cellular phenotypes in the aortic valve leaflets. But due to the pressure difference over the leaflets, more smooth muscle-like cells are expected in the fibrosa compared to the

ventricularis [24]. Pressure levels may influence differences between pulmonary valve leaflets and aortic valve leaflets as well [34] .

The idea that cells within the valve play major roles in overall valve dynamics was further substantiated when a smooth muscle cell system in the leaflets was identified [26]. The smooth muscle cells are terminally differentiated and arranged in small bundles in the *ventricularis*, running circumferentially, or as individual cells [27]. Also, contractile properties of these VICs were observed [28, 36, 37], as well as sensory nerve elements in the leaflets [38]. Therefore, active contraction of the smooth muscle cells within the leaflets might help to sustain the hemodynamic forces that are exerted on the leaflets during systole and diastole, either by assisting the valve in opening or to provide support during diastole [27, 37], and represents a reactive cytoskeleton that can anchor collagen fibrils during valve closure [28].

The endothelial cells covering the surfaces of the leaflets provide a protective, non-thrombogenic layer. It is noteworthy that the endothelial cells on the leaflets are aligned perpendicular to the direction of the flow, as opposed to the alignment of endothelial cells in the direction of the flow in blood vessels. This indicates that a mechanical force, other than flow, induces this endothelial cell alignment on the leaflets. As the alignment is similar to the alignment of the collagen fibers, it has been hypothesized that the pressure stresses during diastole, responsible for the alignment of the collagen fibers, are responsible for the alignment of the leaflet endothelial cells. The only spot where the endothelial cells align in the direction of the flow is at the nodulus [39].

Therefore, it can be concluded that both the VIC and VEC cells within an aortic heart valve perform active and dynamic functions that contribute to the overall structural integrity and functionality of the heart valve. **Thus, when considering tissue engineering applications, these cell types and their distribution must be considered**.

2.2   Heart Valve Disorders

Valvular heart disease, or valvulopathy, is the generic name given to any dysfunction or abnormality of one or more of the heart's four valves. According to the American Heart Association's 2006 Heart and Stroke Statistical Update, valvular heart disease is responsible for nearly 20,000 deaths each year in the United States and is a contributing factor in about 42,000 deaths. The majority of these cases involve disorders of the aortic valve (63 percent) and the mitral valve (14 percent) [40], making the research of treatments for aortic valve disorders an important field. When considering tricuspid valve disease, it affects about 0.8% of the general population in the United States [41], most commonly secondary to left-side valve disease, particularly mitral valve disease [42].

Most experts assert that patients with chronic aortic valve disease can be divided into three primary groups: inflammatory, which includes septic and rheumatic lesions, congenital, and degenerative [43]. Ultimately, however, the resulting pathology is stenosis, insufficiency (regurgitation), or a combination of both [44]. Stenosis is defined as the failure of a valve to open completely, thereby impeding forward flow and is most commonly a result of a cuspal abnormality [45-47]. Insufficiency, regurgitation, or

incompetence, in contrast, results from failure of a valve to close completely, thereby allowing reversed flow, and is most often a result of failure of the valves supporting structures, such as the ventricular wall or the chordae tendinae [45-47]. Dysfunction may vary in degree from slight and physiologically unimportant to severe and rapidly fatal, with the 1-year survival rate in patients with severe tricuspid regurgitation is approximately 60% [48, 49]. Therefore, intervention is in most cases required.

2.2.1 Congenital and Acquired Abnormalities

Even though many patients are asymptomatic, roughly 300,000 patients worldwide have some type of surgical intervention to treat malfunctioning valve annually [42]. However, in children and infants, the prospect of surgical intervention and potential valve replacement poses both technically complex and complicated long-term management issues that differ from those of adults [50].

Of the possible aortic valve dysfunctions, bicuspid aortic valve disease is the most common type of aortic valve abnormality [51]. Bicuspid aortic valve disease is a congenital condition and occurs in about two percent of the population [52]. Instead of the normal three leaflets or cusps, the bicuspid aortic valve has only two. Without the third leaflet, the valve may be well-functioning, as for about two-thirds of people who have this defect have a bicuspid valve that functions well for life, stenotic, which causes the valves to be stiff and therefore leads to the improper opening and closing described above, or leaky (regurgitation), because it is not able to close tightly [52]. Patients with congenital or bicuspid aortic valve disease often do not require aortic valve surgery until

they are adults, however younger patients usually do experience a leaky valve [52]. The leaky valve can lead to insufficiency and peripheral circulatory problems, therefore it is a condition that cannot be ignored.
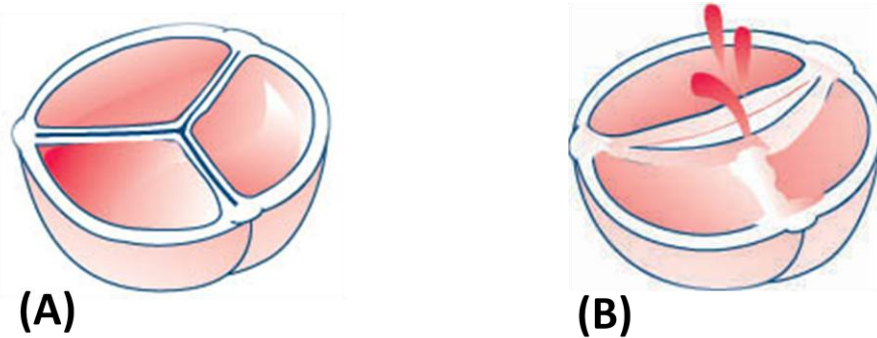
Figure 2.6: (A) Normal, tricuspid aortic valve. (B) Congenital, bicuspid aortic valve [51]

As stated previously, valvular heart disease, particularly in infants and children, is either congenital or acquired. Congenital abnormalities, including structural defects, such as the bicuspid valve described above, whether it be a fused, absent, or extra valve leaflet, and annulus hyperplasia, can be due to abnormal embryonic development. In all, cardiovascular malformations are the most common congenital abnormality, affecting 4 to 6 in 1000 births, with valve defects accounting for up to 30% of these deficiencies [53, 54]. On the other hand, acquired valvular disease, referring to pathologic changes caused by inflammatory or degenerative processes, could result from diseases such as infective endocarditis or acute rheumatic fever [50]. These, however, are less common than the congenital bicuspid valve described above.

2.2.2 Age-related Abnormalities

In addition to the congenital and acquired dysfunctions, there are age-related issues associated with valvular disease witch increases in prevalence with advancing age, afflicting 4% of the population by age 80 years [55]. In particular, one must consider calcific aortic stenosis. The natural progression of this condition has shown that severe symptomatic aortic stenosis is associated with a life expectancy of less than 5 years [56]. But despite the high prevalence of this condition, little is known regarding the molecular basis of calcific aortic stenosis (**Figure 2.7**).

(A)   **(B)**
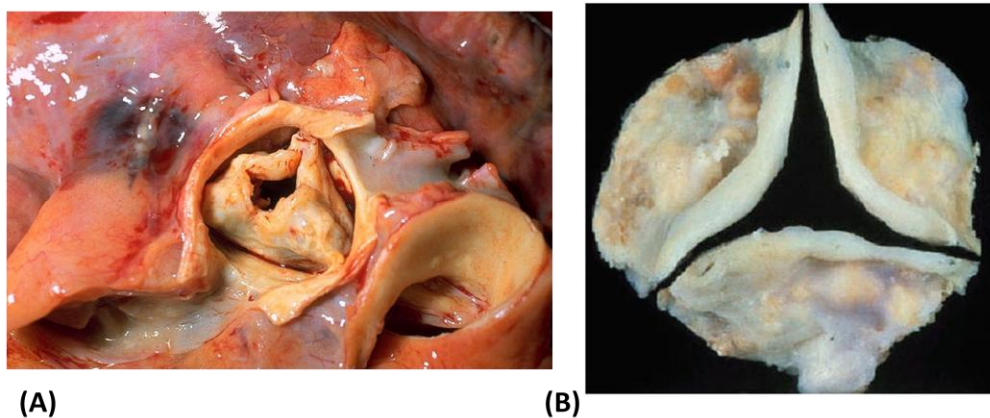
Figure 2.7: (A) shows an aortic valve with **senile calcific aortic stenosis** [57] and (B) a severely calcified aortic valve [58]

Studies have determined that mature lamellar bone formation occurs in calcified human aortic valves and that these valves express osteopontin, a bone matrix protein important in the development of cardiovascular calcification [59, 60]. Furthermore, it has have also been shown that human aortic valve cell cultures *in vitro* contain a calcifying cell population possessing osteoblast-like features [59]. While some have studied this

condition, it is still a significant problem for both aging and bioprosthetic heart valves, as will be discussed below.

2.2.3 Valvular Repair and Remodeling

In response to valvular injury or insult, interstitial cell proliferation and migration occurs-the first events of valve repair [61, 62]. The migration is likely directed by the activation of integrins and other cell-surface receptors that control cell-ECM adhesion [52]. Signaling mechanisms further determine how cytoskeletal proteins react by guiding cell spreading, contraction, and translocation, as would be typical in wound healing [19, 63, 64]. The VICs also play a large part in repair. It has been suggested that the interstitial cells may activate from a quiescent state (as described before) to help establish and guide a biomechanical response when the valve is exposed to a new mechanical environment, as would be expected during injury [19, 23]. This is accomplished by a phenotypic change in the VICs, which is determined by the wall stresses in the leaflets [65]. (Please recall Aortic Valve Cell section for phenotypic changes, page 17)

It is also thought that the interactions between the VICs and the matrix play a large part in regulating interstitial cell-based remodeling, including the induction of cell migration, the secretion of ECM components, and the secretion of proteolytic components- all key parts of the tissue repair process [66]. This is evident by the fact that collagenases, gelatinases, and other matrix metalloproteinases (MMPs) have been isolated from heart valves [32]. Actually, it is thought that MMPs and tissue inhibitor of metalloproteinases (TIMPs) play a key role in tissue remodeling and regeneration [67,

68], with their interactions and the interactions between both the MMPs, TIMPs, and their receptors of particular importance in cardiac remodeling [19]. For example, MMP-1 and MMP-13 have been shown to mediate the initial phase of collagen degradation by disassembling the fibrillar collagen native helix, thus contributing to remodeling [66]. The fibrillar fragments are then susceptible to other proteases, such as gelatinases, or elastases like cathepsin K [69]. And since the level and pattern of MMP and TIMP expression in normal valves is very specific [32], excess levels of these proteolytic enzymes may cause collagen and elastin degradation and result in weakening or destruction of the heart valve. Notably, some valvular pathologies have been associated with an over expression of MMPs by the valve's own cells, leading to ECM degradation [65] (**Figure 2.8**).
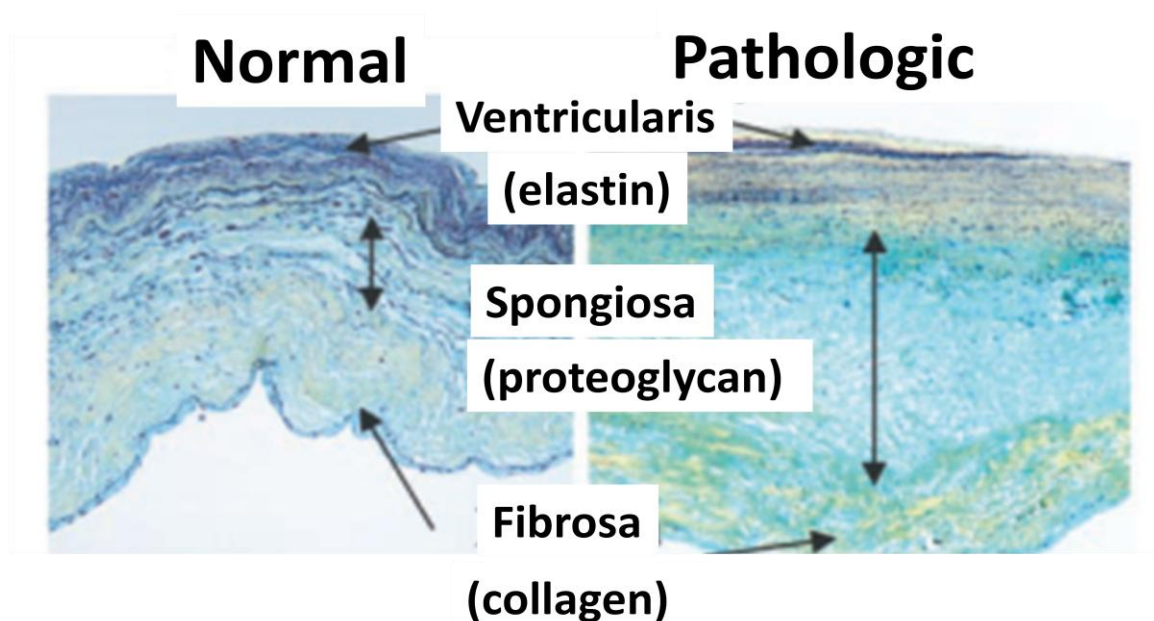
Figure 2.8: Pathologic valves may have an abnormal layered architecture: loose collagen in fibrosa, expanded *spongiosa* strongly positive for proteoglycans, and disrupted elastin in *ventricularis* [adapted from 65]

These findings may suggest that cells are being stimulated to produce and secrete second messengers that prompt native cells to degrade the matrix [70]. Therefore, since MMPs are important for remodeling of tissue engineered scaffolds, their activity must be tightly regulated and controlled in these situations to prevent deleterious events and valve failure.

2.3 Treatments of Valvular Pathology

Even though there are is no medicinal treatment for valvular disease, a physician will most likely recommend medications to control blood pressure and will place limitations on strenuous activity (especially lifting heavy objects), particularly for those with aortic stenosis. However, if symptoms are present or there is severe ventricular dysfunction with either stenosis or regurgitation, further surgical intervention will be warranted [71].

2.3.1 Minimally Invasive Treatments

In some heart conditions minimally invasive surgical approaches via catheters can provide results comparable to those one would expect to experience with surgery. While most patients are able to undergo surgery without difficulty, for people whose heart function is too severely compromised to withstand surgery, several approaches to treat heart valve disease without surgery have been developed. One example is percutaneous valvotomy, or valvuloplasty (**Figure 2.9**) [1].
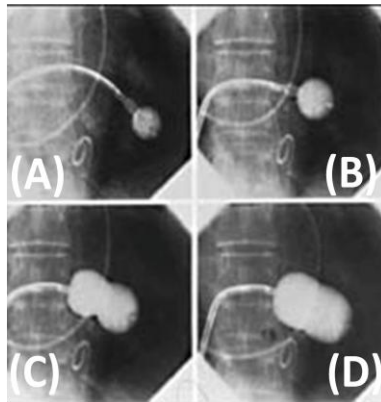
Figure 2.9: Mitral valvotomy [1]. Please see details in text below

Valvotomy can be performed in some patients to treat aortic valve stenosis or mitral valve stenosis [72, 73]. During an aortic valvotomy, a catheter is placed through the femoral vein (in the groin) and guided into the chambers of the heart. The cardiologist then creates a tiny hole in the wall between the heart's two upper chambers, providing an opening for access to the left atrium with a special catheter that has a balloon at the tip. The catheter is positioned so the balloon tip is directly inside the narrowed aortic valve (**Figure 2.9(A)**) while the valve opening is dilated by rapidly inflating and deflating the balloon (**Figure 2.9(B-D)**) [1].

Other investigational options are being explored as alternatives to invasive surgical procedures, the first of which is a possible percutaneous aortic valve replacement (AVR). Percutaneous AVR is a new treatment being investigated for select patients with severe symptomatic aortic stenosis [72]. It is also being investigated as a possible technique for implanting a prosthetic valve inside the diseased calcific aortic valve. The procedure is performed in the catheterization lab [1, 72]. During the procedure a catheter

is placed through the femoral artery and guided into the chambers of the heart. A stent-mounted, compressed tissue heart valve is placed on the balloon-mounted catheter and is positioned directly over the diseased aortic valve. Once in position, the balloon is inflated to secure the valve in place (**Figure 2.10**) [1]. **This holds great possibilities as a deployment method for tissue engineered heart valves. As such, the implantation method must be considered in the design process of the valve.**
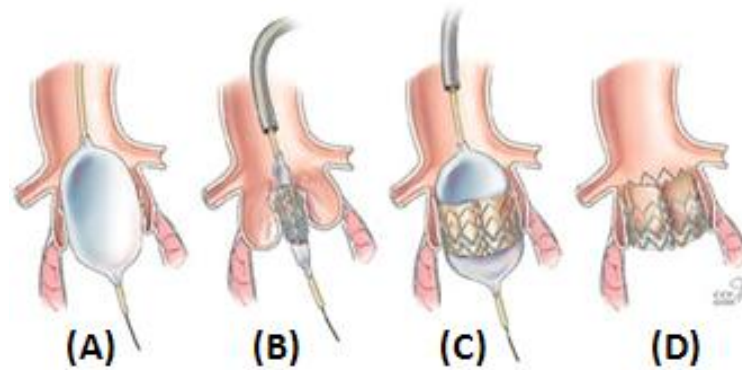
Figure 2.10: Percutaneous aortic valve replacement (AVR) [1]. A balloon catheter is placed in the diseased aortic valve orifice (A,B) and is inflated to deploy the tissue valve (C,D)

2.3.2 Surgical Repair Treatments

There are several options for young adult patients with aortic valve disease. The type of aortic valve surgery that is recommended is based on several factors, including the age of the patient, the expected long-term survival, any co-existing medical conditions including the type of valve disease, other types of heart disease, or other medical conditions, certain surgical risks, including the risk of thromboembolism, the risk of endocarditis, and the overall durability of the valve [74]. Along with the type of valve

29

chosen comes the risk of bleeding complications with long-term anticoagulation therapy. Most adolescent and young adult patients are concerned about aortic valve surgery because they want to maintain an active, normal lifestyle, including sports, travel, pregnancy, etc., and they wish to avoid the use of anticoagulant medications, which some patients are required to take after valve surgery (as for mechanical valves, which will be discussed). They also hope to avoid the need for future surgeries, which are in many cases necessary. Fortunately, in addition to complete valve replacements, there are other options for the treatment of valvular pathologies. One of these options is aortic valve repair [75]. Aortic valve repair may be an option for patients who have bicuspid aortic valve disease or other aortic valve conditions that are associated with valve regurgitation [75].

Even though aortic valve repair is not performed very often because it is technically very difficult, the majority (two-thirds), of leaky bicuspid aortic valves can be repaired with good results [51]. This type of surgery may be advantageous because the natural anatomy of the heart, as well as heart muscle strength, is preserved. There is also a decreased risk of infection, as opposed to complete valve replacement, and need for life-long anticoagulant medication [51, 76-78].

Figure 2.11: Aortic valve repair of a congenital bicuspid aortic valve, depicting shortening of the abnormal cusp [51].

However, there are drawbacks to this type of surgery. For one, this type of aortic valve surgery is technically difficult and is really only an option for leaky aortic valves, not stenotic valves [75]. Although a repaired valve can possibly last a lifetime, about 20 to 25 percent of patients will require a valve replacement within ten years [51, 76]. In the best case scenario, the repaired aortic valve will function like a well-functioning bicuspid valve.
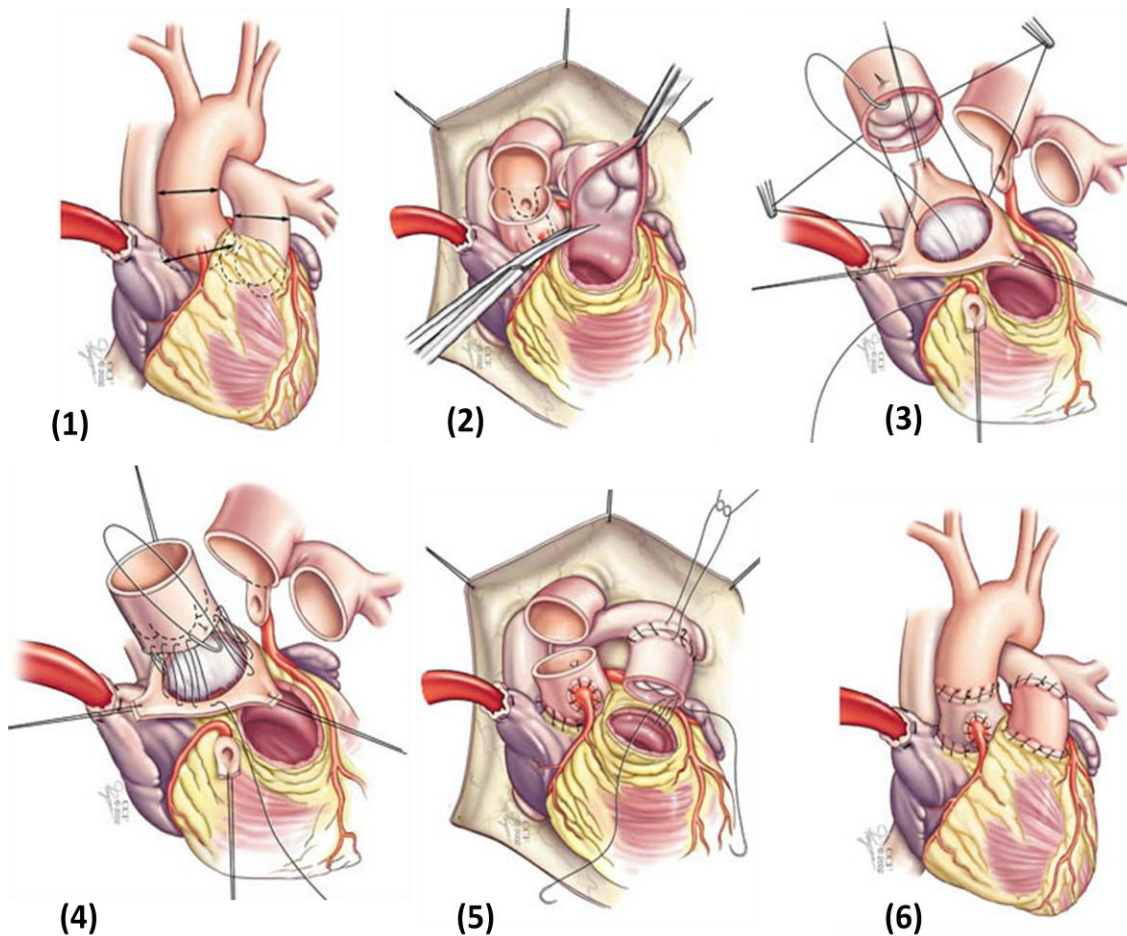
Figure 2.12: The Ross Procedure- In (1), the measurements of the aortic and pulmonic valves are taken, then (2) the aorta and pulmonary artery are opened and the aortic and pulmonary valves are inspected to determine if the Ross is an appropriate procedure.

Next (3), the diseased aortic valve is removed and the pulmonary valve (autograft) is removed and placed in the aortic position. The autograft is sutured in place (4) and the coronary arteries are re-attached. A pulmonary homograft is then attached to the right ventricle outflow tract (5). Finally, the aorta is attached to the autograft and the pulmonary artery is attached to the homograft (6) - the procedure is complete [51].

Another alternative to valve replacement is a procedure known as the Ross operation (**Figure 2.12** above), or the Switch procedure as it is commonly referred [79]. The Ross procedure is usually performed on patients younger than ages 40 to 50 who want to avoid taking long-term anticoagulant medications after surgery [79]. During this procedure, the patient's own pulmonary valve is removed and used to replace the diseased aortic valve. The pulmonary valve is then replaced with a pulmonary homograft [51, 79].

This procedure may be an attractive alternative to replacement with mechanical or xenogenic tissue valves in the aortic position because the pulmonary valve is anatomically very similar to the aortic valve and could be an ideal substitute for the aortic valve. Also, as opposed to mechanical valves, the new aortic autograft is a living valve and it may grow as the young adult grows, making this a good option for young patients. And given that the blood flows with less pressure through the pulmonary valve than the aortic valve, a homograft valve could last longer in the right-sided pulmonary valve position rather than the aortic position. Furthermore, the risk of thromboembolic complications and the risk of valve infection are very low. Moreover, the hemodynamic performance makes the Ross operation an attractive alternative for athletes [10, 51]. Ultimately, the pulmonary autograft valve has a good chance of being a life-lasting solution for the aortic valve (it is speculated that the pulmonary autograft will last a

lifetime in at least half the patients that undergo the Ross procedure [79]), making it an attractive alternative to conventional valve replacements.

However, there are drawbacks to this procedure that make it not the most attractive option for some patients. The Ross procedure is a technically difficult and long surgery, as it requires two valve replacements. As a consequence, this procedure is only recommended for young patients who would tolerate a long surgery time [80]. Also, the pulmonary autograft valve is transplanted from the low pressure pulmonary circulation over to the aortic high pressure system [51]. While the valve cusps are strong enough to withstand the systemic pressure, the pulmonary artery wall does dilate when exposed to systemic pressure, occasionally enough to cause the autograft valve to leak. Therefore, the risk of requiring re-operation for a leaking autograft valve is about 10 percent within 10 years after the operation [79]. Also, the Ross procedure is not recommended for patients with tissue defects (such as Marfan syndrome) or for patients who have an abnormal pulmonary valve [80]. The pulmonary homograft in the pulmonary position could also fail; the most common reason for failure is that it becomes stenotic. The risk of requiring replacement of the pulmonary homograft is about 10 percent within 10 years after the procedure[79]. Therefore, while there are surgical options for repairing a compromised aortic valve, the risk associated with the surgery and the prospect of resurgeries in some instances may be worse than the disorder.

2.3.3 Heart Valve Replacements and Devices

As stated previously, valvular heart disease represents a significant cause of mortality worldwide. Diseases can affect any of the four heart valves, although diseases of the aortic valve occur most frequently, associated with high mortality rates. And when the non- surgical and minimally invasive approaches fail to ameliorate the symptoms caused by a dysfunctional heart valve, the most common treatment for end-stage valvular diseases is surgical replacement of the valve. Historically there have been two types of artificial heart valves that are implanted- mechanical and tissue-based [81, 82]. Today, while mechanical valves contribute to approximately 60% of replacements, tissue valves are used in 40% or more of valve replacements world-wide, whether as autografts or allografts, or more predominantly as stented porcine aortic valve and bovine pericardial valves preserved by glutaraldehyde (collectively termed bioprostheses) [20]. None of these devices, however, is without complications.
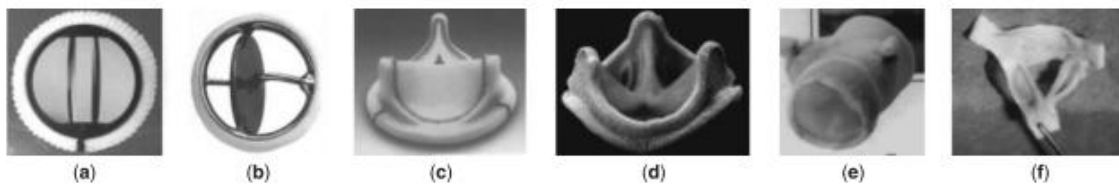
Figure 2.13: Images of contemporary valves implanted into patients today. (a) Bileaflet mechanical   valve, (b) single leaflet mechanical valve, (c) bovine pericardial bioprosthesis, (d) stented porcine xenograft valve, (e) stentless porcine xenograft, and (f) the human aortic valve homograft[83].

2.3.3.1 *Clinical Practice*

The ideal, or ultimate, replacement heart valve would have to function immediately after implantation, would have increased durability than the replaced valve, would be conductive to repopulation with host cells, and would have remodeling potential, or the ability to grow with the patient. Of the currently available replacements, no one valve fulfills all the above requirements. However, each has advantages and disadvantages over the others.

2.3.3.2 *Autografts and Allografts*

Cryopreserved aortic donor valves are the heart valve replacements closest to the natural valve, not being thrombogenic and with a low risk of infection. They are not chemically cross-linked and exhibit good mechanical properties, which prolongs their lifetime [84]. However, their disadvantages are their limited availability, a more difficult implantation technique [85] and failure associated with a specific immune response, especially in young children [86]. The use of cryopreserved pulmonary homografts as aortic heart valve replacements has been shown to result in early failure as the fiber structure of the pulmonary valve is less resistant to the hemodynamic environment in the aortic position compared to cryopreserved aortic valves [87]. Furthermore, these valves were shown to suffer from gross regurgitation *in vitro*, only augmenting the underlying cause for a replacement [88].

A controversial issue regarding cryopreserved homografts concerns the viability of the native endothelial and interstitial cells. A lack of viable cells after implantation was

stated [20] as well as the long-term survival of cellular elements [89]. In general, although cryopreservation reduces cellularity, the expression of strong antigens could still be demonstrated, and this might trigger the immune system of the host, resulting in graft rejection [90].

Figure 2.14: Allograft Valve Replacement- An allograft is an aortic or pulmonic valve that has been removed from a donated human heart, preserved, antibiotic-treated, and frozen under sterile conditions. A homograft may be used to replace a diseased aortic valve, or it may be used to replace the pulmonic valve during the Ross procedure [51].

2.3.3.3 *Mechanical Heart Valves*

Mechanical heart valve replacements display good structural durability, but are associated with a risk of prosthetic valve endocarditis and high rates of thromboembolic complications caused by their non-physiological surface and flow abnormalities[80]. Life-long anticoagulation therapy is necessary in these patients, which is associated with a substantial risk of spontaneous bleeding or embolism, particularly in patients aged over 70 years [91, 92]. Mechanical valves are of rigid construction and because of flow patterns and material properties, induce blood clotting on their surface. In the 1960s and 1970s, some of these valves failed catastrophically by having a leaflet dislodge and

flow into circulation (causing embolic complications) or a portion of the cage break, which could be fatal [83, 93, 94] (**Figure 2.15** below for examples of mechanical valves)
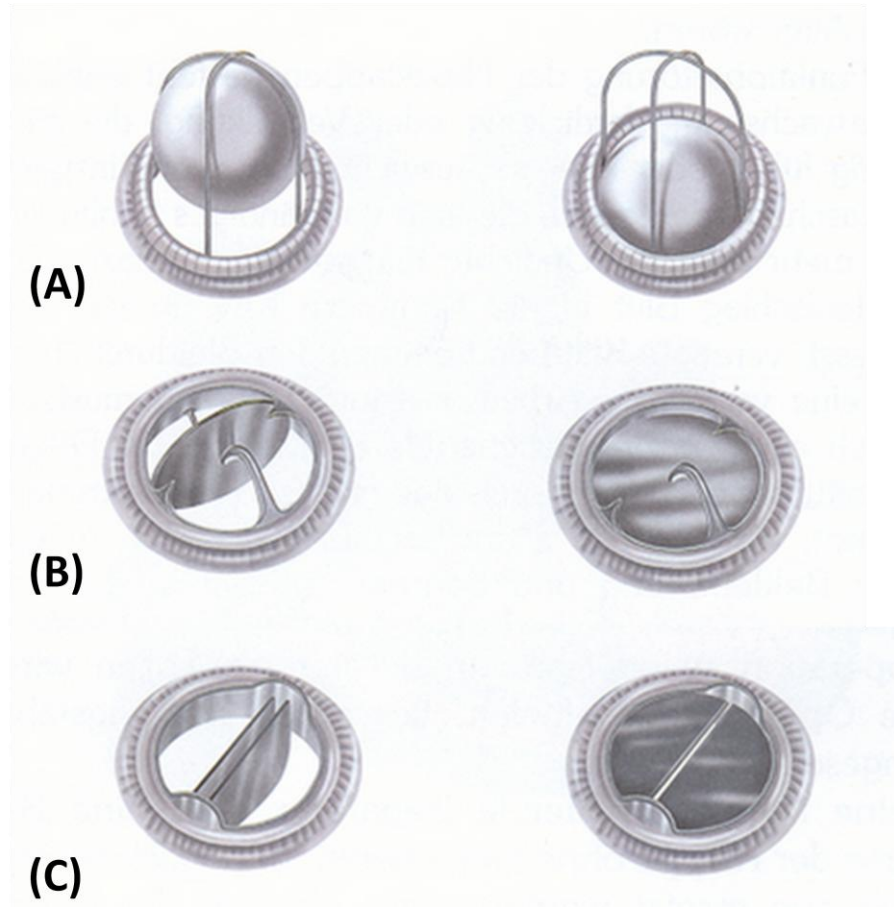
Figure 2.15: **(A)** and **(B)** are examples of a ball and cage and disk mechanical valve, respectively, which are no longer used, while (C) shows a conventional mechanical heart valve in use today [adapted from 95].

Currently, the most serious drawback to the use of mechanical valves is the anticoagulation therapy. Chronic anticoagulation is associated with cumulative morbidity and mortality, often as high as 4% per year [96, 97], which essentially guarantees some serious event within a 25-year implantation period [80]. This is particularly distressing for pediatric applications, where there is not only the prospect of multiple surgeries to

correct valve malfunctions, but the ever changing myocardium of a young mechanical heart valve recipient would necessitate further surgeries to accommodate the growing heart

2.3.3.4 *Bioprosthetic Heart Valves*

Bioprosthetic heart valve (BHV) replacements are of animal origin (xenografts), such as porcine aortic valves and bovine pericardial valves. Xenografts are chemically cross-linked - this inhibits autolysis, enhances the mechanical stability, and creates the possibility of having valves of different size directly available. However, these valves differ in many respects from native valves, for example in their opening and closing behavior due to the chemical pre-treatment [20]. Explanted xenografts were shown to be stiffer in the radial direction and less stiff in the circumferential direction compared to native porcine valves [98]. The risk of thromboembolic complications is much lower, but the valve's durability is limited. Structural failure is strongly age-dependent, making xenografts attractive for the elderly, but less suitable for children and young adults [20].

One important aspect in xenotransplantation is the risk of zoonoses - human diseases caused by infectious agents from animals [99]- which might even be facilitated by the mandatory immunosuppression [100, 101], but this is not necessary for BHVs. The identification of porcine endogenous retroviruses and prionic diseases has given rise to great concern. Recently, epidemiological data have strongly indicated transfer of Creutzfeldt-Jakob disease from cattle into humans either via infected meat, via surgical materials derived from bovine gut, or via drugs or vaccines prepared using fetal calf

serum [102]. Porcine endogenous retroviruses (PERV) can be present in all organs, as multiple copies of PERV can be integrated into germ-line DNA. New and more infectious groups of PERV are being identified [103], as well as their capacity to infect various types of human cells *in vitro* [104, 105]. One antigen that has been implicated in xenogenic transplantation rejection is galactose-alpha(1–3)-galactose (αGal), which are carbohydrate residues present on cell-surface glycoproteins and glycolipids of porcine tissue, but not human tissue [106].

Xenografts are attractive alternatives to homografts as a replacement for an injured valve because sufficient numbers can be obtained [107, 108]. Using the bovine pericardium or porcine heart valves in the manufacture of these valves has become somewhat standard, but these two tissues differ significantly in both structure and overall function. The bovine pericardium is more structurally homogeneous than the porcine tissue with respect to collagen and elastic fiber orientation, while the porcine tissue is less uniform. However, the porcine valve leaflet does contain a *spongiosa* layer, like the human leaflet and unlike the bovine pericardium. This *spongiosa* accumulates large deposits of proteoglycans that serve to reduce friction between the other two layers, again as in the human valve, but upon processing, are usually lost, leaving empty spaces for which may serve as sites for hydroxyapatite crystal nucleation, leading to calcification [109-112]

But, as stated for any tissue implant, the immediate problem with these devices is the preservation and sterilization of the tissue. Initial fixatives included the use of mercury salts and formaldehyde and finally glutaraldehyde (Glut) [109]. Glutaraldehyde

is a five-carbon dialdehyde that reacts directly with primary amines on residues of the amino acids lysine and hydroxylysine (found in abundance in the collagen of pericardial tissue and valves) [113-116]. Since 1970, glutaraldehyde has become the general fixative treatment, but there remain a number of problems with these treatments. Although Glut bioprostheses mimic natural aortic valve structure, their cells are nonviable and thereby incapable of normal turnover or remodeling ECM proteins [20], Glut-fixed tissue is much stiffer than natural cup tissue, which can lead to greater internal stresses in bending [117], and their mechanical properties are markedly different from those of natural aortic valve cusps. Consequently, tissue valves suffer a high rate of progressive and age-dependent structural valve deterioration resulting in stenosis or regurgitation [20].

Two distinct processes- intrinsic calcification and noncalcific degradation of the ECM account for structural valve deterioration. Calcification is a direct consequence of the inability of the nonviable cells of the Glut-preserved tissue to maintain normally low intracellular calcium. Calcification begins in the cells as crystalline deposits, then nucleation of calcium-phosphate crystals occurs in the collagen and elastin [20, 118]. Noncalcific degradation in the absence of physiological repair mechanisms of the valvular structural matrix are largely thought to be due to changes to the natural valves when they are fabricated into a tissue valve and the subsequent interactions with the physiologic environment that are induced following implantation[20]. However, the advantages include the fact that Glut is efficient as a sterilizing agent against bacteria, fungi, and viruses, but one cannot overlook the major problems, that are the propensity of Glut-treated tissue to calcify and clear cytotoxic effects that render cells not viable [119].

As a result, numerous experimental chemical treatments, none of which are in clinical use, are being addressed to alleviate the shortcomings of Glut. Of these, many attempt to stabilize tissue without the use of aldehydes, such as diphenylphosphoryl azide, carbodiimide, and hexamethylene diisocyanate [119-121]. Other treatments have aimed at impeding the harmful effects of glutaraldehye with subsequent treatments with amino acids that block the aldehyde groups [122-127] or pretreatment with chemicals (such as neomycin) that specifically target GAGS, that are not at all stabilized with Glut [128] and subsequently lost in preparations. Another treatment that was used to prepare tissue, in concurrence with Glut, was pressure fixation. Generally, prostheses made of porcine tissue are treated with pressures equivalent to diastolic pressure, but these fixation pressures can affect collagen buckling, loss of endothelium, different degrees of connective tissue cell autolysis, and the tissue can be rigid and inflexible [129]. **Therefore, there is a need for a more adequate fixation method that addresses and alleviates the shortcomings of the fixatives above**.

2.4   Heart Valve Tissue Engineering

The ultimate goal of tissue engineering is to construct tissues from their cellular components which combine and maintain most of the characteristics of the original, healthy tissue. For a functioning heart valve these include durability, adequate mechanical function, which correlates with haemodynamic performance, and a mature extracellular matrix which does not elicit an immunogenic or inflammatory reaction. To this end, the success of tissue engineered heart valves (TEHV) is dependent on three

main issues: (1) the scaffold, which determines the three-dimensional shape and serves as an initial guiding structure for cell attachment and tissue development; (2) the cell source from which a living tissue is grown; and (3) the in vitro culture conditions of the living construct before implantation [20].

In order to overcome the limitations of today's heart valve replacements, researchers have developed different tissue engineering concepts using various scaffold materials. These include biodegradable synthetic scaffolds seeded with autologous cells, decellularized allo- or xenografts seeded with autologous cells (auto-xenograft) or decellularized allo- or xenografts without cell seeding (Table 2) [130].

Matrix	Source	Pre-treatment	Cells	Conditioning	Comments
Synthetical	Various biocompatible, biodegradable polymers	Fabricated into 3D structures, sterilised by ethylenoxide	Seeded with autologous myofibroblasts and endothelial cells	Static or dynamic (bioreactor)	Safe, living, completely autologous, growth
Biological	Xenogenic or Homogenic	Glutaraldehyde fixed	acellular	-	Extensively tested, safe, non-living, calcification
			Seeded with autologous cells	Bioreactor or no conditioning	Difficult to repopulate, increased durability
		Alternative fixation procedures (e.g. photofixation, cryo-preservation)	acellular	-	Biosafety and immunologic situation unclear
			Seeded with autologous cells	Bioreactor or no conditioning	Increased cell attachment /survival
		Decellularised	acellular	-	Biosafety and immunologic situation unclear
			Seeded with autologous cells	Bioreactor or no conditioning	

Table 2.2: Scaffolds and their potential use in tissue engineering [130]

Several attempts have been made to create functional heart valve replacements with the ability to grow, repair, and remodel using the concept of tissue engineering. As demonstrated by the schematic representations below (**Figure 16, A,B**), in one approach to tissue engineering, the patient's own cells, isolated, for example, from a blood vessel and expanded using standard cell culture techniques, are seeded on the scaffold, in the shape of a heart valve.

(A)
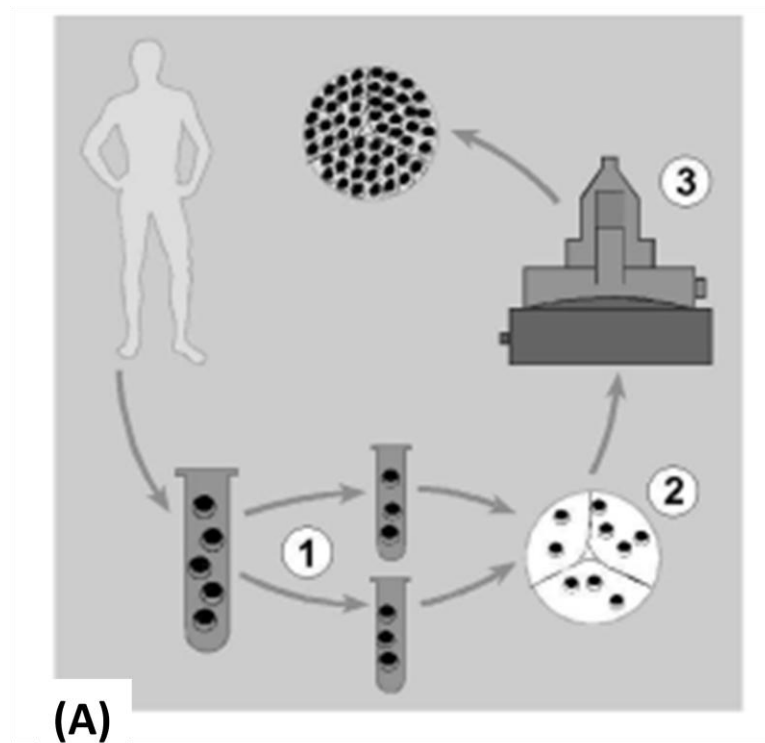
Figure 2.16 (A): Schematic of principle of tissue engineering of heart valves. 1) Isolation of cells from a blood vessel of the patient and separation of myofibroblasts and endothelial cells. 2) Seeding of myofibroblasts onto a scaffold material in the shape of a trileaflet heart valve and subsequent seeding of endothelial cells onto the surfaces. 3) The cell/scaffold construct is placed into a bioreactor to stimulate tissue development [130].

Subsequent stimulation, transmitted via the culture medium (biological stimuli) or via 'conditioning' of the tissue in a bioreactor (mechanical stimuli), promotes tissue

development, resulting in a completely autologous, functional, and living heart valve implant [20]. **However, scaffold seeding has proven to be difficult and incomplete and mechanical properties are not comparable with native tissue, so improvements must be made**.

Another approach, elucidated by **Figure 16 (B)**, is to implant unseeded scaffolds designed to encourage cell migration and proliferation. In either approach, the end goal is the same- to promote cell growth on a tissue engineered scaffold whereby the scaffold will be incorporated into the body as a living tissue.
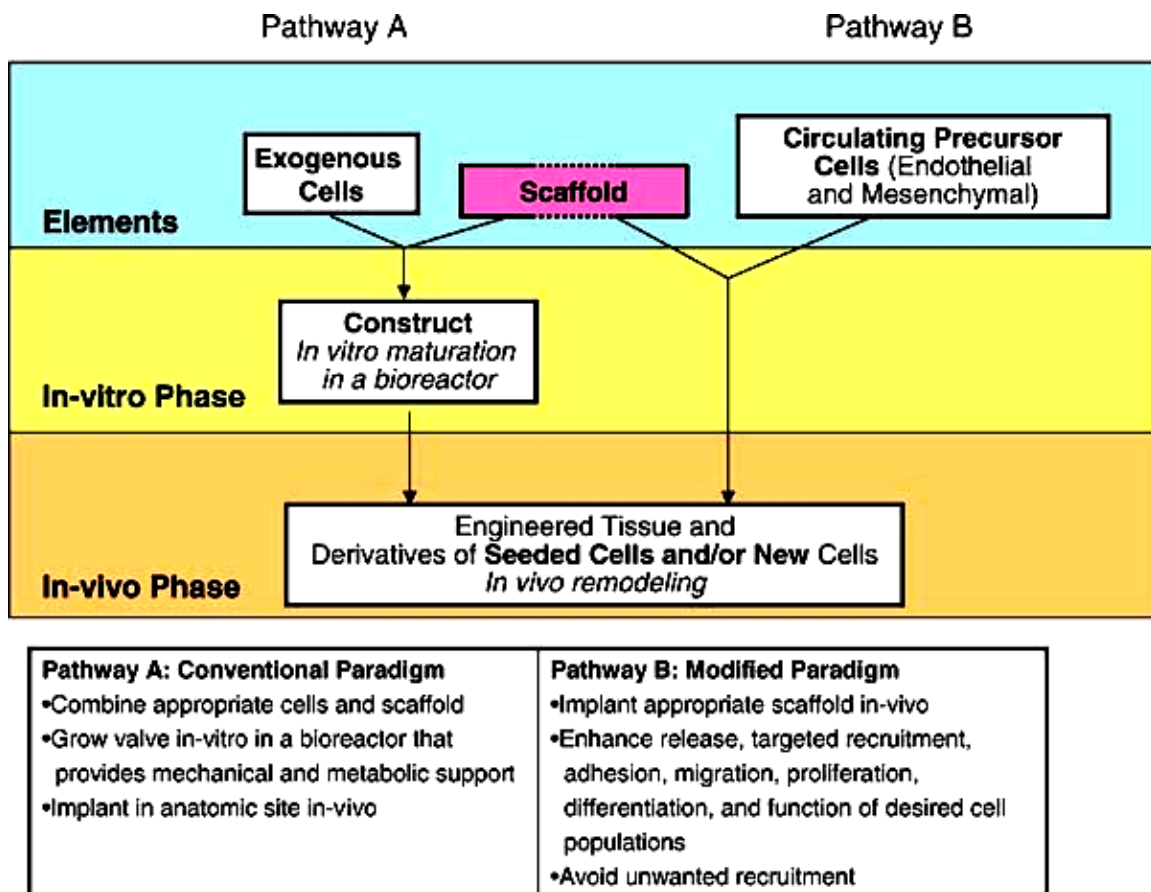
Figure 2.16 (B): The paradigm of tissue engineering (Pathway A) The conventional paradigm of tissue engineering comprises a scaffold that is seeded with cells, an *in vitro* stage of tissue formation typically conducted in a bioreactor, and an *in vivo* stage of tissue

growth and remodeling. The key processes occurring during the *in vitro* and *in vivo* phases are cell proliferation, ECM production and organization, scaffold degradation, and tissue remodeling. The resulting tissue engineered construct will contain some combination of seeded and/or new cells. A modified paradigm (Pathway B) might utilize an unseeded scaffold that is fabricated with biological "information" designed to attract and provide a suitable substrate for differentiation of circulating precursor cells *in vivo* [10].

Heart valve tissue engineering represents a promising approach towards autologous, living, and functional heart valve replacements with the ability to grow, repair, and remodel. Mechanical conditioning of the developing tissue in a bioreactor has rendered heart valve replacements, which have shown excellent functionality in sheep when implanted in the pulmonary position [131]. **The pulmonary position is, however, a low-pressure environment and as most heart valve replacements concern the aortic valve, a high-pressure environment, the tissue properties of the neo-tissue have to be optimized further to serve as aortic heart valve replacements**.

2.4.1 Scaffolds for Heart Valve Tissue Engineering

As stated previously, the heart valve scaffold may be either based on biological or synthetic materials. Donor heart valves or animal derived valves depleted of cellular antigens can be used as a scaffold material. Removing the cellular components results in a material composed of essentially extracellular matrix proteins that can serve as an intrinsic template for cell attachment [132]. In general, non-fixed, acellularized valve leaflets have shown recellularization by the host, as demonstrated in dogs [133] and sheep [134]. However, first clinical applications of this concept in children resulted in rapid failure of the heart valves due to immune rejection as a result of incomplete

decellularization, and was associated with a 75% mortality [135]. In a further approach, specific biological matrix constituents can be used as scaffold material, including collagens and fibrin [136, 137]. These materials have the disadvantage that they are difficult to obtain from the patient in sufficient quantities. Therefore, most of these scaffolds are of animal origin. In this context, identification of retroviruses and prionic diseases has given rise to great concern as to the risk of zoonoses.

An ideal synthetic scaffold for tissue engineering applications must be at least 90% porous [138], and must possess an interconnected pore network, as this is essential for cell growth, nutrient supply, and removal of metabolic waste products. Besides being biocompatible, biodegradable, and reproducible, the scaffold should also display a cell-favorable surface chemistry and, as stated above, match the mechanical properties of the native tissue [20]. The rate of degradation should be proportional to the rate of tissue formation and controllable in order to ensure mechanical stability over time [139, 140]. The use of synthetic materials as scaffolds has already been broadly demonstrated for heart valve tissue engineering. Initial attempts to create single heart valve leaflets were based on synthetic scaffolds, such as polyglactin, PGA (polyglycolic acid), PLA (polylactic acid) and PLGA (copolymer of PGA and PLA). To create complete trileaflet heart valve conduits, PHA based materials (polyhydroxyalkanoates) were used [141]. A combined polymer scaffold consisting of non-woven PGA and P4HB (poly-4-hydroxybutyrate) has shown promising results in sheep, when placed in the pulmonary position [131]. These materials are thermoplastic and can therefore be easily molded into any desired three dimensional shape [130]. These above materials are approved for

surgical use and they are biocompatible and biodegradable. A major advantage of synthetic matrices is the fact that their biodegradation properties and biomechanics can be chemically designed according to the requirements of the particular application. Moreover, specific proteins such as growth factors may be incorporated into the scaffold structure enabling targeted promotion of specific tissue growth [130, 142] . However, success of synthetic leaflet HVs has also been hampered by their impaired haemodynamic performance compared with the performance of natural valves [143] and the fact that they have their limited durability are susceptible to calcification, which leads to leaflet stiffening and tearing [144].

2.4.2 Alternative Cross-linking Methods

As discussed with bioprostheic valves, tissue engineered valve replacements based on biological scaffolds are subject to degradation and stability concerns. And like bioprosthetic replacements a possible way to increase the resistance of natural tissue-engineered scaffolds to proteolytic degradation is to use chemical stabilizing and/or cross-linking agents. Several cross-linking and stabilizing agents (such as glutaraldehyde and proanthocyanidin) and methods have been proposed and tested with different degrees of success [152, 153] however the ideal or at least clinically optimal stabilizing agent has not yet been identified.

Recently tannic acid (TA) and tannic acid mimicking dendrimers (TAMD) have been suggested as potential cross-linking agents for collagen [154-156]. It was also shown that addition of TA to glutaraldehyde (Glut) pretreatment dramatically

improves elastin and collagen stabilization in cardiovascular implants as evidenced by an increased resistance to proteolytic degradation [157]. Moreover, TA has 10 times lower toxicity as compared to Glut [157].

One tannin in particular that is being investigated is penta-galloyl glucose (PGG). It is a naturally derived polyphenol present in plants and is currently available in pure form from several manufacturers. Structurally, it belongs to the galloyl-glucose family (syn. gallotannins), characterized by a D-glucose molecule esterified at all five hydroxyl moieties by gallic acid (3,4,5 -trihydroxybenzoic acid) (**Figure 17**).
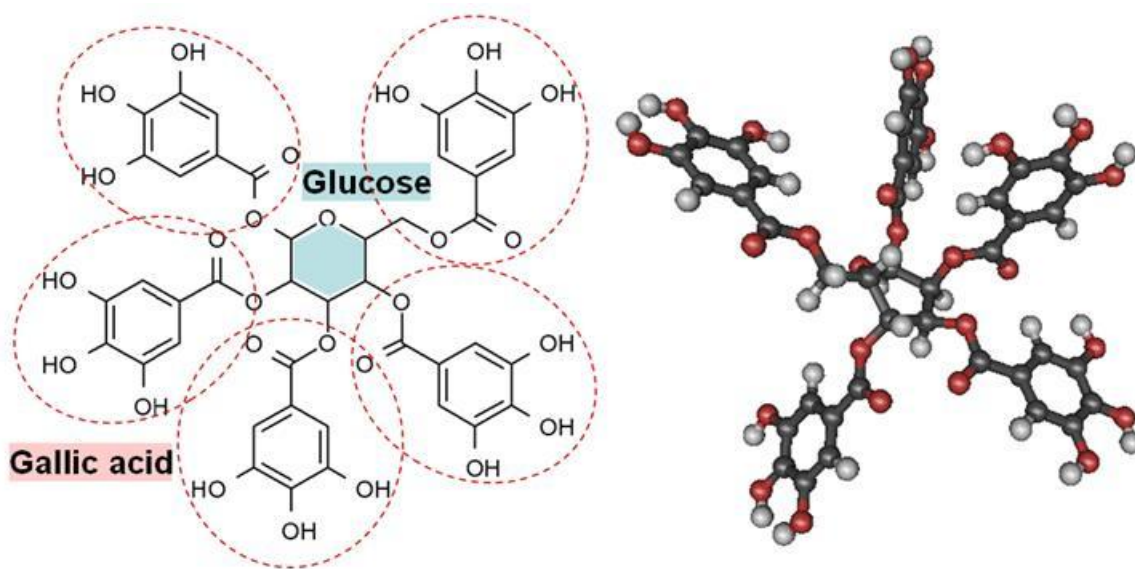
Figure 2.17: Structure of PGG. Five gallic acid residues (pink dotted lines) are bound to each of the hydroxyl groups of a glucose core (blue). At right, spatial configuration of the PGG molecule.

This core molecule may be derived by addition of gallic acid, to yield structures that may contain a total of 10-12 galloyl residues, also known as tannic acids [158] Polyphenols

48

have a hydrophobic internal core and numerous external hydroxyl groups. By virtue of this structure, they react with proteins, specifically binding to hydrophobic regions [159], but also establishing numerous hydrogen bonds, showing particularly high affinity for Proline-rich proteins[160] such as collagen and elastin [161]. In addition, they inhibit many enzymes, are efficient antibacterial agents and reduce inflammation and antigenicity [158]. Polyphenols have very low toxicity in animals (LD50 = 6 g/kg, orally in mice, LD50 = 700 mg/kg i.p. in rats, LD50 = 80 mg/kg i.v. in rats, as per Merck Index). Recently we also showed that peri-arterial delivery of PGG to rat abdominal aorta prevented aneurysm formation or progression and did not elicit any detectable changes in serum liver enzyme activities or liver histology, clearly showing that PGG was not toxic [162]. Moreover, extractables obtained from PGG-fixed tissues exhibited very low in vitro cytotoxicity towards fibroblasts and smooth muscle cells (less than 10%)[163] and thus can be used safely in tissue engineering applications.

2.4.2 Cell Sources for Heart Valve Tissue Engineering

As briefly explained above and visualized in **Figure 16 (A)**, in most cardiovascular tissue engineering approaches cells are harvested from donor tissues. From peripheral arteries, for example, mixed vascular cell populations consisting of myofibroblasts and endothelial cells can be obtained. Out of these, pure viable cell lines can be easily isolated by cell sorters [145] and the subsequent seeding onto the biodegradable scaffold is undertaken in two steps. First the myofibroblasts are seeded and grown in vitro and second, the endothelial cells are seeded on top of the generated neo-

tissue leading to the formation of a native leaflet-analogous histological structure [146].
With regard to clinical applications, several vascular human cell sources have been
investigated [147]. Recently, cells derived from bone marrow or umbilical cord have
been successfully utilized to generate heart valves and conduits *in vitro* [148-150]
(**Figure 18**).
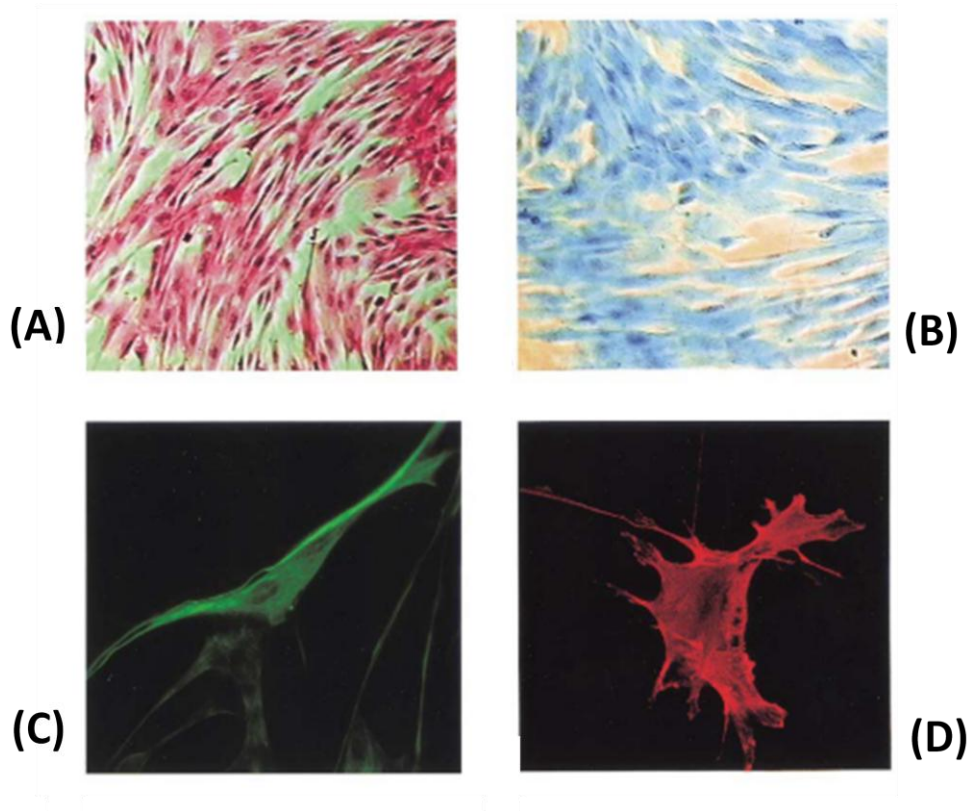
Figure 2.18: Differentiated human umbilical cord cells showing in (A) Hematoxylin-eosin and (B) Masson's trichrome staining cells with a fibroblast morphology and deposition of extracellular matrix proteins. Immunofluorescence staining demonstrated expression of (C) vimentin and (D) alpha-smooth muscle actin [148].

In contrast to vascular cells, these cells can be obtained without surgical
interventions representing an easy-to-access cell source in a possible routine clinical
scenario. Due to their good proliferation and progenitor potential, these cells are

expected to be an attractive alternative for cardiovascular tissue engineering applications. Apart from the use of so called progenitor cells, the research on stem cells and their differentiation pathways is still in its infancy and a drawback is the possible immunogenicity of these cells. This may be solved by genetic engineering [151], although this is still in the experimental phase. **The best option for stem cell use is to use autologous stem cells and, using both mechanical and biochemical cues, differentiate these into VICs**.

2.4.4 Conditioning of Tissue Engineered Heart Valves

Tissue formation can be stimulated by either biological or mechanical conditioning. Biological conditioning involves addition of cytokines either directly to the growth medium or by incorporation into the scaffold material. Cytokines are a group of regulatory molecules that function as mediators of cell communication and can exert multiple biological functions by interaction with specific cell surface receptors. The family of cytokines includes interleukins, hematopoietic growth factors, interferons, tumor necrosis factors, and growth factors [164]. Well-known cytokines that influence vascular cell behavior are fibroblast growth factor (FGF), platelet-derived growth factor (PDGF), transforming growth factor-β (TGF-β), and vascular endothelial growth factor (VEGF) [165, 166] Besides cytokines, regulating cell behavior, matrix metalloproteinases (MMPs) play an important role in tissue development and subsequent remodeling [167]. When cytokines are directly applied to the growth medium, the effect is short term and should be repeated several times. When incorporated into a biodegradable scaffold

material, slow release can be obtained by coupling of the cytokine release to the degradation rate.

Mechanical conditioning involves the application of various mechanical stimuli in a bioreactor, such as flows, inducing shear stresses over the developing tissue, and strains, being either dynamic or static in nature. For engineering of heart valves, the most commonly used bioreactor is a pulse duplicator system, in which the normal opening and closing behavior of the valve is mimicked [168, 169]. In this type of bioreactor, the tissue is exposed to increasing flow rates and pressures. Recently, new bioreactors have been developed for tissue engineering of heart valves, in which the exact physiological conditions of a heart valve *in vivo* can be applied [170-172]. Mechanical and biological stimuli do interact in a very complex way in the regulation of tissue behavior. By mechanical stimuli, the production and secretion of various cytokines by the cells are increased, or conversely, the addition of cytokines during tissue development can increase the effect of mechanical conditioning.

2.4.5 Current Tissue Engineered Heart Valve Approaches

Two of the most recent advancements in the field have striven to incorporate the above concepts of tissue engineering into functional heart valves. The first concept, published by a group in China, is based on the fabrication of a hybrid heart valve leaflet. As has been stated before, the formation of tissue-engineered heart valves can be distinguished by the scaffolding material- bioresorbable polymer scaffold, and decellularized heart valve scaffold [173]. It has been shown that the bioresorbable

polymer scaffold cannot reproduce the functional complex three-dimensional composite heart valve leaflet architecture and has limitations in cellular adhesion. And the use of a decellularized valve tissue matrix offers the advantages of its innate anatomical architecture and remaining biomechanical function. Therefore, they have striven to combine both approaches to form a hybrid biomatrix/polymer heart valve scaffold. The scaffold was fabricated from decellularized porcine aortic heart valve leaflet and coated with basic fibroblast growth factor (bFGF)/chitosan/poly-4-hydroxybutyrate (P4HB) using an electrospinning technique. Then, the hybrid heart valve leaflet was engineered by seeding mesenchymal stem cells (MSCs) onto the scaffold. Results showed that MSCs were present on the scaffolds and the electrospun membrane firmly combined with the surface of the decellularized valve leaflets, concluding that the hybrid leaflets could be useful for heart valve tissue engineering. **However, cellular infiltration into the scaffold has been limited, resulting in only surface population**.
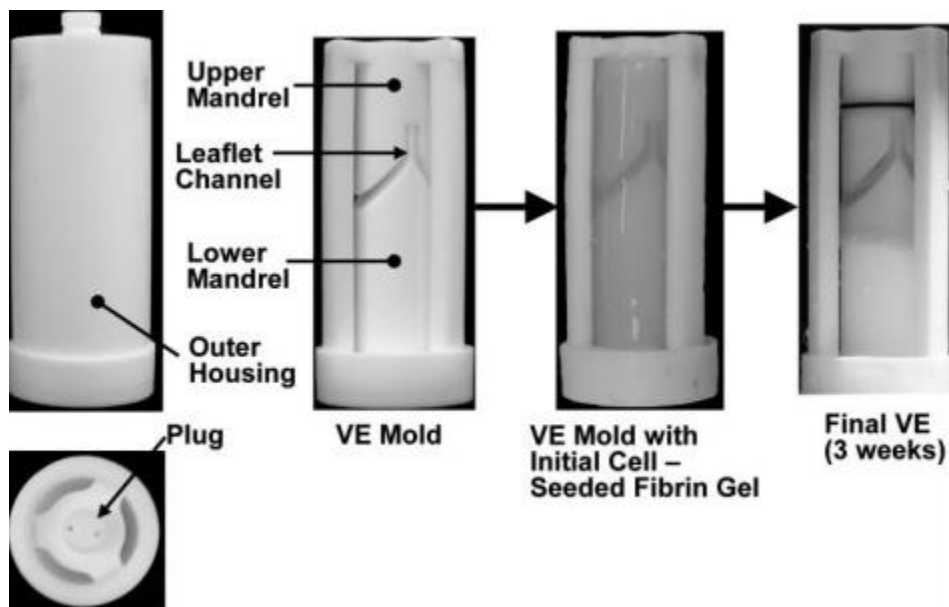
Figure 2.19: Valve-equivalent (VE) mold and fabrication. Cell-seeded fibrin-forming solution is injected into the complete mold (left). After gelation, the outer housing and plug are removed and mold and gel placed in culture medium. Culture for 3 weeks with gentle rocking results in a compacted bi-leaflet VE tissue (right).

The next, and most recently published, by a team lead by Robert Tranquillo, is based on the entrapment of dermal fibroblasts into fibrin gel within a mold, which, following static incubation in the mold, yields the gross geometry and alignment patterns of the native aortic valve [174], as seen in the **Figure 18** (above).

The dermal fibroblast is used because it is a readily available source and generates extensive remodeling of fibrin into a collagenous tissue with tensile mechanical properties approaching those of native tissue [174]. Dermal fibroblasts have also been successfully used for a vascular graft in clinical studies [175]. The fibrin-based TEHVs are cast such that the tubular root and leaflets are a single entity. By using molds with two or three channels cut into the central mandrel, bi- and tri- leaflet VEs have been fabricated.

In contrast to synthetic biodegradable polymers whose initial strength and stiffness values are greater than heart valve tissue, those of biological scaffolds like collagen or fibrin are orders of magnitude smaller. And, as stated earlier, realizing tissue growth to achieve physiological values of leaflet tensile and bending stiffness prior to implantation is crucial for their success. Shown by previous research with fibrin-based tubular constructs prepared with porcine aortic valve interstitial cells, it was illustrated that cyclic stretching with an incremental strain amplitude over three weeks can lead to at minimum an 84% greater ultimate tensile strength compared to statically-incubated controls, which correlates with increased collagen deposition and maturation [176].

54

Therefore, Tranquillo's team is developing a controlled stretch TEHV bioreactor that can apply prescribed cyclic stretching to the VE root and leaflets during the entire incubation (even as the tissue mechanical properties change), while independently controlling the nutrient delivery (see **Figure 2.20** below).

It was concluded that using fibrin-based VEs prepared with human dermal fibroblasts, it is possible to create a TEHV with circumferential fiber alignment in the leaflet manifested as anisotropic stiffness comparable to native leaflets, a property that has not been achieved with TEHVs based on synthetic biodegradable polymers. Though several bioreactors have been proposed to mechanically condition TEHVs, they do not allow for controlled strain to be applied without complicated feedback regulation, which has not been proposed. Using a strategy for controlled cyclic stretching of tubular constructs that they presented previously, they developed a controlled cyclic stretch bioreactor for TEHVs that leads to improved tensile and compositional properties. Despite their exciting accomplishments, in vivo studies have been performed in the less mechanically demanding environment of the pulmonary valve position, where the valve is exposed to pressures far less than would be expected in the aortic position [177]. Furthermore, from preliminary data presented at the Heart Valve and Tissue Engineering meeting in Hilton Head (personal communication, March 2010), Dr. Tranquillo presented data that showed exstensive fibrosis after implantation, suggesting this scaffold may not be suitable for TEHVs.
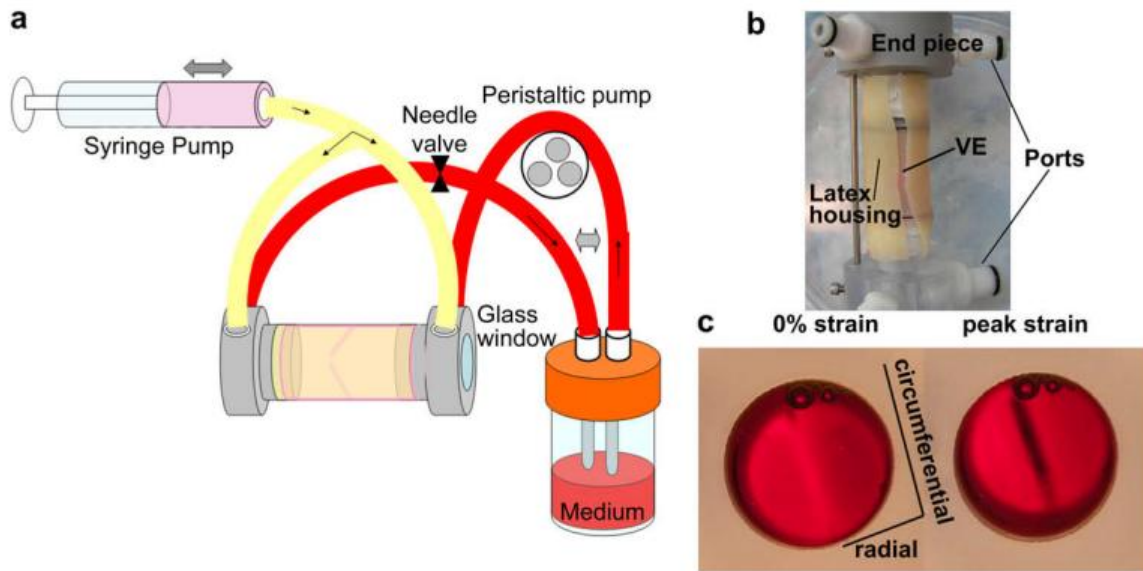
Figure 2.20: (a) Schematic of controlled cyclic stretching TEHV bioreactor showing the reciprocating syringe pump for cyclic pressurization and stretching of the VE mounted within the latex tube, (b) image of the bioreactor with the latex housing slit to reveal the VE mounted within and its tie-down to both end pieces, and (c) end-on view of the VE through the glass window of the bioreactor during a stretching cycle, showing the leaflets coapting when the lumen is not pressurized, and separated when the lumen is pressurized and the root and leaflets are stretched [177].

Thus, research for an ideal scaffold for heart valve tissue engineering is still needed.

2.5   References

1.   *Heart Valve Disease*.   [cited   2009;   Available   from: http://my.clevelandclinic.org/heart/percutaneous/percutaneousValve.aspx.

2.   Netter, F.H., *Atlas of Human Anatomy*. 2 ed. 1997: Rittenhouse Book Distributors Inc. 525.

3.   Costanzo, L.s., *Physiology*. Saunders Text and Review Series. 1998, Philadelphia: W.B. Saunders Company. 429.

4.   Guyton, H., *Textbook of Medical Physiology*, ed. Elsevier. 2006, Philadelphia, PA.

5.   Rahimtoola, S.H., *The Year in Valvular Heart Disease.* Journal of the American College of Cardiology, 2009. **53**(20): p. 1894-1908.

6.   Thubrikar, M.J., R.S. Salzar, and R.T. Eppink, *Correlation between Intramural Stress and Atherosclerotic Lesions in Human Carotid-Artery Bifurcation.* Arteriosclerosis, 1990. **10**(5): p. A821-A821.

7.   Kollar, A.C., S.D. Lick, and V.R. Conti, *Valve-Sparing Aortic Root Reconstruction Using In Situ Three-Dimensional Measurements.* Annals of Thoracic Surgery, 2009. **87**(6): p. 1795-1800.

8.   Mol, A., *Functional tissue engineering of human heart valve leaflets*. 2005, Technische Universiteit Eindhoven. p. 115.

9.   *Background on Heart Valves and Their Function* [cited 2006 October 21]; Available from: http://heartlab.robarts.ca/what.is.2.html.

10.   Mendelson, K. and F.J. Schoen, *Heart valve tissue engineering: concepts, approaches, progress, and challenges.* Ann Biomed Eng, 2006. **34**(12): p. 1799-819.

11.   Thubrikar, M., *The Aortic Valve*. 1990: Boca Raton CRC Press

12.   *Cardiothoracic and Vascular Program Heart Valve Laboratory.*   [cited 2008 July 3]; Available from: http://www.cts.usc.edu/research-heartvalvelaboratory.html.

13.   Schenke-Layland, K., et al., *Impact of cryopreservation on extracellular matrix structures of heart valve leaflets.* Annals of Thoracic Surgery, 2006. **81**(3): p. 918-927.

14.   Scott, M. and I. Vesely, *Aortic-Valve Cusp Microstructure - the Role of Elastin.* Annals of Thoracic Surgery, 1995. **60**(2): p. S391-S394.

15.   Dawn B. Marks, A.D.M., Colleen M. Smith, *Basic Medical Biochemistry*. 1996: Lippincott Williams and Wilkins.

16.   Lehninger, *Principles of Biochemistry*. 4th ed, ed. D.L. Nelson: W.H. Freeman. 1100.

17. Sacks, M.S. and A.P. Yoganathan, *Heart valve function: a biomechanical perspective.* Philosophical Transactions of the Royal Society B-Biological Sciences, 2007. **362**(1484): p. 1369-1391.

18. Balguid, A., et al., *Stress related collagen ultrastructure in human aortic valves - implications for tissue engineering.* Journal of Biomechanics, 2008. **41**(12): p. 2612-2617.

19. Rabkin-Aikawa, E., J.E. Mayer, and F.J. Schoen, *Heart valve regeneration*, in *Regenerative Medicine Ii: Clinical and Preclinical Applications*. 2005. p. 141-179.

20. Schoen, F.J. and R.J. Levy, *Founder's Award, 25th Annual Meeting of the Society for Biomaterials, perspectives. Providence, RI, April 28-May 2, 1999. Tissue heart valves: current challenges and future research perspectives.* J Biomed Mater Res, 1999. **47**(4): p. 439-65.

21. Cebotari, S., et al., *Construction of autologous human heart valves based on an acellular allograft matrix.* Circulation, 2002. **106**(13): p. I63-I68.

22. Cole, W.G., et al., *Collagen Composition of Normal and Myxomatous Human Mitral Heart-Valves.* Biochemical Journal, 1984. **219**(2): p. 451-460.

23. Schoen, F.J., *Future directions in tissue heart valves: impact of recent insights from biology and pathology.* J Heart Valve Dis, 1999. **8**(4): p. 350-8.

24. Chester, A.H. and P.M. Taylor, *Molecular and functional characteristics of heart-valve interstitial cells.* Philosophical Transactions of the Royal Society B-Biological Sciences, 2007. **362**(1484): p. 1437-1443.

25. Davies, P.F., A.G. Passerini, and C.A. Simmons, *Aortic valve: turning over a new leaf(let) in endothelial phenotypic heterogeneity.* Arterioscler Thromb Vasc Biol, 2004. **24**(8): p. 1331-3.

26. Bairati, A. and S. Debiasi, *Presence of a Smooth-Muscle System in Aortic-Valve Leaflets.* Anatomy and Embryology, 1981. **161**(3): p. 329-340.

27. Cimini, M., K.A. Rogers, and D.R. Boughner, *Smoothelin-positive cells in human and porcine semilunar valves.* Histochemistry and Cell Biology, 2003. **120**(4): p. 307-317.

28. Messier, R.H., et al., *Dual Structural and Functional Phenotypes of the Porcine Aortic-Valve Interstitial Population - Characteristics of the Leaflet Myofibroblast.* Journal of Surgical Research, 1994. **57**(1): p. 1-21.

29. Taylor, P.A., et al., *The cardiac valve interstitial cell.* International Journal of Biochemistry & Cell Biology, 2003. **35**(2): p. 113-118.

30. Tomasek, J.J., et al., *Myofibroblasts and mechano-regulation of connective tissue remodelling.* Nature Reviews Molecular Cell Biology, 2002. **3**(5): p. 349-363.

31. Rabkin-Aikawa, E., et al., *Dynamic and reversible changes of interstitial cell phenotype during remodeling of cardiac valves.* Journal of Heart Valve Disease, 2004. **13**(5): p. 841-847.

32. Dreger, S.A., et al., *Profile and localization of matrix metalloproteinases (MMPs) and their tissue inhibitors (TIMPs) in human heart valves.* Journal of Heart Valve Disease, 2002. **11**(6): p. 875-880.

33. Liu, A.C., V.R. Joag, and A.I. Gotlieb, *The emerging role of valve interstitial cell phenotypes in regulating heart valve pathobiology.* American Journal of Pathology, 2007. **171**: p. 1407-1418.

34. Della Rocca, F., et al., *Cell composition of the human pulmonary valve: A comparative study with the aortic valve - The VESALIO* project.* Annals of Thoracic Surgery, 2000. **70**(5): p. 1594-1600.

35. Sartore, S., et al., *Molecular and cellular phenotypes and their regulation in smooth muscle*, in *Reviews of Physiology Biochemistry and Pharmacology; Special issue on signal transduction in smooth muscle*. 1999. p. 235-320.

36. Filip, D.A., A. Radu, and M. Simionescu, *Interstitial-Cells of the Heart-Valves Possess Characteristics Similar to Smooth-Muscle Cells.* Circulation Research, 1986. **59**(3): p. 310-320.

37. Taylor, P.M., S.P. Allen, and M.H. Yacoub, *Phenotypic and functional characterization of interstitial cells from human heart valves, pericardium and skin.* Journal of Heart Valve Disease, 2000. **9**(1): p. 150-158.

38. Marron, K., et al., *Innervation of human atrioventricular and arterial valves.* Circulation, 1996. **94**(3): p. 368-375.

39. Deck, J.D., *Endothelial-Cell Orientation on Aortic-Valve Leaflets.* Cardiovascular Research, 1986. **20**(10): p. 760-767.

40. *Valvular Heart Disease Basics.* [cited 2007 September 26]; Available from: http://yourtotalhealth.ivillage.com/valvular-heart-disease-basics.html.

41.   Singh, J.P., et al., *Prevalence and clinical determinants of mitral, tricuspid, and aortic regurgitation (the Framingham Heart Study).* Am J Cardiol, 1999. **83**(6): p. 897-902.

42.   Chan, K.M., et al., *Tricuspid valve disease: pathophysiology and optimal management.* Prog Cardiovasc Dis, 2009. **51**(6): p. 482-6.

43.   Robicsek, F., M.J. Thubrikar, and A.A. Fokin, *Cause of degenerative disease of the trileaflet aortic valve: review of subject and presentation of a new theory.* Ann Thorac Surg, 2002. **73**(4): p. 1346-54.

44.   Mihaljevic T, *Pathophysiology of Aortic Valve Disease*, in *Cardica Surgery in the Adult*, E.L. Cohn LH, Editor. 2003, McGraw-Hill: New York. p. 791-810.

45.   Cotran, Kumar, and Collins, *Robbins Pathologic Basis of Disease*. 6 ed. 1999: W.B. Sanders Company. 566-78.

46.   LeBoutillier M, D.V., *Valvular and Ischemic Heart Disease*, in *Cardiac Surgery in the Adult*, E.L. Cohn LH, Editor. 2003, McGraw-Hill: New York. p. 1057-1074.

47.   Schoen, F.J., Pandera RF, *Cardiac Surgical Pathology*, in *Cardiac Surgery in the Adult*, Cohn LH and E. LH, Editors. 2003, McGraw-Hill: New York. p. 119-185.

48.   Koelling, T.M., et al., *Prognostic significance of mitral regurgitation and tricuspid regurgitation in patients with left ventricular systolic dysfunction.* Am Heart J, 2002. **144**(3): p. 524-9.

49.   Nath, J., E. Foster, and P.A. Heidenreich, *Impact of tricuspid regurgitation on long-term survival.* J Am Coll Cardiol, 2004. **43**(3): p. 405-9.

50.   Tong, E., *An overview of artificial heart valve replacement in infants and children.* J Cardiovasc Nurs, 1992. **6**(3): p. 30-43.

51.   *Aorta and Aortic Valve Surgery – Keyhole Approaches* [cited 2009; Available from: http://my.clevelandclinic.org/heart/disorders/valve/aorticvalvesurgery.aspx.

52.   Saha, S., et al., *An undiagnosed bicuspid aortic valve can result in severe left ventricular failure.* British Medical Journal, 2007. **334**(7590): p. 420-422.

53.   Ferencz, C., et al., *Congenital heart disease: prevalence at livebirth. The Baltimore-Washington Infant Study.* Am J Epidemiol, 1985. **121**(1): p. 31-6.

54. Loffredo, C.A., *Epidemiology of cardiovascular malformations: prevalence and risk factors.* Am J Med Genet, 2000. **97**(4): p. 319-25.

55. Lindroos, M., et al., *Prevalence of Aortic-Valve Abnormalities in the Elderly - an Echocardiographic Study of a Random-Population Sample.* Journal of the American College of Cardiology, 1993. **21**(5): p. 1220-1225.

56. Ross, J. and Braunwal.E, *Aortic Stenosis.* Circulation, 1968. **38**(1S5): p. V61-&.

57. *Aortic valve, senile calcific aortic stenosis.* [cited 2009; Available from: www.meduweb.com/showthread.php?t=5266.

58. *Calcified aortic heart valve.* [cited 2009; Available from: www.heart-valve-surgery.com/.../pictures/.

59. Mohler, E.R., et al., *Bone formation and inflammation in cardiac valves.* Circulation, 2001. **103**(11): p. 1522-1528.

60. Obrien, K.D., et al., *Osteopontin Is Expressed in Human Aortic Valvular Lesions.* Circulation, 1995. **92**(8): p. 2163-2168.

61. Lester, W.M., et al., *Bovine Mitral-Valve Organ-Culture - Role of Interstitial-Cells in Repair of Valvular Injury.* Journal of Molecular and Cellular Cardiology, 1992. **24**(1): p. 43-53.

62. Lester, W.M. and A.I. Gotlieb, *Invitro Repair of the Wounded Porcine Mitral-Valve.* Circulation Research, 1988. **62**(4): p. 833-845.

63. Meredith, J.E. and M.A. Schwartz, *Integrins, adhesion and apoptosis.* Trends in Cell Biology, 1997. **7**(4): p. 146-150.

64. Woodard, A.S., et al., *The synergistic activity of alpha(v)beta(3) integrin and PDGF receptor increases cell migration.* Journal of Cell Science, 1998. **111**: p. 469-478.

65. Rabkin, E., et al., *Activated interstitial myofibroblasts express catabolic enzymes and mediate matrix remodeling in myxomatous heart valves.* Circulation, 2001. **104**(21): p. 2525-2532.

66. Dreger, S.A., et al., *Potential for synthesis and degradation of extracellular matrix proteins by valve interstitial cells seeded onto collagen scaffolds.* Tissue Eng, 2006. **12**(9): p. 2533-40.

67.   Galis, Z.S. and J.J. Khatri, *Matrix metalloproteinases in vascular remodeling and atherogenesis - The good, the bad, and the ugly.* Circulation Research, 2002. **90**(3): p. 251-262.

68.   Nelson, A.R., et al., *Matrix metalloproteinases: Biologic activity and clinical implications.* Journal of Clinical Oncology, 2000. **18**(5): p. 1135-1149.

69.   Krane, S.M., et al., *Different collagenase gene products have different roles in degradation of type I collagen.* Journal of Biological Chemistry, 1996. **271**(45): p. 28509-28515.

70.   Decker, R.S. and J.T. Dingle, *Cardiac Catabolic Factors - the Degradation of Heart-Valve Inter-Cellular Matrix.* Science, 1982. **215**(4535): p. 987-989.

71.   *Aortic Valve Disease.* [cited 2009; Available from: http://www.healthscout.com/ency/416/656/main.html#TreatmentofAorticValveDisease.

72.   Vahanian, A. and I.F. Palacios, *Percutaneous approaches to valvular disease.* Circulation, 2004. **109**(13): p. 1572-1579.

73.   Buellesfeld, L. and E. Grube, *Percutaneous Aortic Valve Replacement - Pro.* Herz, 2009. **34**(2): p. 124-129.

74.   Song, X., et al., *Grape seed proanthocyanidin suppression of breast cell carcinogenesis induced by chronic exposure to combined 4-(methylnitrosamino)-1-(3-pyridyl)-1-butanone and benzo[a]pyrene.* Mol Carcinog, 2010. **49**(5): p. 450-63.

75.   Shrestha, M., et al., *Valve-Sparing Aortic Root Stabilization in Acute Type A Aortic Dissection.* Asian Cardiovasc Thorac Ann, 2009. **17**(1): p. 22-24.

76.   Baig, K.a.P.P., *Heart Valve Surgery.* Surgery, 2008. **26**(12): p. 491-95.

77.   Yacoub, M.H. and L.H. Cohn, *Novel approaches to cardiac valve repair: From structure to function: Part II.* Circulation, 2004. **109**(9): p. 1064-1072.

78.   Yacoub, M.H. and L.H. Cohn, *Novel approaches to cardiac valve repair: From structure to function: Part I.* Circulation, 2004. **109**(3): p. 942-950.

79.   Raja, S.G. and J.C. Pollock, *Current outcomes of ross operation for pediatric and adolescent patients.* Journal of Heart Valve Disease, 2007. **16**(1): p. 27-36.

80.   Hanke, T., et al., *Autograft regurgitation and aortic root dimensions after the ross procedure - The German ross registry experience.* Circulation, 2007. **116**(11): p. I251-I258.

81.   Migneco, F., S.J. Hollister, and R.K. Birla, *Tissue-engineered heart valve prostheses: 'state of the heart'.* Regen Med, 2008. **3**(3): p. 399-419.

82.   Simionescu, D., *Artificial Heart Valves*, in *Wiley Encyclopedia of Biomedical Engineering*, M. Akay, Editor. 2006. p. 1-10.

83.   Vesely, I., *Heart Valve Tissue Engineering*, in *Wiley Encyclopedia of Biomedical Engineering*, M. Akay, Editor. 2006. p. 1-6.

84.   Lee, T.C., et al., *The effect of elastin damage on the mechanics of the aortic valve.* Journal of Biomechanics, 2001. **34**(2): p. 203-210.

85.   Senthilnathan, V., et al., *Heart valves: which is the best choice?* Cardiovascular Surgery, 1999. **7**(4): p. 393-397.

86.   Rajani, B., R.B. Mee, and N.B. Ratliff, *Evidence for rejection of homograft cardiac valves in infants.* Journal of Thoracic and Cardiovascular Surgery, 1998. **115**(1): p. 111-117.

87.   Koolbergen, D.R., et al., *Structural degeneration of pulmonary homografts used as aortic valve substitute underlines early graft failure.* European Journal of Cardio-Thoracic Surgery, 2002. **22**(5): p. 802-807.

88.   Jennings, L.M., et al., *The pulmonary bioprosthetic heart valve: Its unsuitability for use as an aortic valve replacement.* Journal of Heart Valve Disease, 2002. **11**(5): p. 668-678.

89.   Angell, W.W., et al., *Durability of the Viable Aortic Allograft.* Journal of Thoracic and Cardiovascular Surgery, 1989. **98**(1): p. 48-56.

90.   Oei, F.B.S., et al., *The presence of immune stimulatory cells in fresh and cryopreserved donor aortic and pulmonary valve allografts.* Journal of Heart Valve Disease, 2002. **11**(3): p. 315-324.

91.   Aagaard, J. and J. Tingleff, *Fifteen years' clinical experience with the CarboMedics prosthetic heart valve.* J Heart Valve Dis, 2005. **14**(1): p. 82-8.

92.   Vesely, I., *Heart valve tissue engineering.* Circ Res, 2005. **97**(8): p. 743-55.

93. Gonzalez-Lavin, L., et al., *Strut fracture and other events after valve replacement with the 60 degree convexoconcave Bjork-Shiley prosthesis.* Circulation, 1987. **76**(3 Pt 2): p. III137-40.

94. Schoen, F.J., *Cardiac valve prostheses: review of clinical status and contemporary biomaterials issues.* J Biomed Mater Res, 1987. **21**(A1 Suppl): p. 91-117.

95. *Particle deposition in an artificial heart valve.* [cited 2009; Available from: http://www.ifdmavt.ethz.ch/education/student_projects/heart_valve_II.

96. Hammermeister, K.E., et al., *A comparison of outcomes in men 11 years after heart-valve replacement with a mechanical valve or bioprosthesis. Veterans Affairs Cooperative Study on Valvular Heart Disease.* N Engl J Med, 1993. **328**(18): p. 1289-96.

97. Jamieson, W.R., et al., *Multiple mechanical valve replacement surgery comparison of St. Jude Medical and CarboMedics prostheses.* Eur J Cardiothorac Surg, 1998. **13**(2): p. 151-9.

98. Adamczyk, M.M. and I. Vesely, *Biaxial strain distributions in explanted porcine bioprosthetic valves.* Journal of Heart Valve Disease, 2002. **11**(5): p. 688-695.

99. Takeuchi, Y., *Risk of zoonosis in xenotransplantation.* Transplantation Proceedings, 2000. **32**(8): p. 2698-2700.

100. Weiss, R.A., S. Magre, and Y. Takeuchi, *Infection hazards of xenotransplantation.* Journal of Infection, 2000. **40**(1): p. 21-25.

101. Moza, A.K., et al., *Heart valves from pigs and the porcine endogenous retrovirus: Experimental and clinical data to assess the probability of porcine endogenous retrovirus infection in human subjects.* Journal of Thoracic and Cardiovascular Surgery, 2001. **121**(4): p. 697-701.

102. Knight, R., M. Brazier, and S.J. Collins, *Human prion diseases: Cause, clinical and diagnostic aspects*, in *Contributions to Microbiology:A CHALLENGE FOR SCIENCE, MEDICINE AND THE PUBLIC HEALTH SYSTEM*. 2004. p. 72-97.

103. Patience, C., et al., *Multiple groups of novel retroviral genomes in pigs and related species.* Journal of Virology, 2001. **75**(6): p. 2771-2775.

104. Martin, U., et al., *Expression of pig endogenous retrovirus by primary porcine endothelial cells and infection of human cells.* Lancet, 1998. **352**(9129): p. 692-694.

105. Specke, V., S. Rubant, and J. Denner, *Productive infection of human primary cells and cell lines with porcine endogenous retroviruses.* Virology, 2001. **285**(2): p. 177-180.

106. Sprangers, B., M. Waer, and A.D. Billiau, *Xenograft rejection - all that glitters is not Gal.* Nephrology Dialysis Transplantation, 2006. **21**(6): p. 1486-1488.

107. Carpentier, A., *From Valvular Xenograft to Valvular Bioprosthesis - 1965-1970.* Annals of Thoracic Surgery, 1989. **48**(3): p. S73-S74.

108. Angell, W.W., J.D. Angell, and A. Sywak, *Selection of Tissue or Prosthetic Valve - 5-Year Prospective, Randomized Comparison.* Journal of Thoracic and Cardiovascular Surgery, 1977. **73**(1): p. 43-53.

109. Paez, J.M.G. and E. Jorge-Herrero, *Assessment of pericardium in cardiac bioprostheses. A review.* Journal of Biomaterials Applications, 1999. **13**(4): p. 351-388.

110. Ferrans, V.J., et al., *Structural-Changes in Implanted Cardiac Valvular Bioprostheses Constructed of Glycerol-Treated Human Dura-Mater.* European Journal of Cardio-Thoracic Surgery, 1991. **5**(3): p. 144-154.

111. Hilbert, S.L., et al., *Ionescu-Shiley Bovine Pericardial Bioprostheses - Histologic and Ultrastructural Studies.* American Journal of Pathology, 1992. **140**(5): p. 1195-1204.

112. Ishihara, T., et al., *Structure of Bovine Parietal Pericardium and of Un-Implanted Ionescu-Shiley Pericardial Valvular Bioprostheses.* Journal of Thoracic and Cardiovascular Surgery, 1981. **81**(5): p. 747-757.

113. Cheung, D.T. and M.E. Nimni, *Mechanism of Crosslinking of Proteins by Glutaraldehyde .1. Reaction with Model Compounds.* Connective Tissue Research, 1982. **10**(2): p. 187-199.

114. Cheung, D.T. and M.E. Nimni, *Mechanism of Crosslinking of Proteins by Glutaraldehyde .2. Reaction with Monomeric and Polymeric Collagen.* Connective Tissue Research, 1982. **10**(2): p. 201-216.

115. Cheung, D.T., et al., *Mechanism of Crosslinking of Proteins by Glutaraldehyde .3. Reaction with Collagen in Tissues.* Connective Tissue Research, 1985. **13**(2): p. 109-115.

116. Ionescu, M.I., et al., *Heart-Valve Replacement with Ionescu-Shiley Pericardial Xenograft.* Journal of Thoracic and Cardiovascular Surgery, 1977. **73**(1): p. 31-42.

117. Duncan, A.C. and D. Boughner, *Effect of dynamic glutaraldehyde fixation on the viscoelastic properties of bovine pericardial tissue.* Biomaterials, 1998. **19**(7-9): p. 777-783.

118. Wang, D., et al., *Mitigated calcification of glutaraldehyde-fixed bovine pericardium by tannic acid in rats.* Chinese Medical Journal, 2008. **121**(17): p. 1675-1679.

119. Nimni, M.E., et al., *Chemically Modified Collagen - a Natural Biomaterial for Tissue Replacement.* Journal of Biomedical Materials Research, 1987. **21**(6): p. 741-771.

120. Naimark, W.A., et al., *Hmdc Cross-Linking of Bovine Pericardial Tissue - a Potential Role of the Solvent Environment in the Design of Bioprosthetic Materials.* Journal of Materials Science-Materials in Medicine, 1995. **6**(4): p. 235-241.

121. Damink, L., et al., *Cross-Linking of Dermal Sheep Collagen Using Hexamethylene Diisocyanate.* Journal of Materials Science-Materials in Medicine, 1995. **6**(7): p. 429-434.

122. Chanda, J., et al., *Prevention of Calcification of Tissue Valves.* Artificial Organs, 1994. **18**(10): p. 752-757.

123. Grimm, M., et al., *Improved Biocompatibility of Bioprosthetic Heart-Valves by L-Glutamic Acid Treatment.* Journal of Cardiac Surgery, 1992. **7**(1): p. 58-70.

124. Hoffman, D., et al., *Spontaneous Host Endothelial Growth on Bioprostheses - Influence of Fixation.* Circulation, 1992. **86**(5): p. 75-79.

125. Jorge-Herrero, E., et al., *Calcification of pericardial tissue pretreated with different amino acids.* Biomaterials, 1996. **17**(6): p. 571-575.

126. Simionescu, A., D. Simionescu, and R. Deac, *Lysine-Enhanced Glutaraldehyde Cross-Linking of Collagenous Biomaterials.* Journal of Biomedical Materials Research, 1991. **25**(12): p. 1495-1505.

127. Wika, K.E., et al., *Quantification of the Edge Effect in Calcified Bioprosthetic Tissues.* Journal of Biomedical Materials Research, 1993. **27**(10): p. 1293-1299.

128. Raghavan, D., D.T. Simionescu, and N.R. Vyavahare, *Neomycin prevents enzyme-mediated glycosaminoglycan degradation in bioprosthetic heart valves.* Biomaterials, 2007. **28**(18): p. 2861-8.

129. Flomenbaum, M.A. and F.J. Schoen, *Effects of Fixation Back Pressure and Antimineralization Treatment on the Morphology of Porcine Aortic Bioprosthetic Valves.* Journal of Thoracic and Cardiovascular Surgery, 1993. **105**(1): p. 154-164.

130. Neuenschwander, S. and S.P. Hoerstrup, *Heart valve tissue engineering.* Transplant Immunology, 2004. **12**(3-4): p. 359-365.

131. Hoerstrup, S.P., et al., *Functional living trileaflet heart valves grown in vitro.* Circulation, 2000. **102**(19): p. 44-49.

132. Samouillan, V., et al., *Thermal analysis characterization of aortic tissues for cardiac valve bioprostheses.* Journal of Biomedical Materials Research, 1999. **46**(4): p. 531-538.

133. Wilson, G.J., et al., *Acellular Matrix - a Biomaterials Approach for Coronary-Artery Bypass and Heart-Valve Replacement.* Annals of Thoracic Surgery, 1995. **60**(2): p. S353-S358.

134. Elkins, R.C., et al., *Decellularized human valve allografts.* Annals of Thoracic Surgery, 2001. **71**(5): p. S428-S432.

135. Simon, P., et al., *Early failure of the tissue engineered porcine heart valve SYNERGRAFT (TM) in pediatric patients.* European Journal of Cardio-Thoracic Surgery, 2003. **23**(6): p. 1002-1006.

136. Lee, K.Y. and D.J. Mooney, *Hydrogels for tissue engineering.* Chemical Reviews, 2001. **101**(7): p. 1869-1879.

137. Rothenburger, M., et al., *Tissue engineering of heart valves: Formation of a three-dimensional tissue using porcine heart valve cells.* Asaio Journal, 2002. **48**(6): p. 586-591.

138. Agrawal, C.M. and R.B. Ray, *Biodegradable polymeric scaffolds for musculoskeletal tissue engineering.* Journal of Biomedical Materials Research, 2001. **55**(2): p. 141-150.

139. Hutmacher, D.W., *Scaffold design and fabrication technologies for engineering tissues - state of the art and future perspectives.* Journal of Biomaterials Science-Polymer Edition, 2001. **12**(1): p. 107-124.

140. Hutmacher, D.W., J.C.H. Goh, and S.H. Teoh, *An introduction to biodegradable materials for tissue engineering applications.* Annals Academy of Medicine Singapore, 2001. **30**(2): p. 183-191.

141. Sodian, R., et al., *Early in vivo experience with tissue-engineered trileaflet heart valves.* Circulation, 2000. **102**(19): p. 22-29.

142. Zisch, A.H., et al., *Cell-demanded release of VEGF from synthetic, biointeractive cell-ingrowth matrices for vascularized tissue growth.* Faseb Journal, 2003. **17**(13): p. 2260-+.

143. Antunes, M., Daebritz, and T. Bottio, *Introduction of a flexible polymeric heart valve prosthesis with special design for aortic position - Appendix A. Conference discussion.* European Journal of Cardio-Thoracic Surgery, 2004. **25**(6): p. 952-952.

144. Ghanbari, H., et al., *Polymeric heart valves: new materials, emerging hopes.* Trends in Biotechnology, 2009. **27**(6): p. 359-367.

145. Hoerstrup, S.P., et al., *Fluorescence activated cell sorting: A reliable method in tissue engineering of a bioprosthetic heart valve.* Annals of Thoracic Surgery, 1998. **66**(5): p. 1653-1657.

146. Zund, G., et al., *The in vitro construction of a tissue engineered bioprosthetic heart valve.* European Journal of Cardio-Thoracic Surgery, 1997. **11**(3): p. 493-497.

147. Schnell, A.M., et al., *Optimal cell source for cardiovascular tissue engineering: Venous vs. aortic human myofibroblasts.* Thoracic and Cardiovascular Surgeon, 2001. **49**(4): p. 221-225.

148. Hoerstrup, S.P., et al., *Living, autologous pulmonary artery conduits tissue engineered from human umbilical cord cells.* Annals of Thoracic Surgery, 2002. **74**(1): p. 46-52.

149. Hoerstrup, S.P., et al., *Tissue engineering of functional trileaflet heart valves from human marrow stromal cells.* Circulation, 2002. **106**(13): p. I143-I150.

150. Rezai, N., T.J. Podor, and B.M. McManus, *Bone marrow cells in the repair and modulation of heart and blood vessels: Emerging opportunities in native and engineered tissue and biomechanical materials.* Artificial Organs, 2004. **28**(2): p. 142-151.

151.   Odorico, J.S., D.S. Kaufman, and J.A. Thomson, *Multilineage differentiation from human embryonic stem cell lines.* Stem Cells, 2001. **19**(3): p. 193-204.

152.   Schmidt, C.E. and J.M. Baier, *Acellular vascular tissues: natural biomaterials for tissue repair and tissue engineering.* Biomaterials, 2000. **21**(22): p. 2215-31.

153.   Han, B., et al., *Proanthocyanidin: a natural crosslinking reagent for stabilizing collagen matrices.* J Biomed Mater Res A, 2003. **65**(1): p. 118-24.

154.   Heijmen, F.H., et al., *Cross-linking of dermal sheep collagen with tannic acid.* Biomaterials, 1997. **18**(10): p. 749-54.

155.   Isenburg, J.C., et al., *Structural requirements for stabilization of vascular elastin by polyphenolic tannins.* Biomaterials, 2006. **27**(19): p. 3645-3651.

156.   Isenburg, J.C., D.T. Simionescu, and N.R. Vyavahare, *Tannic acid treatment enhances biostability and reduces calcification of glutaraldehyde fixed aortic wall.* Biomaterials, 2005. **26**(11): p. 1237-45.

157.   Isenburg, J.C., D.T. Simionescu, and N.R. Vyavahare, *Elastin stabilization in cardiovascular implants: improved resistance to enzymatic degradation by treatment with tannic acid.* Biomaterials, 2004. **25**(16): p. 3293-302.

158.   Haslam, E., *Plant polyphenols; vegetable tannins revisited.* Chemistry and Pharmacology of Natural Products, ed. J. Phillipson. 1989, Cambridge, UK: Cambridge University Press.

159.   Shi, B., X.Q. He, and E. Haslam, *Gelatin - Polyphenol Interaction.* Journal of the American Leather Chemists Association, 1994. **89**(4): p. 98-104.

160.   Charlton, A.J., et al., *Tannin interactions with a full-length human salivary proline-rich protein display a stronger affinity than with single proline-rich repeats.* Febs Letters, 1996. **382**(3): p. 289-292.

161.   Luck, G., et al., *Polyphenols, Astringency and Proline-Rich Proteins.* Phytochemistry, 1994. **37**(2): p. 357-371.

162.   Isenburg, J.C., et al., *Elastin stabilization for treatment of abdominal aortic aneurysms.* Circulation, 2007. **115**(13): p. 1729-37.

163.   Isenburg, J.C., et al., *Structural requirements for stabilization of vascular elastin by polyphenolic tannins.* Biomaterials, 2006. **27**(19): p. 3645-51.

164. Takehara, K., *Growth regulation of skin fibroblasts.* Journal of Dermatological Science, 2000. **24**: p. S70-S77.

165. Ziegler, T., R.W. Alexander, and R.M. Nerem, *An Endothelial Cell-Smooth Muscle-Cell Coculture Model for Use in the Investigation of Flow Effects on Vascular Biology.* Annals of Biomedical Engineering, 1995. **23**(3): p. 216-225.

166. Bos, G.W., et al., *Proliferation of endothelial cells on surface-immobilized albumin-heparin conjugate loaded with basic fibroblast growth factor.* Journal of Biomedical Materials Research, 1999. **44**(3): p. 330-340.

167. Streuli, C., *Extracellular matrix remodelling and cellular differentiation.* Current Opinion in Cell Biology, 1999. **11**(5): p. 634-640.

168. Hoerstrup, S.P., et al., *New pulsatile bioreactor for in vitro formation of tissue engineered heart valves.* Tissue Engineering, 2000. **6**(1): p. 75-79.

169. Hoerstrup, S.P., et al., *Optimized growth conditions for tissue engineering of human cardiovascular structures.* International Journal of Artificial Organs, 2000. **23**(12): p. 817-823.

170. Dumont, K., et al., *Design of a new pulsatile bioreactor for tissue engineered aortic heart valve formation.* Artificial Organs, 2002. **26**(8): p. 710-714.

171. Hildebrand, D.K., et al., *Design and hydrodynamic evaluation of a novel pulsatile bioreactor for biologically active heart valves.* Annals of Biomedical Engineering, 2004. **32**(8): p. 1039-1049.

172. Mol, A., et al., *Tissue engineering of human heart valve leaflets: A novel bioreactor for a strain-based conditioning approach.* Annals of Biomedical Engineering, 2005. **33**(12): p. 1778-1788.

173. Schmidt, D., U.A. Stock, and S.P. Hoerstrup, *Tissue engineering of heart valves using decellularized xenogeneic or polymeric starter matrices.* Philosophical Transactions of the Royal Society B-Biological Sciences, 2007. **362**(1484): p. 1505-1512.

174. Robinson, P.S., et al., *Functional tissue-engineered valves from cell-remodeled fibrin with commissural alignment of cell-produced collagen.* Tissue Engineering Part A, 2008. **14**(1): p. 83-95.

175. L'Heureux, N., et al., *Technology Insight: the evolution of tissue-engineered vascular grafts - from research to clinical practice.* Nature Clinical Practice Cardiovascular Medicine, 2007. **4**(7): p. 389-395.

176.	Syedain, Z.H., J.S. Weinberg, and R.T. Tranquillo, *Cyclic distension of fibrin-based tissue constructs: Evidence of adaptation during growth of engineered connective tissue.* Proceedings of the National Academy of Sciences of the United States of America, 2008. **105**(18): p. 6537-6542.

177.	Syedain, Z.a.T., Robert Tranquillo, *Controlled cyclic stretch bioreactor for tissue-engineered heart valves.* Biomaterials, 2009. **xxx**: p. 1-7.

CHAPTER 3

PROJECT RATIONALE

3.1   <u>Hypothesis</u>

Replacement or regeneration of heart valves, exquisite examples of hemodynamics, durability, design and adaptability has challenged engineers and surgeons for the last 40 years. Since about 300,000 diseased valves are replaced each year worldwide, this study is highly relevant to public health. Aortic heart valves are composed of three distinct layers: *fibrosa*, *ventricularis* and *spongiosa*. These layers are populated by interstitial cells which actively degrade and remodel the extracellular matrix to withstand billions of bending cycles without significant wear and tear. Tissue engineering, the emerging science of combining scaffolds, cells and specific mechanical and biochemical signals is feasible and holds great promise for treatment of heart valve disease [1]. Typical approaches include use of biodegradable polymers or decellularized porcine valves as scaffolds for in vitro cell seeding or in vivo cell infiltration and remodeling. Valves made by these procedures are either not strong enough to withstand aortic pressures or cannot be fully repopulated by cells. Recognizing the vital importance of the three leaflet layers [2], the outstanding hemodynamics of natural valve homografts [3] and the need for reconstruction of the physiologic valve design, **we hypothesized** that combination of four elements can be utilized for tissue engineering of the "ideal" aortic heart valve: A) Constructs made from partially stabilized collagenous scaffolds, B) Anatomically analogous 3-D heart valve shapes made from tri-layered structures that

mimic the native heart valve histo-architecture, C) Autologous multipotent mesenchymal stem cells for repopulation and remodeling and D) Mechanical cues to induce stem cell differentiation into valvular cells capable of maintaining matrix homeostasis.

3.2   Specific Aims

Aim 1: Preparation of engineered heart valve scaffolds

Hypothesis: Functional heart valves can be created from layering of stabilized collagen scaffolds.

Approach: Collagen layers to be used as *fibrosa* and *ventricularis* layers were prepared from decellularized pericardium and lightly cross-linked with penta-galloyl-glucose, a collagen binding polyphenolic tannin, to allow for delayed biodegradation. For the *spongiosa* layer, highly porous collagen scaffolds were prepared from decellularized, elastase-treated arteries and enriched with valve-specific glycosaminoglycans. **Innovative features** include unique engineering of tri-layered valvular structures from partially stabilized collagen scaffolds specifically designed to replace *fibrosa*, *spongiosa* and *ventricularis*.

Aim 2: Adhering the three scaffolds used to form engineered heart valves

Hypothesis: Functional heart valves can be created from layering of stabilized collagen scaffolds and adhered together using a biological glue.

Approach: To assemble the 3D heart valve structures from layers of collagen scaffolds, we developed and implemented use of biological adhesives in tissue engineering. After comparing several adhesives including cyanoacrylate, albumin, gelatin and fibrin-based glues, we chose to implement a modified albumin/glutaraldehyde adhesive for the construction of living heart valves and tested for mechanical properties and biocompatibility.

Innovative features include unique use of a biological glue to assemble the tri-layered constructs, which has never been described before.

Aim 3: Molding, assembly, and bioreactor testing of tri-layered scaffolds used for heart valve tissue engineering

Hypothesis: Tissue engineered scaffolds that more closely mimic the 3D ultra-structure and histo-architecture of a native aortic heart valve will functionally perform similar to a natural valve.

Approach: Being aware of the vital importance of these layers, we assembled fibrous and spongy scaffolds in a three-layered structure based on anatomically accurate molds of aortic valves, in which the *spongiosa* layer is inserted between two purely collagen fibrous collagenous layer (*fibrosa* and *ventricularis*). Both gluing and layering techniques were used to create a fully-functional tri-layered construct. Layered collagenous constructs were tested for functionality in a custom-made bioreactor.

Innovative features include unique use of molds to form the accurate shape and corrugations of each leaflet and the assembly of different scaffolds into a tri-layered construct.

Aim 4: Differentiation of stem cells in tissue engineered heart valves into valvular interstitial-like cells

Hypothesis: Stem cells exposed to 3D mechanical stimuli should share many similarities to natural valvular interstitial cells. These studies should indicate that physiologic mechanical stimuli offered by our 3D tissue engineered heart valve constructs and the heart bioreactor encouraged differentiation of stem cells into activated valvular interstitial cells, a much sought-after outcome of cardiovascular tissue engineering. We hypothesize that conditioning of stem cell-seeded engineered aortic heart valves in a bioreactor will induce cell differentiation.

Approach: To prove that relevant mechanical can help maturation of tissue engineered valves, we subjected stem cell-seeded constructs to in vitro cycling in a bioreactor that is similar to the intra-cardiac environment. We then evaluated cell differentiation.

Innovative features include the fact that remodeling behavior of stem cells seeded within tri-layered tissue engineered heart valves has not been studied before.

4.3   Clinical Significance and Translational Scenario

Cardiovascular malformations are the most common congenital abnormality, affecting 4 to 6 in 1000 births, with valve defects accounting for up to 30% of these deficiencies [4, 5]. It is projected that by 2020 at least 1.4 million children will be affected [6]. A major problem associated with available valve replacements is that no existing replacements grow with the patient, which could mean a pediatric patient could need 2-4 valve replacements before 18 years old. Each of these surgeries is associated with a high operative mortality rate (10-36%) [7]. Furthermore, each operation on average could cost of a at least $54,000 (US average) [8], placing a large financial burden not only on the families of those affected but the entire health care industry in general. Therefore, tissue engineered heart valve replacements hold promise to solve this problem by creating a living heart valve that can grow with the patient.

Our vision of a potential translational scenario using stabilized collagen scaffolds and autologous stem cells involves the following steps. After initial diagnosis and collection of mesenchymal stem cells from the patient, imaging of the diseased heart valve would provide anatomical coordinates for reconstruction of the heart valve geometry into solid molds using appropriate software and hardware. Minimizing size mismatch in implanted heart valve devices is an important aspect of heart valve surgery [1]. Concomitant with stem cell isolation, valves will be made from decellularized collagen scaffolds by assembly into tri-layered constructs and then cusps seeded with autologous stem cells as described in current study. After conditioning in bioreactors for

1-2 weeks for stem cell pre-differentiation into VIC-like cells, the patient-tailored engineered heart valve would be surgically implanted back into the patient.
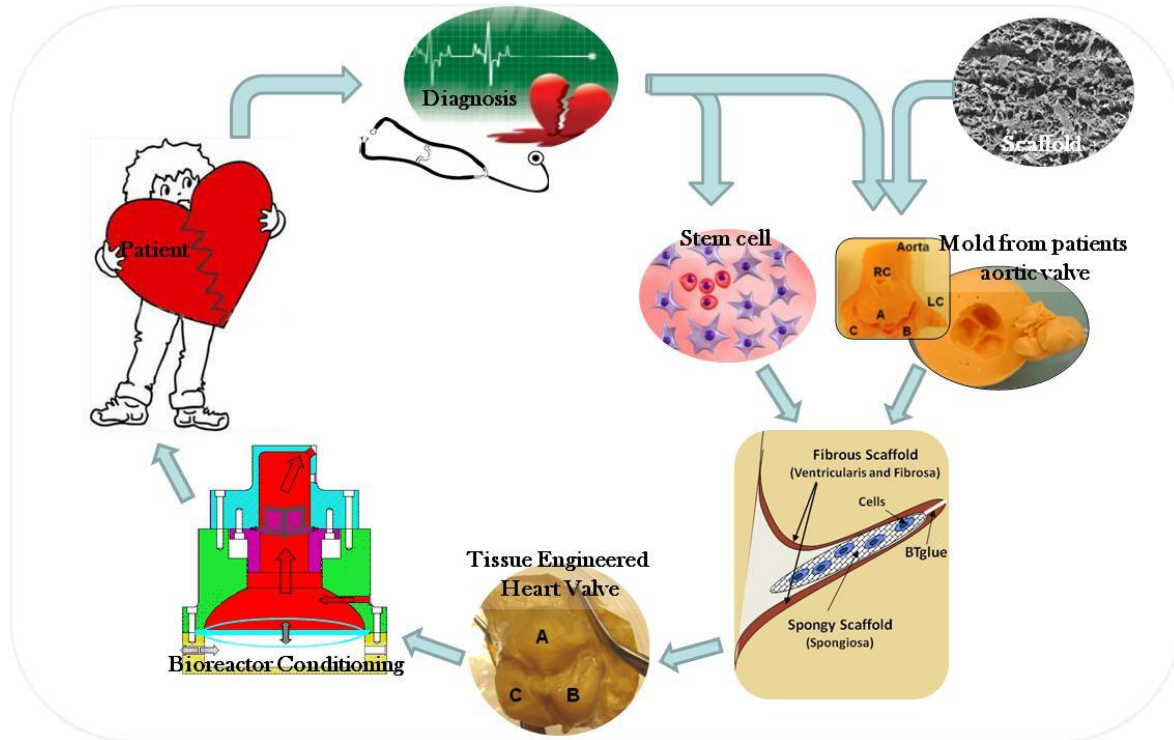
Figure 3.1: Translational scenario for tissue engineered heart valve.

References

1.   Yacoub, M., *Viewpoint: Heart valve engineering. Interview by James Butcher.* Circulation, 2007. **116**(8): p. f44-6.

2.   Schoen, F.J., *Cardiac valves and valvular pathology: update on function, disease, repair, and replacement.* Cardiovasc Pathol, 2005. **14**(4): p. 189-94.

3.   Sodian, R., et al., *Application of stereolithography for scaffold fabrication for tissue engineered heart valves.* Asaio J, 2002. **48**(1): p. 12-6.

4.   Loffredo, C.A., *Epidemiology of cardiovascular malformations: Prevalence and risk factors.* American Journal of Medical Genetics, 2000. **97**(4): p. 319-325.

5.   Wollins, D.S., et al., *A population-based study of coarctation of the aorta: Comparisons of infants with and without associated ventricular septal defect.* Teratology, 2001. **64**(5): p. 229-236.

6.   [June 4, 2010]; Available from: http://emedicine.medscape.com/article/893646-overview.

7.   Irving, C., et al., *Outcomes following infant listing for cardiac transplantation: the impact of strategies introduced to counteract limited donor availability.* Archives of Disease in Childhood.

8.   [June 2, 2010]; Available from: http://www.medpathgroup.com/coronary_artery_bypass_surgery.php.

CHAPTER 4

SCAFFOLD PREPARATION AND CHARACTERIZATION
(AIM 1)

4.1   Introduction

Strategies for heart valve tissue engineering fall into two main categories [3]: a) preparation of decellularized heart valves by enzyme/detergent methods followed by repopulation with appropriate cell types *in vitro* before implantation or relying on host cells to repopulate and remodel the scaffolds in vivo. This approach has limitations, as complete valve decellularization was proven difficult to attain and cell repopulation is difficult due to lack of adequate porosity. A second approach is assembly of synthetic biodegradable matrices populated by cells and bioreactor conditioning to express adequate properties before implantation. While this approach seems appealing, the polymeric matrices lack sufficient mechanical strength and have not withstood the test of time under arterial pressure [3].

Therefore, a biologically-based scaffold may hold promise. Pericardium has been widely researched as a biomaterial, including examination of its mechanical and fiber orientation properties by mapping techniques [4], isolation of pericardial fibroblasts and analysis of their biosynthetic abilities [5,6] and detailed analysis of its collagen and proteoglycan components [5,6]. Glutaraldehyde (Glut) fixed bovine pericardium has a long history of being used in manufacturing of bioprosthetic heart valves, a good record of implantation in humans, is well characterized mechanically and biologically [1-4], has been used in development of collapsible percutaneous heart valves [10] and for mitral

valve repair [11]. Only recently has decellularized pericardium attracted attention as a scaffold for tissue engineering [9,12].

Our working premise was that the ideal scaffolds for heart valve applications should be porous, strong, biocompatible, and conducive to cell repopulation and remodeling, while maintaining mechanical functions. Our novel strategy relies on use of stabilized collagen scaffolds that mimic the natural valve fibrous layers, based on decellularized porcine pericardium [5] and delicate, highly hydrated porous collagen scaffolds to be used as the middle *spongiosa* layer. **We hypothesized** that partially cross-linked collagen scaffolds would fulfill these requirements. To test this hypothesis, collagen scaffolds were cross-linked with either ultraviolet (UV) light or penta-galloyl glucose (PGG) and then tested for biodegradation, mechanical properties and in vivo biocompatibility and remodeling. Their properties were compared to Glut-treated scaffolds**. In the current study we demonstrate that PGG partially cross-links collagen and preserves the excellent mechanical properties of pericardium.** PGG-treated collagen scaffolds do not calcify in vivo and support progressive host cell infiltration and matrix remodeling, indicating that among the treatments tested, PGG is a most promising collagen stabilization process for heart valve tissue engineering.

4.2 Materials and Methods

4.2.1 Materials

High purity 1,2,3,4,6-Penta-*O*-galloyl-beta-D-glucose (penta-galloyl-glucose, PGG) was a generous gift from N.V. Ajinomoto OmniChem S.A., Wetteren, Belgium

(www.omnichem.be). Pure DNA, ribonuclease, glutaraldehyde (50% stock), and collagenase Type VII from *Clostridium histolyticum*, were purchased from Sigma-Aldrich Corporation (St. Louis, MO). Deoxyribonuclease I was from Worthington Biochemical Corporation (Lakewood, NJ) and Bicinchoninic acid protein assay kits from Pierce Biotech (Rockford, IL). Electrophoresis apparatus, chemicals and molecular weight standards were from Bio-Rad, Hercules, CA and elastase was from Elastin Products Company, Owensville, MO. All other chemicals were of highest purity available and typically obtained from Sigma Aldrich, St. Louis, MO.

4.2.2 Methods

4.2.2.1 *Spongy Scaffold Preparation*

For preparation of *spongiosa* scaffolds, porcine pulmonary arteries obtained from Animal Technologies Inc. (Tyler, TX) were decellularized. In the first step, tissues were stored in double distilled water overnight at 4^oC to induce hypotonic shock and cell lysis. After rinsing, tissues were treated with 0.25% Na-Deoxycholate, 0.15% Triton X-100, 0.1% EDTA, 0.02 % NaN_3, in 50 mM Tris-HCl buffer (pH 7.8) with mild agitation for six days at 22ºC, and changes of the solution after three days. After rinsing with double-distilled water and 70% ethanol to remove detergents, tissues were treated with a deoxyribonuclease / ribonuclease mixture (360 milliunits/ml for each enzyme) at 37ºC for 24 hours to fully digest away nucleic acids. This was followed by rinsing twice with double distilled water and incubation in ultra pure elastase (10 Units/ml) in 50 mM Tris buffer, 1 mM $CaCl_2$, 0.02% NaN_3 (pH=8), at 37^oC for six days with mild agitation.

Elastase was replaced with fresh solution after three days. Tissues were rinsed in double distilled water at 22ºC until Bicinchoninic acid protein assay revealed undetectable levels of soluble proteins. Scaffolds were finally rinsed with 70% ethanol and then stored in sterile saline supplemented with 0.02% NaN_3 at 4^oC.

4.2.2.2 *Spongy Scaffold characterization*

For histology, paraffin-embedded samples were stained with Hematoxylin and Eosin (H&E) and Masson's trichrome (n=6 slides per group per stain). To detect Galα we performed lectin histochemistry using biotinylated *Griffonia simplicifolia* lectin as the primary reactant, followed by ABC-peroxidase complex and DAB detection with Hematoxylin counterstaining [6]. Scanning electron microscopy (SEM) sample preparation was performed according to standard procedures [7] and imaged on a Hitachi S4800. To test for cytocompatibility, rat dermal fibroblasts were seeded (10^5 cells per cm^2) onto sterile scaffolds and cell viability and proliferation evaluated weekly for up to 5 weeks using LIVE/DEAD® stain (Molecular Probes, Carlsbad, CA) and CellTiter 96® AQueous One Solution Cell Proliferation Assay MTS (Promega, Madison, Wisconsin) as per manufacturers' directions. Samples were also stained with 4-6 Diamidino-2-phenylindole (DAPI) blue fluorescent nuclear stain.

Total genomic DNA was extracted and purified from scaffolds and from fresh arteries as controls (n = 3 per group), using a Fibrous Tissue DNeasy Kit (Qiagen, Valencia, CA), subjected to agarose/ethidium bromide gel electrophoresis followed by densitometry using Gel-Pro Analysis Software (MediaCybernetics, Silver Spring, MD).

Water content was calculated gravimetrically from weights obtained before and after freeze-drying of fresh artery and scaffold samples (n = 6 per group). Glycosaminoglycan (GAG) content was analyzed by full digestion of fresh tissue and scaffolds with protease K followed by reaction of released GAGs with 1,9-dimethylmethylene blue dye and colorimetry [8, 9].

4.2.2.3 *Fibrous Scaffold preparation*

Fresh adult swine pericardial sacs obtained from Animal Technologies Inc. (Tyler, TX) were cleaned, rinsed in sterile saline, cut into strips, and then decellularized as follows. In the first step, tissues were stored in double distilled water overnight at 4°C to induce hypotonic shock and cell lysis. After rinsing, tissues were treated with 0.25% Na-Deoxycholate, 0.15% Triton X-100, 0.1% EDTA, 0.02 % NaN_3, in 50 mM Tris-HCl buffer (pH 7.8) with mild agitation for six days at 22ºC, and changes of the solution after three days. After rinsing with double-distilled water and 70% ethanol to remove detergents, tissues were treated with a deoxyribonuclease / ribonuclease mixture (360 milliunits/ml for each enzyme) at 37ºC for 24 hours to fully digest away nucleic acids. This was followed by rinsing twice with double distilled water and incubation in ultra pure elastase (10 Units/ml) in 50 mM Tris buffer, 1 mM $CaCl_2$, 0.02% NaN_3 (pH=8), at 37°C for six days with mild agitation. Elastase was replaced with fresh solution after three days. Tissues were rinsed in double distilled water at 22ºC until Bicinchoninic acid protein assay revealed undetectable levels of soluble proteins. Scaffolds were finally

rinsed with 70% ethanol and then stored in sterile saline supplemented with 0.02% NaN_3 at 4^oC.

4.2.2.4 *Fibrous Scaffold characterization*

For histological evaluation, paraffin-embedded samples were stained with Hematoxylin and Eosin for general morphology and confirmation of cell removal and with Verhoeff van Gieson to confirm removal of elastin (n=6 slides per group per stain). Digital pictures were taken of Hematoxylin and Eosin stained samples (n=2 slides per group) at 400X magnification and open spaces (pores) between intact collagen fibers were measured using AxioVision Release 4.6.3 digital imaging software (Carl Zeiss MicroImaging, Inc. Thornwood, NY). To further validate decellularization, total genomic DNA was extracted and purified from collagen scaffolds and from fresh pericardium as controls (n=3 per group), using a Fibrous Tissue DNeasy Kit (Qiagen, Valencia, CA) following manufacturers' instructions. DNA samples were subjected to agarose electrophoresis alongside pure DNA standards (10-100 ug/ml) followed by densitometry using Gel-Pro Analysis Software (MediaCybernetics, Silver Spring, MD). DNA levels were calculated from the standard curve and normalized to initial tissue wet weight. To detect Galα we performed lectin histochemistry using biotinylated *Griffonia simplicifolia* lectin as the primary reactant, followed by ABC-peroxidase complex and DAB detection with Hematoxylin counterstaining [6].

To test for presence of soluble proteins, scaffolds and fresh pericardial samples (n=2 per group) were pulverized in liquid N_2, proteins extracted in an extraction buffer

(50 mM Tris-HCl, 150 mM NaCl, 1 mM EDTA, 1% Triton X-100, 1% Sodium Deoxycholate, 0.1% SDS, pH 7.4, with protease inhibitor cocktail) and protein content determined using BCA assay. Samples normalized to initial dry weight were analyzed for detergent-soluble proteins by sodium dodecyl sulfate polyacrylamide gel electrophoresis followed by silver staining (SilverSnap, Pierce Biotech, Rockford, IL). For detection of matrix metalloproteinase 2 (MMP-2) same protein extracts were analyzed by an MMP-2 ELISA kit (Amersham Biosciences, Piscataway, NJ) and results normalized to mg soluble protein.

Chemotaxis assays were conducted using a Boyden chamber (NeuroProbe, Gaithersburg, MD) and a polycarbonate filter with 8 μm diameter pores, as per manufacturers' instructions. Soluble collagen peptides (matrikines) were prepared by treatment of decellularized porcine pericardium with collagenase (10 U/ml) for 24 hours. The supernatant was filtered through Microcon YM-3 centrifugal devices and peptides smaller than 3 kDa were collected in the flow-through for chemotaxis assays. Rat aortic fibroblasts (10x105/well, prepared in house by an explant technique) suspended in DMEM/0.1% bovine serum albumin were used in these tests; undiluted Fetal Bovine Serum (100%) was used as a positive control and DMEM/0.1% bovine serum albumin as the negative control. Cells migrated for 4 hours at 37ºC and 5% CO_2. After incubation, the non migrated cells were removed with a wiper blade and the filter fixed and stained using a DiffQuick® kit (Dade Behring Inc, Newark, DE) dried, and screened for migrated cells using an inverted microscope. Results were reported as negative (0-2 cells per 10x field), slightly positive (2-10 cells), or positive (> 10 cells).

4.2.2.5 *Evaluation of PGG cross-linking and stability*

To evaluate the cross-linking efficiency of PGG, fibrous scaffolds were treated with different concentrations of PGG (0%, 0.1%, 0.15%, and 0.3%) and leaching of PGG was tested. Briefly, ½" diameter circles of decellularized pericardium were cut using a core borer. The circles were then placed in PBS. For a long wash procedure, the circles were next placed in corresponding PGG concentrations for fixation (for 24 hrs.). The circles were then removed from PGG after 24 hrs., and placed in sterile PBS w/ 0.02% azide (making sure to keep groups separated) and shaken on an oscillating shaker at room temp. The wash was removed and replaced with new PBS every day for 5 days. At the end of the long wash procedure, circles designated for a short wash were placed in corresponding concentrations of PGG (as for long wash). All circles were then washed 2X in sterile PBS by gentle inversion, then place circles in 70% ethanol for 10 mins. in sterile 50 ml conical tube.. The circles were then washed 2x in sterile PBS by gentle inversion in sterile 50 ml conical tube. The circles, keeping differing concentrations of PGG-fixed circles separated, were placed in 50/50 FBS/DMEM (in sterile 50 ml conical tubes) for 24 hrs in an incubator at 37°. The disks were then removed from 50/50 tubes and placed in new tubes with glycine for ~2hrs. The disks were then removed from glycine and each disk placed in a well of a 12-well plate (NOT tissue culture treated). Approximately 50,000 rat aortic fibroblasts were placed directly to top of each circle. The plate was placed in an incubator @ 37° for 2 hrs. Live/Dead and MTS assays were then preformed on the samples.

Next, fibrous scaffolds were treated with different concentrations of PGG (0%, 0.0375%, 0.075%, 0.10%, and 0.15%, n=6 per concentration) and exposed to collagenase to test degradation properties. The long wash procedure was followed as above. At the end of the washes, the circles were then placed in collagenase (as described in section 4.2.3.5) for 7 days.

4.2.2.6 *Properties of cross-linked fibrous collagen scaffolds*

Scaffolds were prepared as above and treated with one of three methods: (a) Glutaraldehyde (Glut), (b) Penta-galloyl-glucose (PGG), and (c) Ultraviolet light (UV) ,. For UV treatment, scaffold samples were first dried flat in sterile conditions (2 days in a cell culture hood at 22ºC), then UV-treated in a Spectrolinker XL-1000 UV cross linker (Spectronics Corporation, Westbury, NY) at optimal density (1200 x 100 µJ/cm2) for 30 minutes. Samples were stored dry at 4oC until use. For Glut fixation, wet scaffold samples were incubated in 0.6% glutaraldehyde in 50 mM 4-(2-hydroxyethyl)-1-piperazineethanesulfonic acid (HEPES) buffered saline (pH=7.4) overnight at 22ºC and subsequently rinsed and stored in sterile saline. For PGG fixation, the scaffolds were incubated with 0.15% PGG in 50 mM phosphate buffer (pH 5.5) containing 4% isopropanol, for 24 hours at 22oC, rinsed and stored in sterile saline.

To evaluate cross-linking efficacy, scaffold samples were tested for resistance to collagenase. Treated and untreated samples (n=18 per group) of about 15 x 5 mm were rinsed 3 times in ddH20 at 22ºC and lyophilized to record dry weight. Each sample was then incubated separately with 1 ml of collagenase (6.25 units/ml) dissolved in 100 mM

Tris buffer, 1 mM CaCl2, 0.02% NaN3 (pH=7.8) for 1, 2, and 7 days at 37ºC with mild agitation. At each time point, 6 samples from each group were rinsed 4 times with ddH20 by centrifugation (12,000 rpm, 1.5 minutes, 18ºC) after which the samples were lyophilized to obtain dry weights after collagenase, and percent of digested tissue was calculated.

Three specimens from each group of (1) control (no fixation), (2) Glut, (3) PGG-treated scaffolds, and (4) UV were also subjected to thermal denaturation temperature (Td) analysis by Differential Scanning Calorimetry (DSC-131, Setaram Instrumentation, Caluire, France). Specimens were tested at a heating rate of $10˚C/min$ from $20˚C$ to $110˚C$ in a N2 gas environment. Td, a well known indicator of collagen cross-linking was defined as the temperature at the endothermic peak [13].

4.2.2.7 In vivo *evaluation of fibrous scaffolds*

Male, juvenile Sprague-Dawley rats (weighing around 50 grams, from Harlan Laboratories; Indianapolis, IN) were sedated with acepromazine (0.5 mg/kg, Ayerst Laboratories, Rouse Point, NJ) and maintained on 2% isoflurane during surgery. A small transverse incision was made on the backs of the rats and two subdermal pouches (one superior and one inferior to the incision) were created. Samples were prepared for implantation by overnight soaking in sterile saline. Controls (no cross-linking), Glut-treated, PGG-treated, and UV-treated scaffold samples (as prepared above) were implanted into the subdermal pouches (n=8 implants per group per time point) and incisions closed with surgical staples. After surgery the rats were allowed to recover and

permitted free access to water and food. The animal protocol was approved by the Animal Research Committee at Clemson University and NIH guidelines for the care and use of laboratory animals (NIH publication #86-23 Rev. 1996) were observed throughout the experiment.

The rats were humanely euthanized by CO2 asphyxiation at 1, 3, and 6 weeks after surgery and samples retrieved for analysis. A small section of each explant with its associated capsule was maintained for histological evaluation. The remainder of explants were cleaned free of capsule rinsed in saline and then divided for DNA, calcium and matrix metalloproteinase (MMP) analysis.

For histology samples were placed in formalin and paraffin sections (5 µm) were stained with Hematoxylin and Eosin \ for general morphology. For identification of infiltrating cell types, samples tagged for immunohistochemistry were placed in formalin [17,18] and paraffin-embedded. Sections (5 µm) were exposed to 0.1% Proteinase K solution (25 units/500 ml, from Qiagen DNeasy Tissue Kit) in Tris Buffer Saline (TBS), pH=7.5 at 22ºC for 30 seconds. Endogenous peroxidases were blocked with 0.3% H2O2 in 0.3% normal sera (Vectastain Elite ABC kit for rabbit IgG, Burlingame, CA). Sections were immunostained using mouse anti-rat monoclonal antibodies to macrophages (1:200 dilution, Chemicon, Temecula, CA), vimentin (1:500 dilution, Sigma, St. Louis, MO) and Prolyl-4-hydroxylase (1:200 dilution, Chemicon, Temecula, CA) at 22ºC for 1 hour. To minimize cross reactivity, rat-absorbed biotinylated anti-mouse IgG was used in place of biotinylated secondary antibody provided with the staining kit. Negative staining controls were performed with the omission of the primary antibody. Diaminobenzidine

tetrahydrochloride peroxidase substrate kit was used to visualize the specific staining (Vector Laboratories, Burlingame, CA) and sections were lightly counter-stained with Hematoxylin. As positive controls we stained paraffin sections from rat spleen (macrophage control) and rat skin (fibroblast control) in parallel with the explant sections.

To visualize phenol groups within PGG-treated samples we used an iron-based histology stain [19] [10][10][9][12][12]. Briefly, tissues were stained en-bloc with FeCl3, embedded in Tissue Tek OCT compound (Sakura Finetek, USA Inc., Torrance, CA) and six micrometer thick sections counterstained with Light green. PGG appears brown with this staining.

For DNA analysis explants (n=3 per group per time point) were weighed and then subjected to DNA extraction and purification using the Qiagen Kit and DNA content evaluated by agarose gel electrophoresis followed by densitometry as described above. Explanted samples (n=4 per group per time point) were rinsed in saline, lyophilized to obtain dry weight and individually hydrolyzed in 6N HCl, dried under nitrogen, and reconstituted in 1.0 ml of 0.01 N HCl. Calcium content was then measured using atomic absorption spectrophotometry as described before [20,21].

For matrix metalloproteinase detection, proteins were extracted in 50 mM Tris, 1% Triton X-100, 0.1% SDS, 1% Deoxycholate, 150 mM NaCl, with protease inhibitor mixture, pH=7.4 buffer and protein content determined using the Bicinchoninic acid assay as described before [19]. Samples were subjected to gelatin zymography using 6 μg of protein per lane alongside molecular weight standards [22]. Intensity of MMP bands

(white bands on dark background) were evaluated by densitometry using Gel-Pro Analysis Software (MediaCybernetics, Silver Spring, MD) and expressed as relative density units (RDU) normalized to protein content.

Glycosaminoglycan content in explanted tissues was determined by a dimethylmethylene blue assay as described before [13]. Briefly, a sample of extracted protein (described above for MMP assay) was digested with papain and released glycosaminoglycans were incubated with dimethylmethylene blue reagent and OD read at 525nm. Glycosaminoglycan content was calculated from a standard curve of pure chondroitin sulfate (0-25 ug/ml) and values expressed as µg/mg protein.

Statistics

Results are represented as means ± the standard error of the mean (SEM). Statistical analysis was performed with one way Analysis Of Variances (ANOVA) and results were considered significantly different at $p < 0.05$.

4.3   Results

4.3.1   Scaffold Characterization

4.3.1.1 *Spongy Scaffold characterization*

Highly hydrated, collagen scaffolds to be used as valvular *spongiosa* were prepared from porcine pulmonary aorta by decellularization and removal of elastin. Histology showed complete cell and elastin removal from the pulmonary aorta (**Figure**

4.1), leaving behind a porous collagen scaffold with pore sizes ranging between 20 and 100 microns.
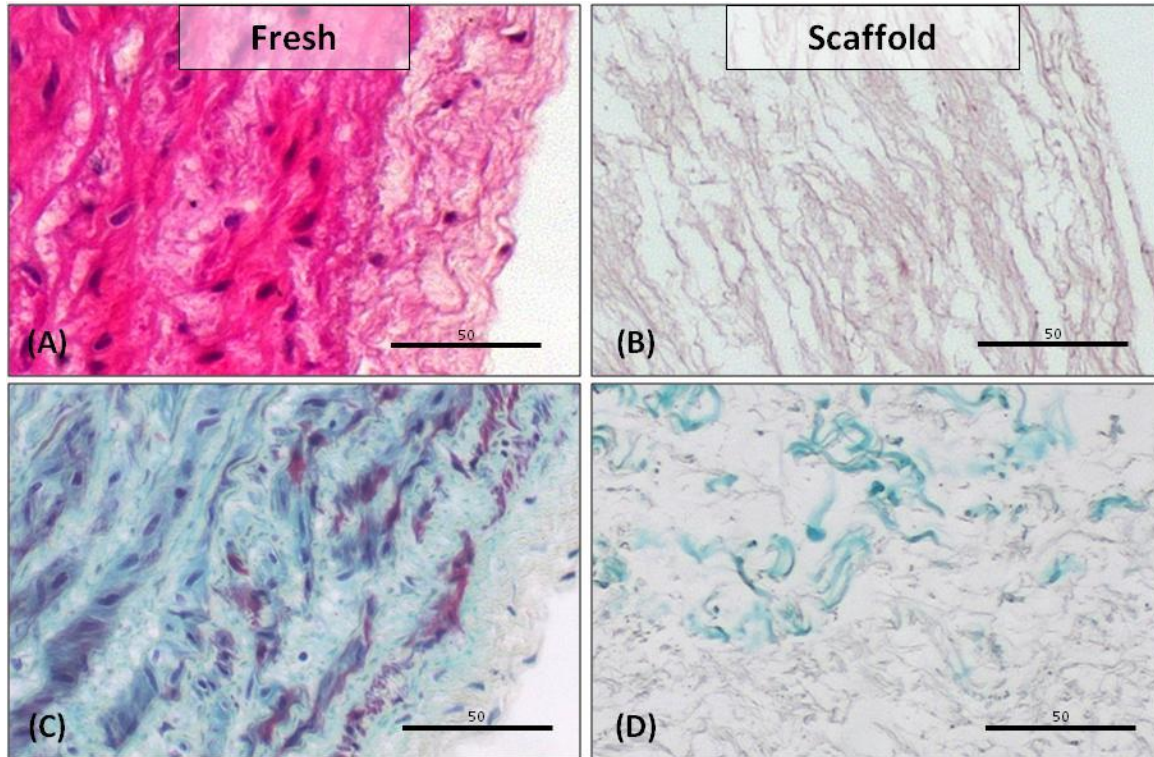

Figure 4.1: Histology of spongy collagen scaffolds. (A, C) fresh porcine pulmonary artery and (B, D) decellularized pulmonary artery scaffolds were stained with H&E stain (A, B), Trichrome stain (C, D, collagen blue, cells dark pink).

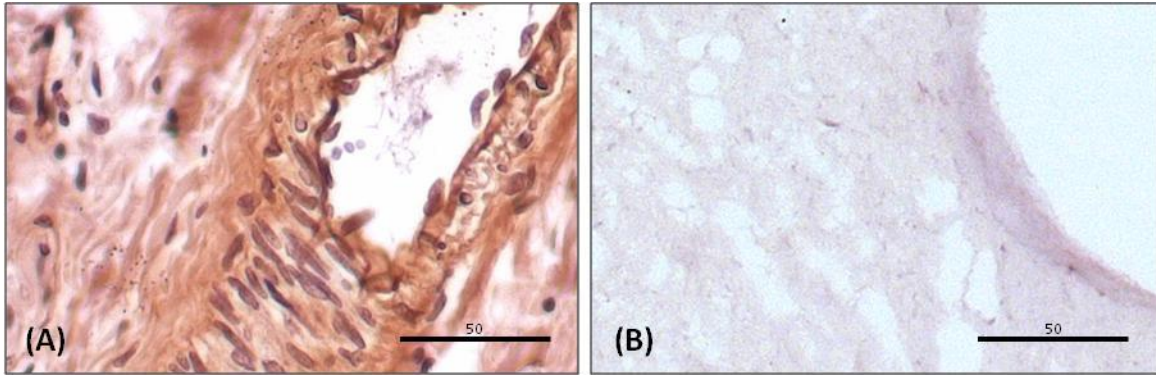Histochemical staining showed the *spongiosa* scaffold lacked Galα antigen.

Figure 4.2: Histology of spongy collagen scaffolds. (A) fresh porcine pulmonary artery and (B) decellularized pulmonary artery scaffolds stained with *GS* lectin for Galα antigen (A & B, dark brown = positive staining). Bars are 50 μm.

Analysis of *spongiosa* scaffold by contrast phase microscopy and SEM revealed a 3-D matrix composed of insoluble collagen fibrils of 1-2 microns in diameter assembled into larger fibers and wavy bundles.
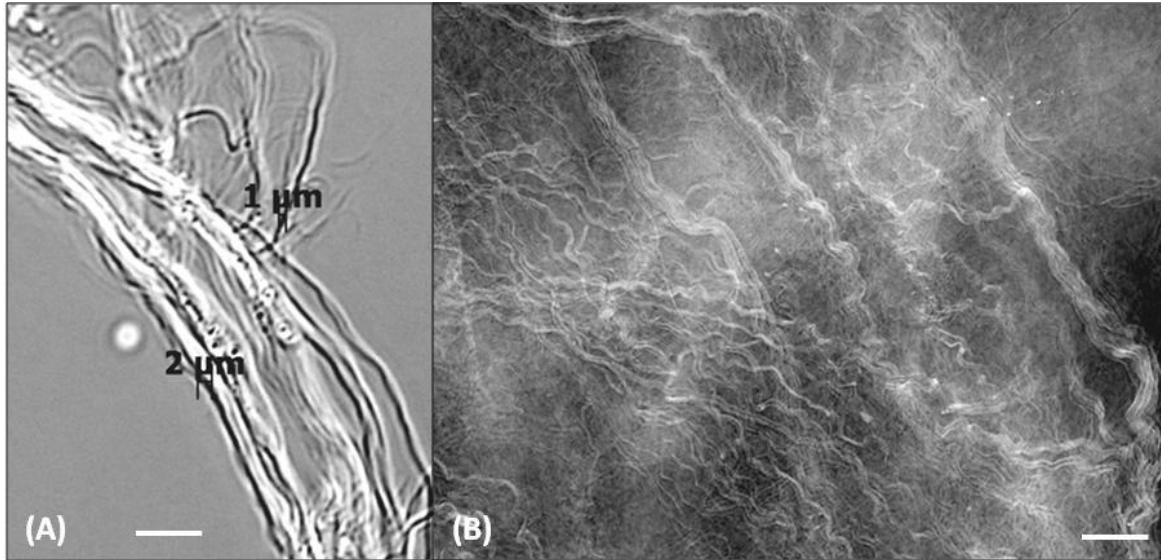
Figure 4.3: Properties of *spongiosa* scaffolds. (A,B) Phase contrast micrographs of fresh scaffolds. Bars are 100 μm
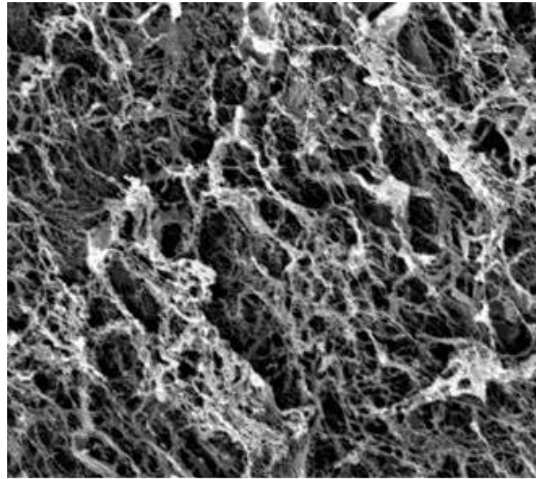
Figure 4.4: Properties of *spongiosa* scaffolds. (A) SEM image of scaffold surface.

The spongy scaffold was fully degradable by collagenase *in vitro* (not shown) and supported fibroblast growth and proliferation for up to 5 weeks (**Figure 4.5**).

Figure 4.5: Properties of *spongiosa* scaffolds. (A, B) Cytocompatibility testing with fibroblasts stained with Live/Dead stains (live cells green, dead cells red) and DAPI nuclear stain (light blue), respectively. Bars are 100 μm.

Semi quantitative DNA analysis revealed almost complete cell removal. Specifically, levels of high molecular weight genomic DNA were significantly reduced and there was no sign of morphologically identifiable cells by histology, thus we considered the scaffolds acellular. As can be seen on the agarose gels (**Figure 4.6**), m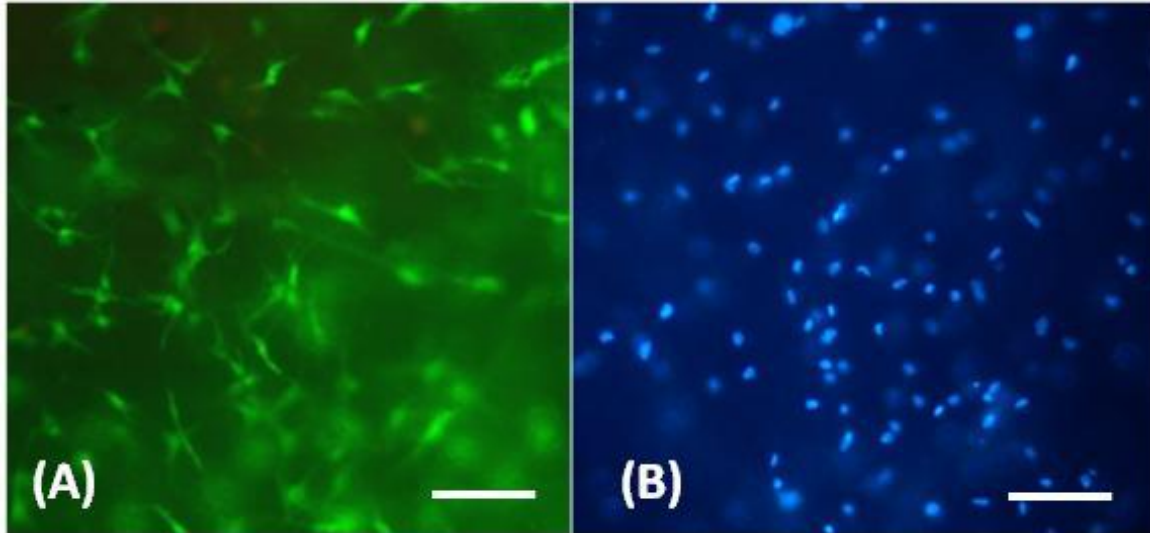inute amounts of low molecular weight DNA fragments may have been trapped in the scaffolds but we did not consider this a sign of cell presence.

Macroscopically, *spongiosa* collagen scaffolds appeared as white, highly hydrated matrices which, when compared to the native tissue, occupied almost 4 times larger volumes than the original artery while maintaining the original shape and more than 90% water (**Figure 4.7**).
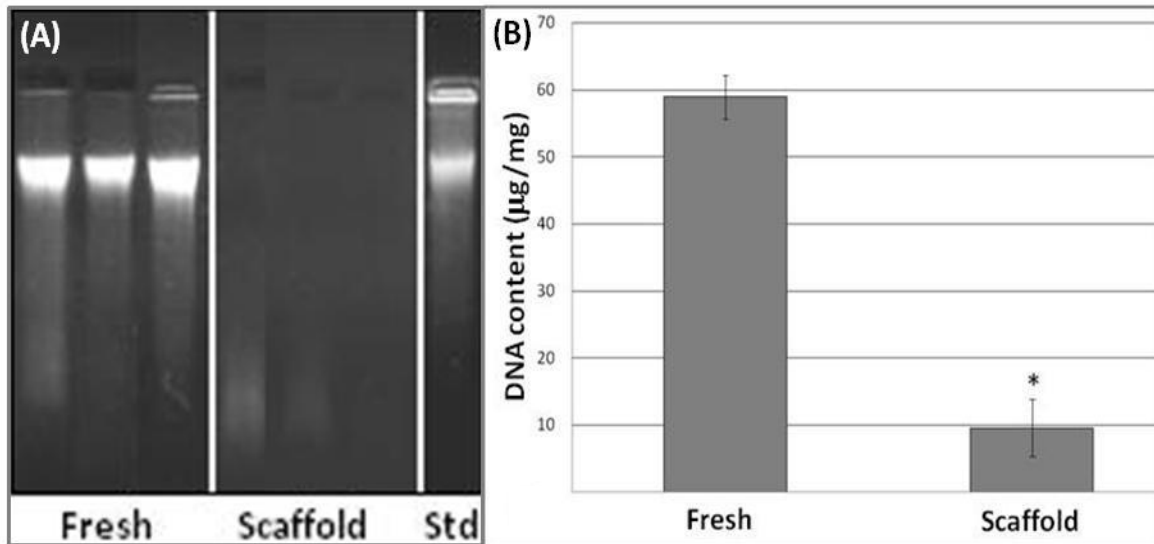

Figure 4.6: Properties of *spongiosa* scaffolds. (A) Shows agarose/Ethidium bromide electrophoresis, of extracted DNA, alongside pure DNA standard while (B) quantifies DNA content of fresh and decellularized scaffolds
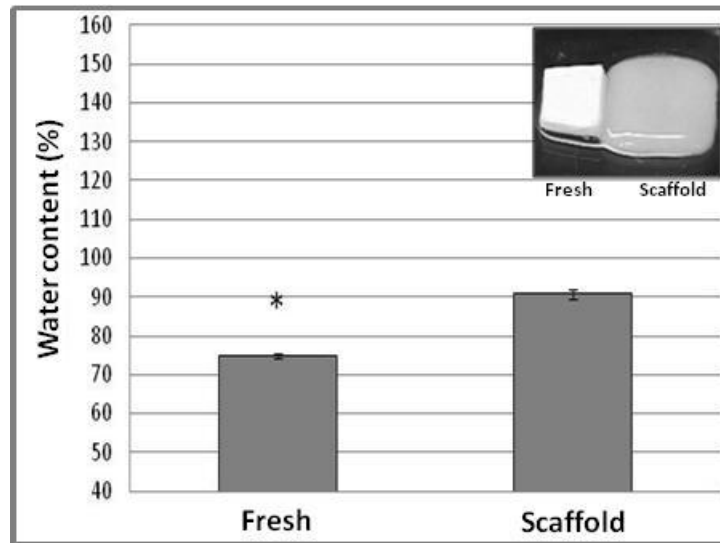
Figure 4.7: Properties of *spongiosa* scaffolds. Water content of fresh and decellularized scaffolds; insert shows macroscopic aspects of 10 x 10 mm arterial tissue samples before (left) and after (right) decellularization/elastase treatment.

Glycosaminoglycans (GAGs) were also analyzed in tissues and scaffolds. As compared to fresh pulmonary artery (14.6 ug GAGs/mg dry), the *spongiosa* layer contained about 8.5 ug GAGs/mg dry, which is about 3 times lower than values reported in the literature for the whole aortic cusp (25 ug GAGs/mg dry). To date we have no knowledge of precise GAG content of the *spongiosa* layer alone in native aortic heart valves.

4.3.1.2 *Fibrous Scaffold Characterization*

Our technique for decellularizing porcine pericardium involved hypotonic shock, detergent extractions, nuclease digestions and elastase treatment. Results showed that an acellular structure of histologically intact pure wavy collagen fibers with long inter-fibril open spaces (pores) of 8-30 microns in diameter was obtained (**Figure 4.8 (A-D)**).
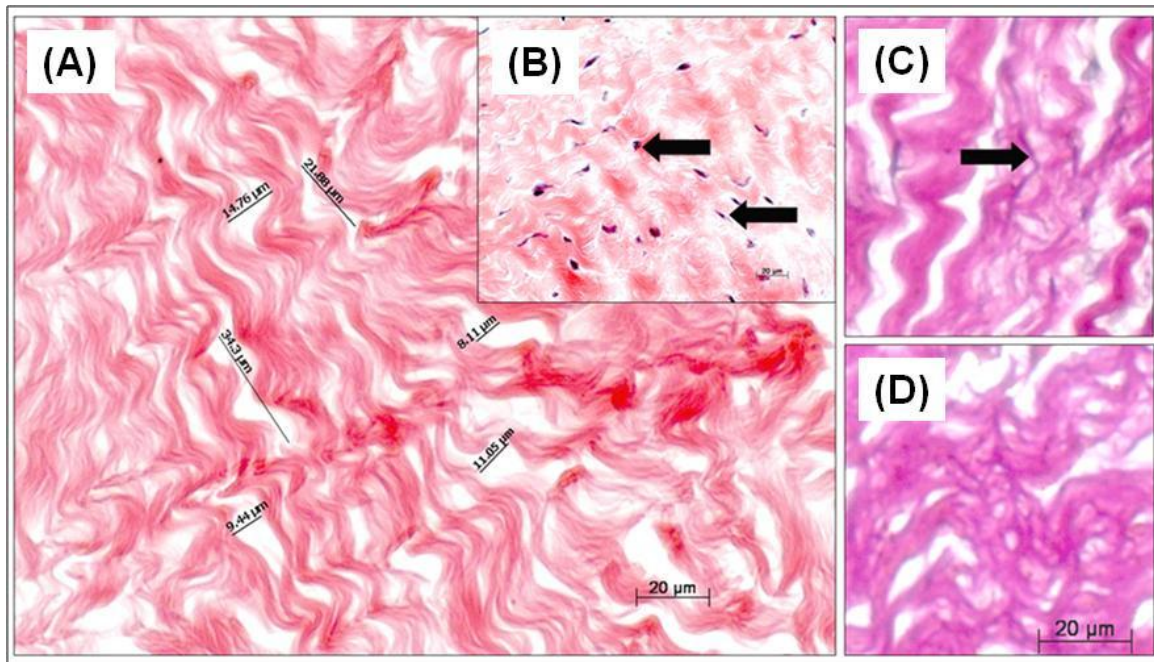
Figure 4.8: Histology of fibrous scaffolds. (A) H&E staining of acellular scaffold showing wavy collagen fibers interspersed with pores. Note complete lack of cell staining, as compared to native tissue (B) where cells are outlined by black arrows. (C) VVG staining showed fine elastin fibers (black arrow) throughout the native pericardial tissue, which were completely removed (D) by elastase treatment
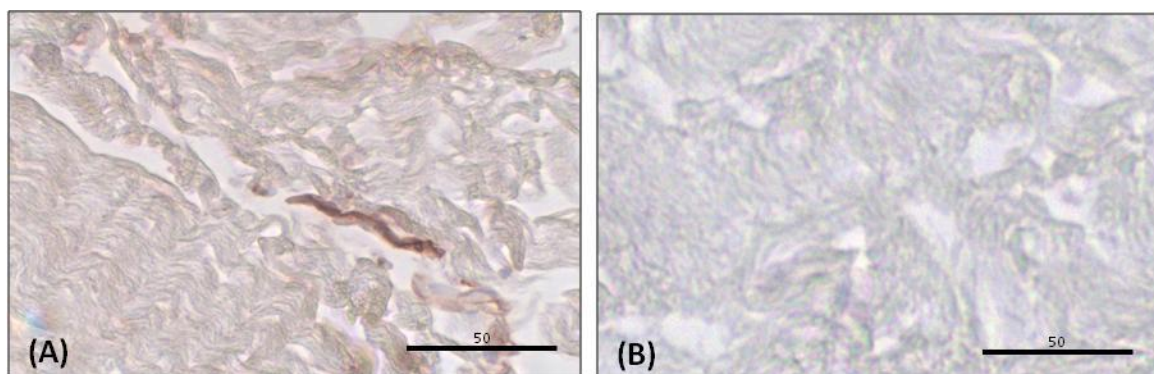
Figure 4.9: Histology of spongy collagen scaffolds. (A) fresh porcine pericardium, and (B) decellularized pericardium scaffolds stained with *GS* lectin for Galα antigen (A & B, dark brown= positive staining). Bars are 50 μm.

Histochemical staining showed the fibrous scaffold lacked Galα antigen.

The large majority of the fibers were insoluble since strong detergent extractions

yielded very few extractable proteins as evidenced by electrophoresis and silver-staining

(**Figure 4.10**).
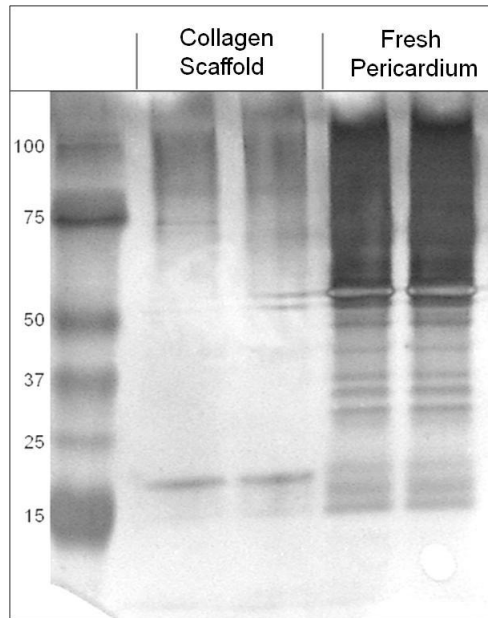
Figure 4.10: Properties of fibrous scaffolds. Presence of SDS-soluble proteins in fresh
pericardium and acellular collagen scaffolds was evaluated by SDSPAGE and silver
staining

Decellularization was confirmed by DNA extraction and evaluation using agarose

gel electrophoresis (**Figure 4.11 (A)**) followed by densitometry (**Figure 4.11 (B)**), which

showed more than 94% reduction in DNA content.

Furthermore, histochemical staining showed that both the fibrous scaffold

(derived from pericardium) as well as the *spongiosa* scaffold lacked Galα antigen.

ELISA measurements showed significantly lower levels of remnant MMP-2 activity in

scaffolds as compared to fresh pericardium (**Figure 4.12**).
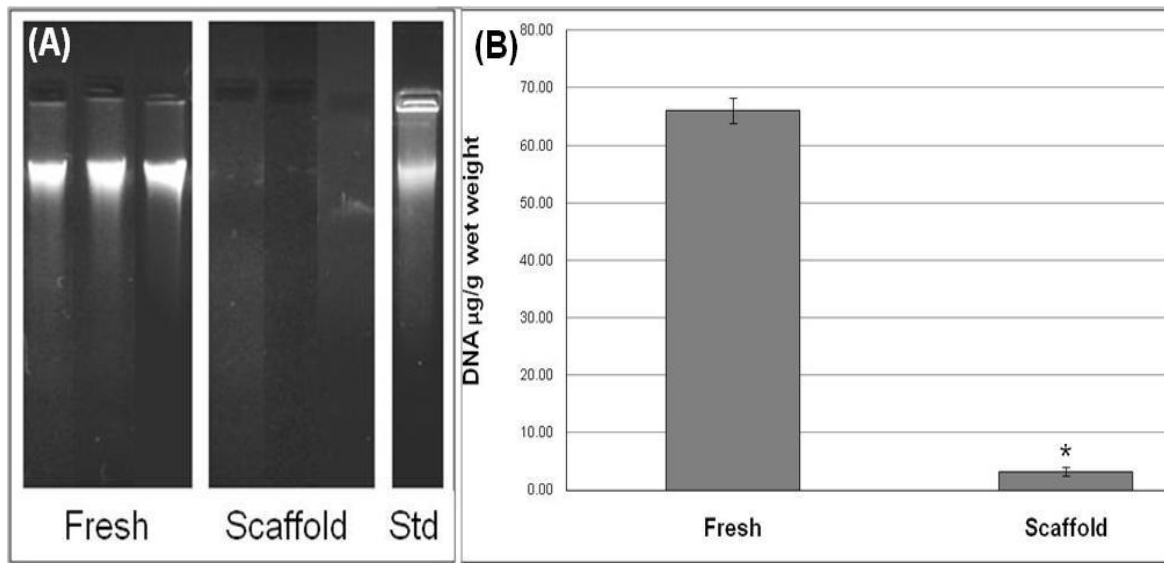
Figure 4.11: Properties of fibrous scaffolds. (A) Agarose/ethidium bromide gel electrophoresis of DNA extracted from fresh pericardium and the acellular collagen scaffolds; (B) densitometry of DNA bands in (A)
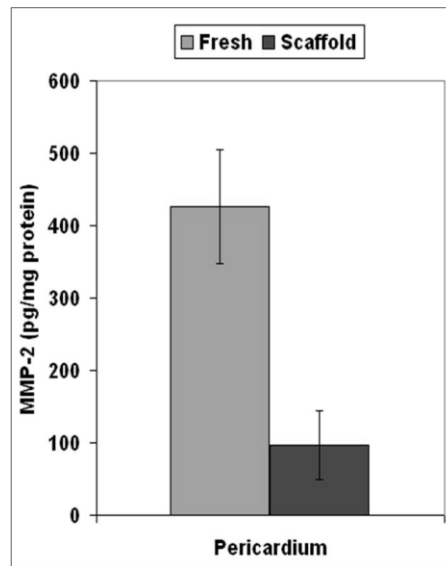
Figure 4.12: Properties of fibrous scaffolds. ELISA for MMP-2 in fresh pericardium and the acellular collagen scaffolds.

Fibroblasts exhibited a strong positive chemotaxis toward collagen peptides obtained from decellularized pericardium (**Figure 4.13**) suggesting that scaffold degradation products could encourage repopulation by acting as matrikines.
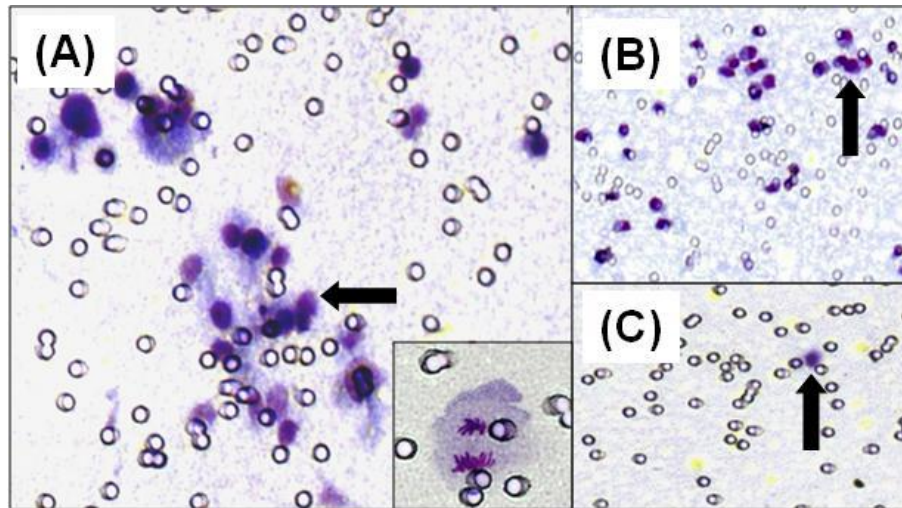
Figure 4.13: Characteristics of acellular porcine collagen scaffolds: Chemotaxis of fibroblasts towards collagen peptides obtained from acellular pericardium; inset in (A) shows a cell undergoing mitosis after chemotaxis, (B) positive chemotaxis control, (C) negative control.

4.3.1.3 Evaluation of PGG cross-linking and stability

To evaluate the cross-linking efficiency of PGG, fibrous scaffolds were treated with different concentrations of PGG (0%, 0.1%, 0 .15%, and 0 .3%) and leaching of PGG was tested. There was no significant difference in cell viability between the 3 concentrations tested as given by MTS assays (**Table 4.1**)

Cell viability % of control		
PGG conc.	Short Wash	Long Wash
0.10%	27.1	57.7
0.15%	22.8	44.8
0.30%	33.3	60.6

Table 4.1

However, there is a noticeable difference in the cell viability on each of the scaffolds

when the Live/Dead assay was used, with the 0.15% scaffold being the highest

concentration with viable cells. The 0.3%-fixed scaffold showed no live cells upon

evaluation (Live/Dead shown for 0.15%-treated scaffold).
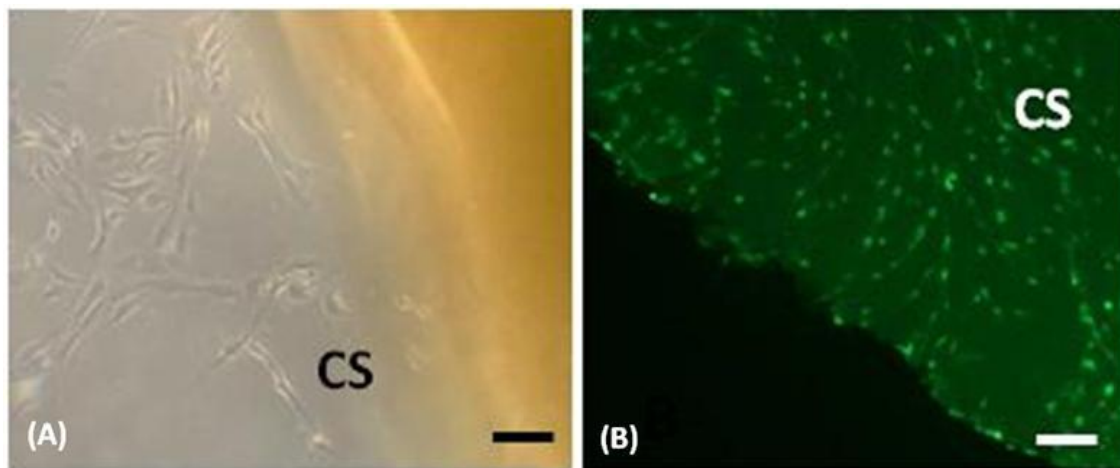
Figure 4.14: Phase contrast (A) and Live/Dead (B) of 0.15%-fixed scaffold that was washed over a weeks time.
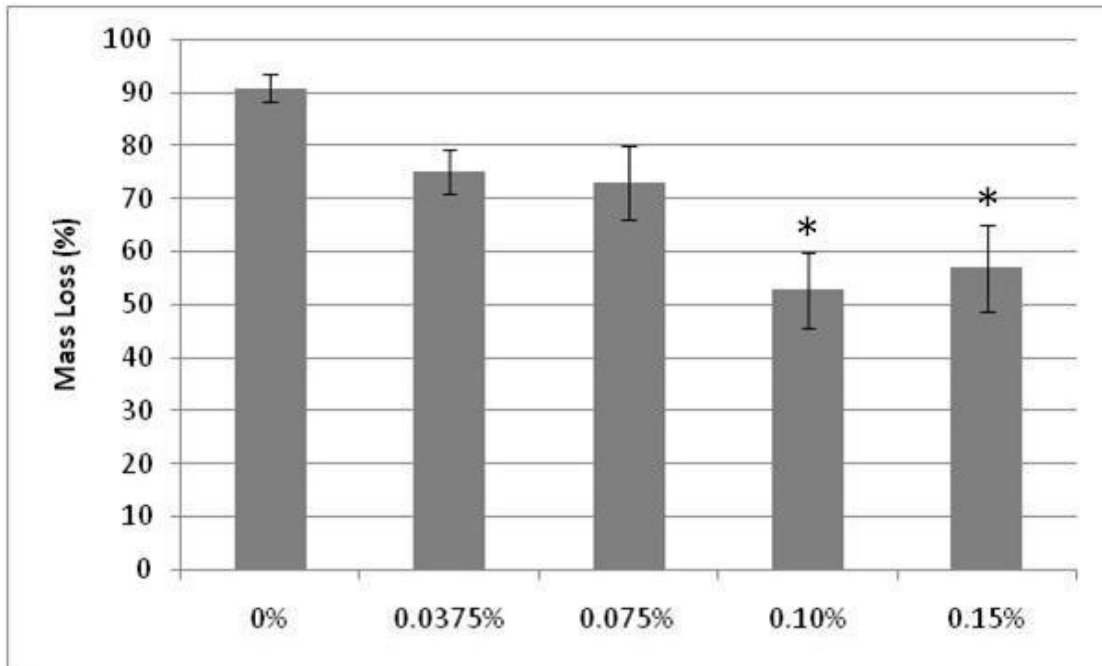
Figure 4.15: Collagenase study with scaffolds washed for a week.

The PGG, fibrous scaffolds were then treated with different concentrations of PGG (0%, 0.0375%, 0.075%, 0.10%, and 0.15%) based on leaching studies above and washed over a one week time, then exposed to collagenase to test degradation properties.

Results showed there was a significant difference between 0.10% and 0.15% PGG-fixation and all other concentrations, as well as there is a significant difference between 0.10% and 0.15%, therefore the 0.10% and 0.15% concentrations prevent degradation of the scaffold more effectively than the other concentrations.

4.3.1.4 *Properties of cross-linked fibrous collagen scaffolds*

Collagen scaffolds were treated with Glut, a known protein cross linker [11], PGG, a compound known to interact with Proline-rich proteins such as collagen [12], and

UV-light. Samples were then tested in vitro for resistance to collagenase, mechanical properties and thermal denaturation characteristics. Collagenase was used as an accelerated model for degradation and a widely accepted test that reveals extent of collagen cross-linking [13, 14]. Results showed that control, untreated scaffolds were almost completely digested by collagenase in 1-2 days (**Figure 4.16**), suggesting that decellularized porcine pericardium is highly biodegradable.
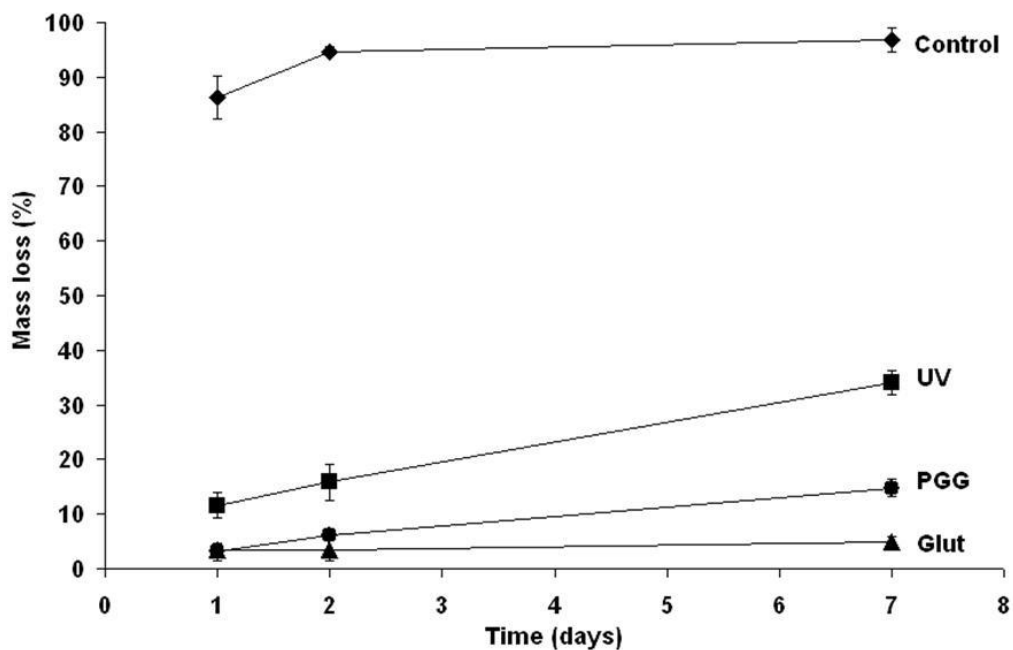
Figure 4.16: Resistance to collagenase of treated collagen scaffolds; a time-course study. Percent mass loss after collagenase treatment is shown for untreated scaffolds (control) and for UV, Glut and PGG-treated scaffolds. Control values were all significantly higher than other groups. *ANOVA statistical significance between groups.

Expectedly, Glut-treated collagen was highly resistant to collagenase at all time points, indicating that glutaraldehyde fixation of collagen is very strong and practically irreversible. PGG-treated collagen scaffolds exhibited excellent resistance to collagenase at 1 and 2 days with a slight but significant ($p<0.05$) increase in mass loss at 7 days

103

(almost 15% degradation by collagenase). These data suggest that PGG and UV treatment are good short-term collagen fixatives.

Differential scanning calorimetry analysis showed Td values of 76.9±1.0oC (mean ±SEM) for control scaffolds, 86.9±0.2oC for Glut and 78.2±0.6oC for PGG-treated scaffolds. All values were statistically different among groups (ANOVA, p<0.05), with the exception of PGG vs. control (p=0.454).

4.3.1.5 In vivo *biocompatibility studies of fibrous scaffolds*

To study biocompatibility and cell repopulation potential of our scaffolds we implanted samples subdermally in juvenile rats and analyzed them at 1, 3, and 6 weeks post-implantation. H&E staining (**Figure 4.17**) revealed a time dependent increase in cell infiltration in control (untreated) scaffolds associated with visible collagen fiber degeneration, confirming the fact that the collagen scaffold is degradable in vivo. Glut-fixed collagen scaffolds showed good collagen fiber preservation and significantly less cell infiltration (**Figure 4.17 (C)**) validating the fact that Glut-treated collagen is not an ideal substrate for cell-mediated remodeling.
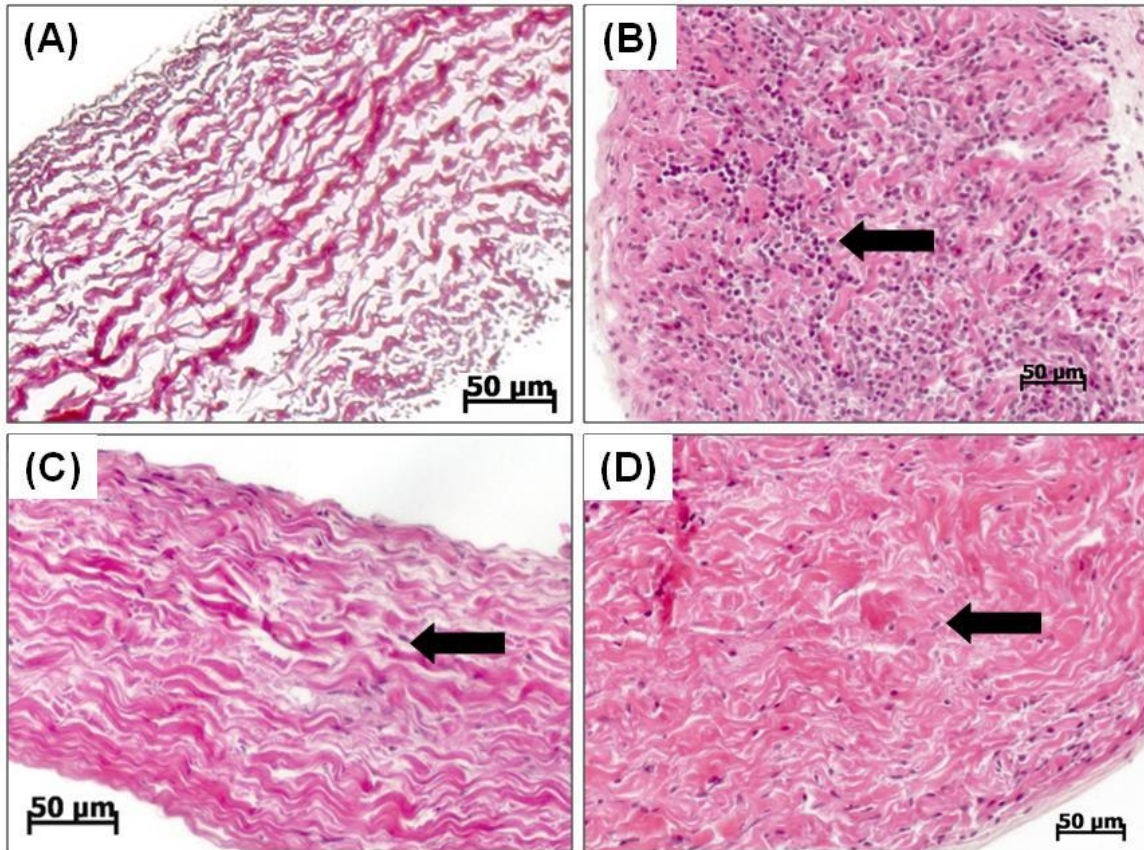
Figure 4.17: Histological analysis of subdermally implanted scaffolds. Representative H&E micrographs from 3 weeks samples showing (A) pre-implant collagen scaffolds, (B) explanted control scaffolds, (C) explanted Glut-treated scaffolds, and (D) explanted PGG-treated scaffolds. Black arrows point to cells present within implants.

PGG-treated scaffolds (**Figure 4.17 (D)**) exhibited clear signs of collagen fiber degradation, visibly less than control untreated collagen and more than Glut-fixed collagen. Similarly, larger numbers of infiltrating cells were found in PGG-treated collagen as compared to Glut-fixed collagen, but less than in untreated controls. Cell infiltration in PGG treated scaffolds increased with time, clearly showing that PGG treatment is not cytotoxic. UV-treated scaffolds exhibited a dramatically collapsed structure, practically impenetrable to cells at all time points (**Figure 4.18**).
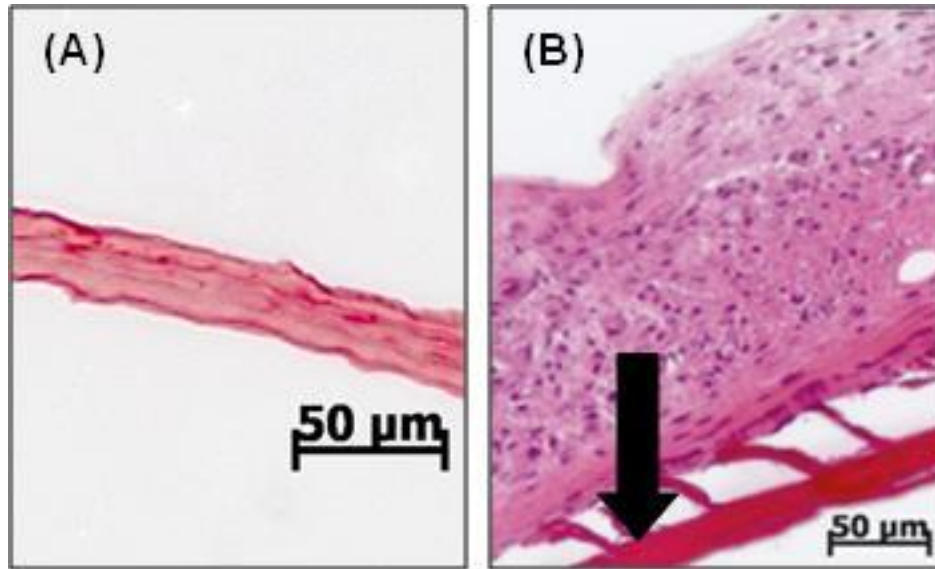
Figure 4.18: Histological analysis of subdermally implanted scaffolds. Representative H&E micrographs from 3 weeks samples showing UV-treated scaffold before (A) and after implantation (B). Black arrows point to cells present within implants.

Histology data was confirmed by quantitative DNA analysis. Despite considerable biological variability among samples, data showed significant DNA present at all time points in most tissues, with less DNA present in Glut-fixed tissues at 3 weeks ($p < 0.05$). Comparative analysis of 6 week vs. 3 week data revealed that DNA content apparently reached a plateau after 3 weeks, indicating that cell infiltration is complete within this time frame in subdermal implants (**Table 4.2**).

DNA levels in explanted collagen scaffolds

Samples	DNA content (µg / gram wet weight ± SEM, n=3)		
	1 week	3 weeks	6 weeks
Control	910 ± 130^{b}	1459 ± 185	961 ± 373
UV	1108 ± 145	$3258 \pm 1102^{a, b}$	2179 ± 488
Glut	1121 ± 318	$578 \pm 21^{a, b}$	1396 ± 341
PGG	2662 ± 538	2287 ± 172	642 ± 128^{a}

[a] statistical significance among time points within each fixation group ($p<0.05$).
[b] statistical significance among groups at each time point ($p<0.05$).
Table 4.2

A large majority of cells infiltrating collagen scaffolds were vimentin-positive cells resembling fibroblasts (**Figure 4.19 (A)**). Cell density apparently increased with time of implantation for control and PGG scaffolds, while cell infiltration in Glut-fixed scaffolds was significantly reduced at all time points. Infiltrating cells were also positive for proline-hydroxylase, an enzyme involved in collagen synthesis (**Figure 4.19 (B)**). Macrophage infiltration was very scarce in all implants at all time points (**Figure 4.19 (C)**).
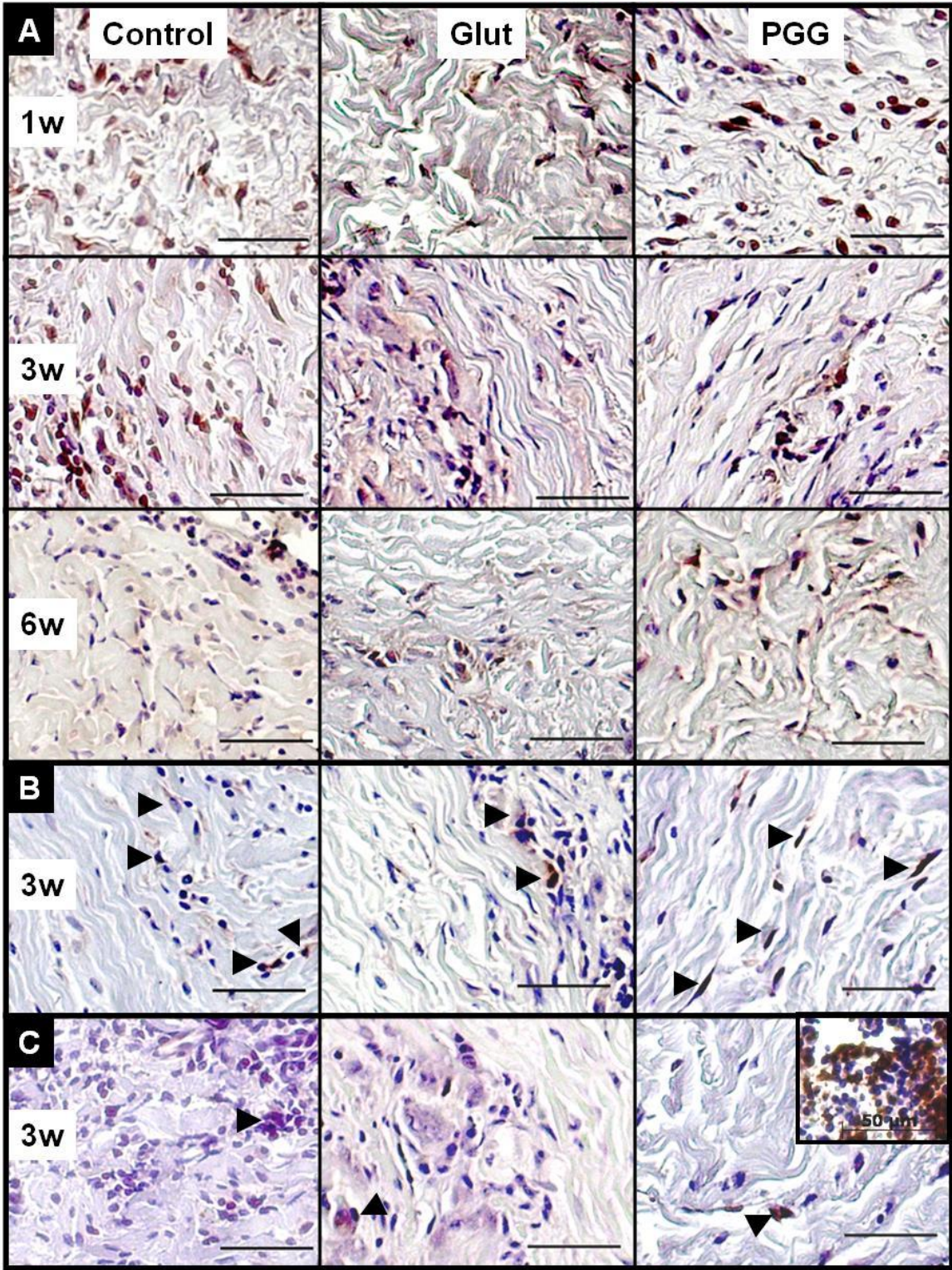
Figure 4.19: Immunohistochemical identification of infiltrating cells. a) Vimentin stain showing extensive fibroblast-like infiltrating cells in all implant groups at 1 week (1w), 3 weeks (3w) and 6 weeks (6w) after implantation. b) Proline-hydroxylase immunohistochemical staining; arrowheads point to positively stained cells. c) Specific staining showing very few macrophages (arrowheads). Inset in (c) shows macrophage staining of rat spleen sections used as a positive control. Sections were counterstained with hematoxylin (nuclei dark blue). Bars are 50 microns in all micrographs.

Calcium analysis in explanted scaffolds (**Table 4.3**) revealed significantly high levels in Glut-fixed and UV-treated collagen while control, untreated collagen scaffold samples, as well as PGG-treated scaffolds did not accumulate any significant amounts of calcium, indicating that despite effective collagen stabilization, PGG treatment may not induce collagen calcification while UV treatment induces significant calcification of the scaffolds.

Calcium levels in explanted collagen scaffolds

Samples	Ca content (μg / mg dry weight $\pm$ SEM, n=4)		
	1 week	3 weeks	6 weeks
Control	1.4 ± 0.5	1.2 ± 0.3	0.5 ± 0.1
UV	32.6 ± 17.5^{b}	$97.3 \pm 17.2^{a, b}$	$121.9 \pm 11.7^{a, b}$
Glut	2.8 ± 1.4	5.4 ± 3.8	4.6 ± 2.6
PGG	1.4 ± 0.4	1.5 ± 0.5	1.1 ± 0.2

[a] statistical significance among time points within each fixation group ($p < 0.05$).
[b] statistical significance among groups at each time point ($p < 0.05$)
Table 4.3

Phenol staining showed tight binding of PGG to collagen (**Figure 4.20 (A)**) which appeared to be maintained even after 3 weeks of subdermal implantation (**Figure 4.20(B)**) suggestive of stable PGG-collagen interactions.
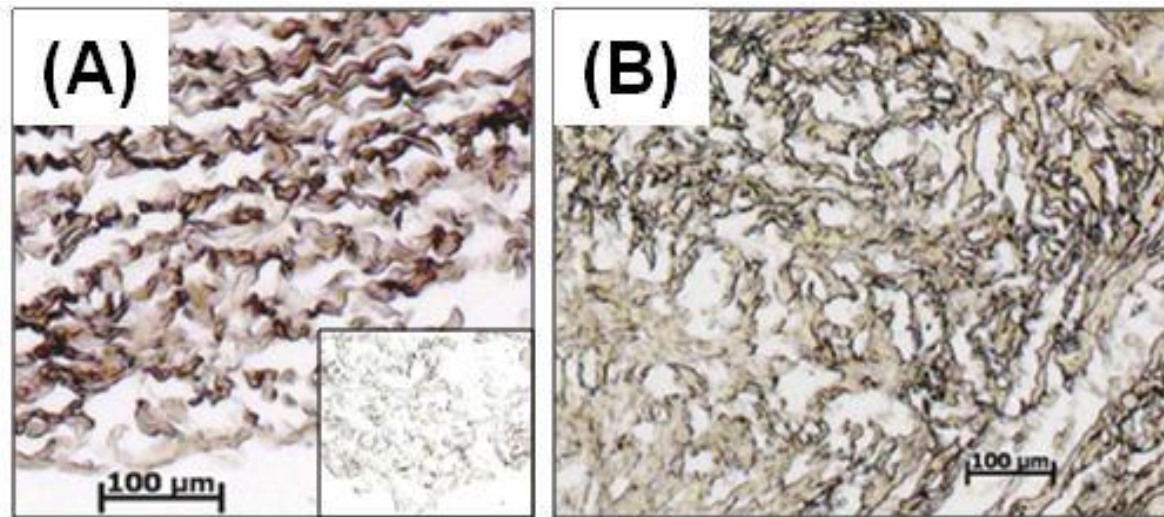
Figure 4.20: Histological analysis of subdermally implanted scaffolds. (A) Phenol staining showing collagen-bound PGG (brown) before implantation and (B) 3 weeks after subdermal implantation. Insert in (A) represents phenol staining of a negative control (scaffold not treated with PGG).

Matrix metalloproteinase (MMP) activity was measured in explants from all time points using gelatin zymography (**Figure 21**). Two major proteases were identified in tissue extracts, namely MMP-9 (migrating at around 90-95 kDa) and MMP-2 (65-80 kDa). Band intensity was measured for each sample (normalized to protein content) and represented as relative density units or RDU (**Figure 21**). Similar trends were observed for MMP-9 and MMP-2, i.e. high enzyme levels at 1 and 3 weeks, leveling off at 6 weeks. Activity of MMP-2 was about 10 times higher in all samples as compared to

MMP-9. The total MMP enzyme activity distribution resembled that of the DNA content. In addition, glycosaminoglycan levels within all implant groups showed a mean overall value of 175 +/- 30 ug per mg extracted protein, but without showing statistical significance among treatment groups and time points ($p > 0.05$). Overall results suggest the presence of cells actively involved in matrix remodeling.
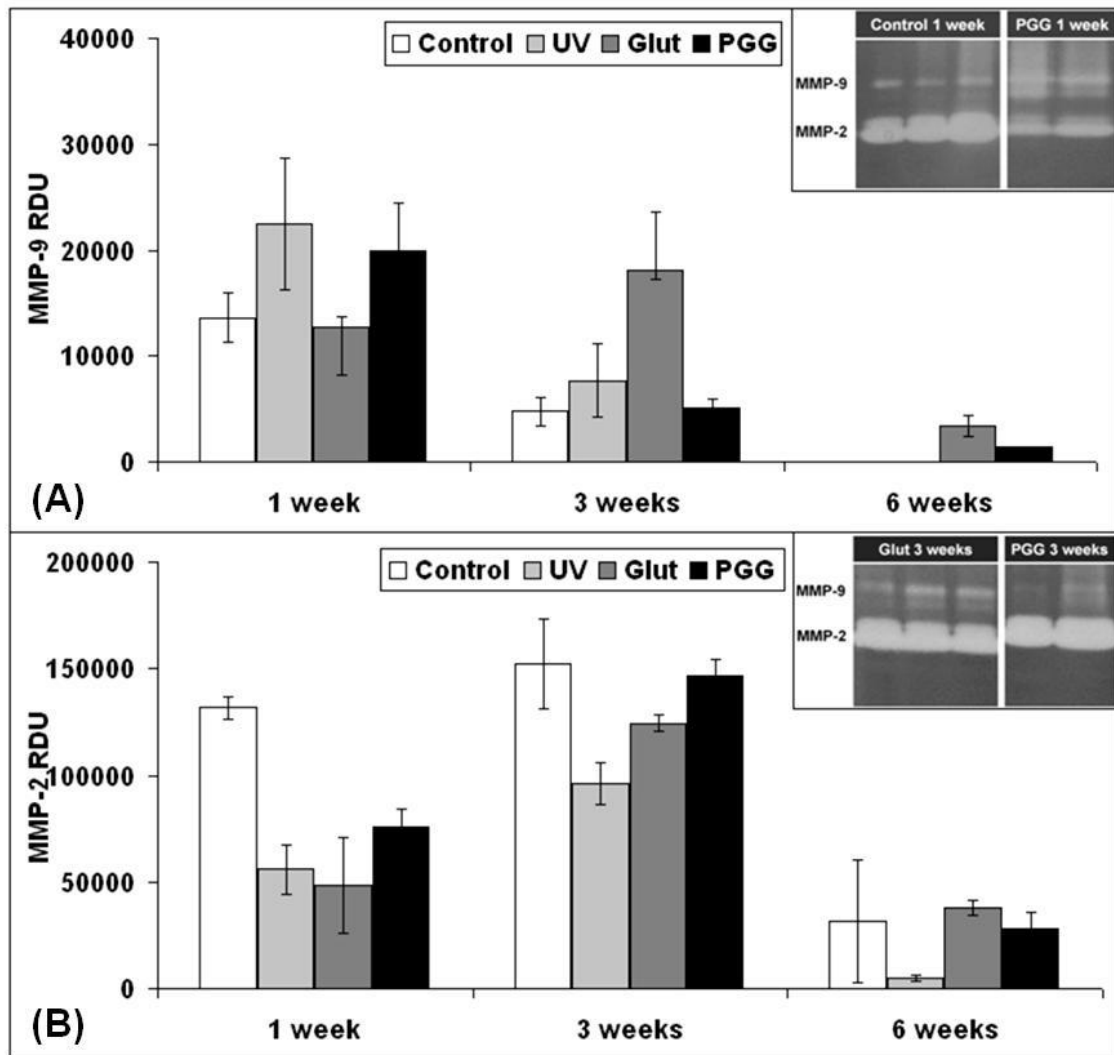
Figure 4.21: MMP activities in explanted scaffolds. Densitometry of active MMP bands are expressed as relative density units (RDU) normalized to protein content. MMP-9 (A)

and MMP-2 (B) were identified from their relative migration on gelatin containing 10% polyacrylamide gels (insets show representative zymograms).

4.4 **Discussion**

It is our premise that the outstanding performance of allografts is mainly due to the fact that they very closely mimic the natural valve anatomy. Since collagen represents the predominant component of heart valves we hypothesized that use of collagen membranes engineered to mimic the native anatomical heart valve structure would serve as an effective approach to heart valve tissue engineering.

It is vital that implanted heart valves function immediately after implantation but also support host cell infiltration and remodeling. It is our working hypothesis that such properties can be achieved by development of partially cross-linked collagen scaffolds. Full cross-linking would reduce cell infiltration and remodeling capacity to a minimum and thus may prevent tissue regeneration. Conversely, uncross-linked scaffolds may degrade too rapidly after implantation and thus reduce functionality of the tissue engineered heart valves. Moderately cross-linked scaffolds would allow for slow but sustained cell infiltration with temperate remodeling of the scaffold, without alterations in valve properties. In current study we evaluated non-Glut fixation methods such as UV light and PGG treatments of acellular porcine pericardium for development of novel scaffolds for heart valve tissue engineering.

In current study we illustrated development of a new scaffold to be used as a *spongiosa* layer for heart valve tissue engineering. The middle *spongiosa* layer, composed primarily of glycosaminoglycans (GAGs) and collagen, is easily deformed in

the presence of shear forces and cushions shock during the valve cycle and is not readily compressed. This resistance to compression during bending aids in cuspal mechanics by preventing buckling during flexion (systole), which could result in overall cuspal damage [15]. To obtain pure collagen scaffolds with constant and predictable composition and properties, porcine pulmonary artery was successfully decellularized using hypotonic shock, detergent extraction and nuclease digestion. The scaffold was further treated with elastase. Removal of elastin created supplementary pores for cell infiltration and assisted with tissue decellularization. The *spongiosa* has a gelatinous consistency, due in large part to the hydrophillicity of the GAG molecules. This novel acellular scaffold composed of collagen and GAGs was highly hydrated, porous and hydrophilic, showed good preservation of matrix components, lacked Galα antigens and supported in vitro cell repopulation. Enhanced scaffold characterization could be obtained by more extensive ultra structural analysis of collagen and elastin fiber integrity, GAG components and presence of minute cell debris [16, 17].

Porcine pericardium was successfully decellularized using hypotonic shock, detergent extraction and nuclease digestion. This is an accepted decellularization approach for fibrous connective tissues [29]. Since pericardium contains about 10% elastin, we added an extra step, elastase treatment, to fully remove elastin, increase porosity and make mechanical properties more homogenous. Histology, DNA and protein analysis showed that decellularization was complete and the scaffold was predominantly composed of insoluble collagen fibrils devoid of inter-fibrillar matrix or cells.

To evaluate cross-linking possibilities, we treated decellularized pericardium with UV, PGG and Glut and compared their properties with untreated scaffolds as controls. Native, untreated scaffolds degraded quickly in vitro and in vivo, were rapidly invaded by host cells, showed signs of remodeling and lack of calcium deposition. UV treatment had the most dramatic effects on collagen scaffolds including irreversible and aggressive changes in tissue structure, full collapse of the porous configuration and significant changes in mechanical properties. UV treated scaffolds appeared to have been partially cross-linked because they exhibited initial resistance to collagenase in the first 1-2 days of exposure to the enzyme, subsequently losing more than 1/3 of its mass after 7 days in collagenase.

Upon implantation, UV treated collagen scaffolds were not infiltrated by host cells, calcified massively and adhered strongly to their fibrous capsules. The mechanisms of UV-induced collagen cross-linking are thought to include radical mediated alterations in aromatic amino acids [18]. These changes may be responsible for observed in vitro resistance to collagenase. It is not clear at this point how UV treatment induces collagen calcification but we speculate that it does so through dramatic changes in molecular structure and ultra structure, including loss of fibrillar architecture [19]. Although this cross-linking procedure appears advantageous for tissue engineering applications, the propensity of UV treated collagen towards calcification needs to be further addressed. Notably, subdermal implantation in juvenile rats serves as a model for calcification [34] as well as for degradation of matrix components and remodeling [35,36].

Glut treatment effectively stabilized decellularized pericardium against collagenase, an expected feature known in the bioprosthetic heart valve field [2]. Moreover, Glut-fixed scaffolds exhibited typical mechanical properties and high Td (as compared to native collagen). Upon implantation, Glut-fixed collagen calcified to some extent, but not to levels reported for bioprosthetic heart valves analysis, where Glut-fixed pericardium showed calcification levels of about 100 µg/mg [30]. This may be because of absence of pericardial cells which are presumably the initial calcification nucleation sites [31]. Cell infiltration was noted to occur to some extent in Glut-fixed scaffolds but cell numbers did not increase with time and, despite the fact that some infiltrating cells were fibroblast-like cells expressing MMPs, Proline-hydroxylase and glycosaminoglycans; it is unlikely that these scaffolds will undergo remodeling after implantation.

PGG treatment revealed substantial initial collagen stabilization versus the action of collagenase in vitro, with the potential for reversibility. It should be noted that the *in vitro* collagenase system is an accelerated model for degradation as collagenase activities in vivo are not expected to be so harsh [32]. Differential scanning calorimetry analysis showed a slightly higher Td when compared to native scaffold and lower than Glut (but not statistically different) partially confirming collagenase results. This phenomenon of tissue resistance to collagenase in the absence of high Td values was reported previously for the Photofix stabilization procedure [33]. Mechanical properties of PGG-treated scaffolds were similar to untreated and Glut treated samples except for a relatively higher hysteresis (data not shown). Despite effective collagen stabilization, PGG treated collagen did not calcify in vivo, suggesting that the nature of the cross-linker may

determine the outcome of collagenous implants. Host cells infiltrated implants relatively rapidly indicating that PGG-treated collagen is not cytotoxic. Moreover these fibroblast-like cells secreted MMPs, expressed Proline-hydroxylase and secreted GAGs and thus may exhibit true potential for remodeling. Because long-term, adequate control of local inflammation and MMP activities may be difficult to achieve and may be accompanied by adverse side effects, such as failure of the implant, [20] demonstrating that the tissue has potential to remodel, as indicated by the types of cells infiltrating over the time course of the *in vivo* study, further supports the notion that PGG may be a safe and effective collagen stabilizing agent.

Mechanisms of PGG-induced collagen stabilization are not fully understood. PGG is a naturally derived polyphenol characterized by a D-glucose molecule derivatized at all five hydroxyl moieties by gallic acid, i.e. 3,4,5-trihydroxybenzoic acid (Fig. 2b). Polyphenols have a hydrophobic internal core and numerous external hydroxyl groups. By virtue of this structure, they react with proteins, specifically binding to hydrophobic regions [37], but also establishing numerous hydrogen bonds, showing particularly high affinity for Proline-rich proteins [38] such as collagen and elastin [39]. In addition, they are efficient antibacterial agents and reduce inflammation and antigenicity [40]. Recently we showed that peri-arterial delivery of PGG to rat abdominal aorta prevented aneurysm formation or progression and did not elicit any detectable changes in serum liver enzyme activities or liver histology, clearly showing that PGG was not toxic at local or systemic levels [10]. Moreover, extractables obtained from PGG-fixed tissues exhibited very low in vitro cytotoxicity towards fibroblasts and smooth muscle cells [41] and thus can be

116

used safely in tissue engineering applications [42-46]. In current studies we have shown that PGG binds strongly to pericardial collagen and this binding was stable for at least 3 weeks in vivo.

4.5   Conclusions

Decellularized pulmonary arteries can be prepared by our method to be used as the *spongiosa* layer in our aortic heart valve constructs. Decellularized pericardium fulfills many properties required for use in valvular tissue engineering, including adequate mechanical properties, minimal cytotoxicity, excellent cell repopulation potential and propensity for matrix remodeling. Such collagen scaffolds emerge superior to polymer scaffolds in terms of mechanical and biological properties, but also maintain a natural tendency to degenerate rapidly in vivo unless stabilized. Glut cross-linking fully stabilizes collagen but does not allow for tissue remodeling and also induces calcification when implanted subdermally in rats. Conversely, PGG is a mild, non-toxic, reversible collagen stabilizing agent capable of controlling tissue degradation. PGG treated collagen does not calcify in vivo and supports host cell infiltration and matrix remodeling. In contrast, UV treatment induced exstensive changes in the mechanical properties and induced profuse calcification of the fibrous collagen scaffold, therefore the use of UV cross-linking was no investigated further as a fixation option. In conclusion, PGG treatment is a promising collagen stabilization process for heart valve tissue engineering.

4.6   References

1.   Liao, J., et al., *Molecular orientation of collagen in intact planar connective tissues under biaxial stretch.* Acta Biomater, 2005. **1**(1): p. 45-54.

2.   Obermiller, J.F., et al., *A comparison of suture retention strengths for three biomaterials.* Med Sci Monit, 2004. **10**(1): p. PI1-5.

3.   Oswal, D., et al., *Biomechanical characterization of decellularized and cross-linked bovine pericardium.* J Heart Valve Dis, 2007. **16**(2): p. 165-74.

4.   Simionescu, D., A. Simionescu, and R. Deac, *Mapping of glutaraldehyde-treated bovine pericardium and tissue selection for bioprosthetic heart valves.* J Biomed Mater Res, 1993. **27**(6): p. 697-704.

5.   Tedder, M.E., et al., *Stabilized Collagen Scaffolds for Heart Valve Tissue Engineering.* Tissue Eng Part A, 2008.

6.   Strokan, V., et al., *Heterogeneous expression of Gal alpha1-3Gal xenoantigen in pig kidney: a lectin and immunogold electron microscopic study.* Transplantation, 1998. **66**(11): p. 1495-503.

7.   Lu, Q., et al., *Novel porous aortic elastin and collagen scaffolds for tissue engineering.* Biomaterials, 2004. **25**(22): p. 5227-37.

8.   Barbosa, I., et al., *Improved and simple micro assay for sulfated glycosaminoglycans quantification in biological extracts and its use in skin and muscle tissue studies.* Glycobiology, 2003. **13**(9): p. 647-53.

9.   Farndale, R.W., C.A. Sayers, and A.J. Barrett, *A direct spectrophotometric microassay for sulfated glycosaminoglycans in cartilage cultures.* Connect Tissue Res, 1982. **9**(4): p. 247-8.

10.   Isenburg, J.C., et al., *Elastin stabilization for treatment of abdominal aortic aneurysms.* Circulation, 2007. **115**(13): p. 1729-37.

11.   Simionescu, A., D. Simionescu, and R. Deac, *Lysine-enhanced glutaraldehyde crosslinking of collagenous biomaterials.* J Biomed Mater Res, 1991. **25**(12): p. 1495-505.

12.   Tang, H.R., A.D. Covington, and R.A. Hancock, *Structure-activity relationships in the hydrophobic interactions of polyphenols with cellulose and collagen.* Biopolymers, 2003. **70**(3): p. 403-13.

13.   Isenburg, J.C., D.T. Simionescu, and N.R. Vyavahare, *Tannic acid treatment enhances biostability and reduces calcification of glutaraldehyde fixed aortic wall.* Biomaterials, 2005. **26**(11): p. 1237-45.

14.   Kasyanov, V., et al., *Tannic acid mimicking dendrimers as small intestine submucosa stabilizing nanomordants.* Biomaterials, 2006. **27**(5): p. 745-51.

15.   Sacks, M.S. and A.P. Yoganathan, *Heart valve function: a biomechanical perspective.* Philosophical Transactions of the Royal Society B-Biological Sciences, 2007. **362**(1484): p. 1369-1391.

16.   Simionescu, D., R.V. Iozzo, and N.A. Kefalides, *Bovine pericardial proteoglycan: biochemical, immunochemical and ultrastructural studies.* Matrix, 1989. **9**(4): p. 301-10.

17.   Simionescu, D., J. Lovekamp, and N. Vyavahare, *Degeneration of bioprosthetic heart valve cusp and wall tissues is initiated during tissue preparation; an ultrastructural study.* J Heart Valve Dis, 2002. **in press**.

18.   Lee, J.E., et al., *Characterization of UV-irradiated dense/porous collagen membranes: morphology, enzymatic degradation, and mechanical properties.* Yonsei Med J, 2001. **42**(2): p. 172-9.

19.   Schoen, F.J., et al., *Onset and progression of calcification in porcine aortic bioprosthetic valves implanted as orthotopic mitral valve replacements in juvenile sheep.* J Thorac Cardiovasc Surg, 1994. **108**(5): p. 880-7.

20.   Isenburg, J.C., D.T. Simionescu, and N.R. Vyavahare, *Elastin stabilization in cardiovascular implants: improved resistance to enzymatic degradation by treatment with tannic acid.* Biomaterials, 2004. **25**(16): p. 3293-302.

CHAPTER 5

**INVESTIGATION OF SCAFFOLD ADHERENCE METHODS FOR TRI-
LAYERED TISSUE ENGINEERED HEART VALVES
(AIM 2)**

5.1   Introduction

Native aortic valve leaflets are complex structures composed of external layers, the *fibrosa* (composed of collagen) on the arterial aspect and the *ventricularis* (collagen and elastin) on the ventricular aspect. The fibrous layers are sustained internally by a highly hydrated central *spongiosa* layer (rich in proteoglycans) that serves as a cushion material to mediate deformations of the fibrous layers, allows shearing between the outer layers and absorbs compressive forces during valve function [1-3]. Lack of a buffering layer results in large shear stress and tissue buckling when subjected to bending [4].

Tissue engineering, the science of combining scaffolds, cells and specific signals to create living tissues is feasible and holds great promise for treatment of heart valve disease [5]. Two main strategies have been developed in recent years. The first is based on use of decellularized porcine valves followed by *in vitro* or *in vivo* repopulation with cells of interest. Despite their excellent mechanics, acellular valves are very dense and thus difficult to repopulate with desired cells. The second approach employs cell seeded polymeric biodegradable matrices [6] or scaffolds built from fibrin [7]. While polymeric and fibrin-based scaffolds shown very promising results, decellularized these degradable matrices have insufficient strength to withstand arterial pressures immediately after implantation.

Our novel strategy relies on use of stabilized collagen scaffolds that mimic the natural valve fibrous layers, based on decellularized porcine pericardium [8] and delicate, highly hydrated porous collagen scaffolds to be used as the middle *spongiosa* layer. Chemically stabilized pericardium has outstanding mechanical properties, a good record of implantation in humans as valves, and as reconstructive surgery biomaterial patches in other organs [9-15]. To reduce scaffold biodegradation, we have also investigated the use of penta-galloyl glucose (PGG), a naturally derived collagen-binding polyphenol [8, 16]. No reports to date have documented the use of PGG-stabilized acellular pericardium for construction of tissue engineered heart valves. Since the xenoantigen $Gal\alpha1-3Gal$ ($Gal\alpha$), is responsible for rejection of vascularized organ transplants we are paying special attention to $Gal\alpha$ detection in decellularized scaffolds [17-21].

Recognizing the outstanding mechanical performance of natural valve homografts, the vital importance of the three leaflet layers [22], and the need for reconstruction of the physiologic valve design, we developed five building blocks for this new approach: a) partially stabilized collagenous scaffolds which degrade slowly with time, b) anatomically analogous 3-D heart valve shapes made from solid molds, c) tri-layered constructs that mimic the native heart valve histo-architecture, d) autologous multipotent mesenchymal stem cells for repopulation and remodeling and e) mechanical cues to induce stem cell differentiation into valvular cells capable of maintaining matrix homeostasis.

To assemble the 3D heart valve structures we developed and implemented use of biological adhesives in tissue engineering. At a minimum, these adhesives need to exhibit

adequate bond strength and elasticity, long term stability and biocompatibility. In current study we chose to implement a modified albumin/glutaraldehyde adhesive for the construction of living heart valves. In Chapter 4 we reported on extensive characterization of the acellular fibrous pericardial scaffolds and spongy pulmonary artery used to mimic the *fibrosa* and *ventricularis* layers and *spongiosa* layers, respectively [8]. In current study we describe the use of these novel scaffolds to be used as the layers and utilization of a biological glue to assemble the tri-layered constructs.

5.2   Materials and Methods

5.2.1   Materials

High purity 1,2,3,4,6-Penta-O-galloyl-beta-D-glucose (penta-galloyl-glucose, PGG) was a generous gift from N.V. Ajinomoto OmniChem S.A., Wetteren, Belgium (www.omnichem.be). Human bone marrow derived stem cells (hBMSCs) were obtained from Cell Applications, Inc. San Diego, CA) and all other chemicals were of highest purity available from Sigma Aldrich, St. Louis, MO.

5.2.2   Methods

5.2.2.1 *Development and testing of the scaffold adhesive*

Since bonding layers of collagen scaffolds is essential for our approach, we developed a scaffold adhesive based on protein-aldehyde mixtures, inspired from the FDA-approved BioGlue™ (CryoLife, Kennesaw, GA) developed as a haemostatic agent. BioGlue™ is composed of 45% (w/v) bovine serum albumin and 10% glutaraldehyde

solutions which are stored independently in a double-barreled syringe and dispensed through a mixing tip to yield a quickly setting gel. Initial testing of the original BioGlue™ on acellular pericardial scaffolds showed that setting time was too short and once bonded, of insufficient mechanical strength for creation of engineered heart valves. Thus we increased albumin concentration to 55% and decided to apply it in two steps, first the protein layer and then glutaraldehyde using single-barreled syringes. This approach ensured that the albumin solution first infiltrated several scaffold layers before being fully crosslink by the aldehyde. The volumetric ratio of albumin to glutaraldehyde was maintained at about 5 to 1. This higher protein concentration reduced the fluidity of the solution and allowed for precise positioning of the gluing spots. The new adhesive was coined "BTglue" and used in all studies shown below.

5.2.2.2 *Lap shear*

The test was performed according to ASTM 2255-05. Fibrous scaffolds were cut into 2.5 x 7 cm strips, overlapped over a 1 cm wide area and bonded using the BTglue. The specimens were subjected to increasing loads in the testing frame of a MTS Synergy 100 (Eden Prairie, MN) machine at a crosshead speed of 5 mm/min at room temperature (**Figure 5.1**).
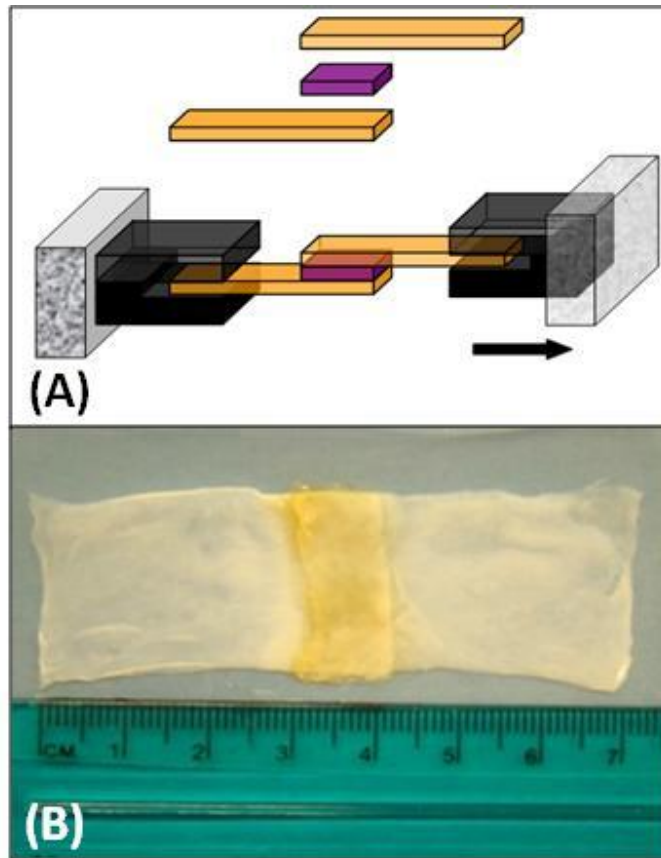
Figure 5.1: Testing of the scaffold adhesive. To test bond strength samples were glued by partial overlap subjected to pullout forces and shear strength calculated.

The apparent shear strength was calculated as the maximum load divided by the bonded area and expressed as Pa.

5.2.2.3 *Shear properties*

Squares (20 x 20 mm) of fibrous scaffolds incorporating 10 x 10 mm of *spongiosa* layer were glued together using BTglue as described above. The samples were mounted onto a micromechanical testing device (Mach-1 Micromechanical Systems, Biosyntech,

MN) and sheared horizontally to mimic physiologic movements of valve leaflets (**Figure 5.2**).
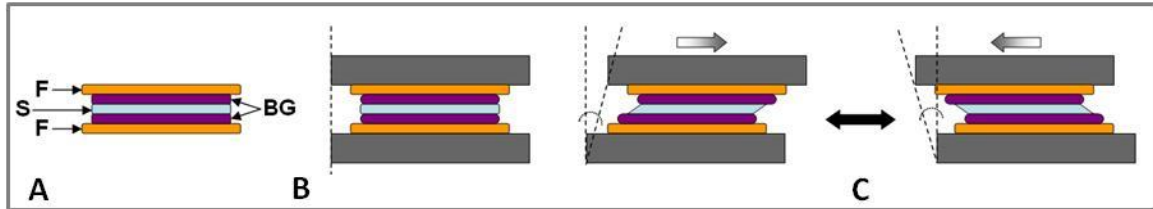

Figure 5.2: Testing of the scaffold adhesive. Shear properties of glued layers in which *spongiosa* scaffolds (S) were glued between two fibrous scaffolds (F) using BTglue (BG).

A deflection was applied by moving one of the shear plates with the linear positioner of the Mach-1 (**Figure 5.2 (B)**). The shear angle was calculated by finding the arctangent of the ratio of deflection over tissue thickness (**Figure 5.2 (C)**). Shear force was recorded by the load cell and converted to shear stress by normalizing to the area of specimen. Shear stress-shear angle relationships were compared to fresh valve cusps and 0.5% glutaraldehyde-fixed valve cusps.

5.2.2.4 *Cytotoxicity studies on BTglue*

Fibrous scaffold samples (15 x 15 mm) were prepared and BTglue (200 μl albumin followed by 40 μl glutaraldehyde) was applied on one surface of the scaffold. Scaffolds were then divided into two groups; one group (n = 3) was treated with 50% FBS/DMEM mixture for surface passivation (24 hours at 37 $^{\circ}$C), rinsed and then treated for 2 hours in 1% Glycine in PBS for complete aldehyde group neutralization.
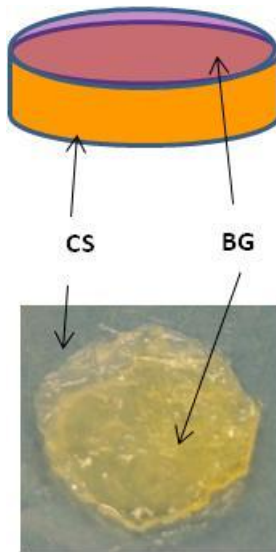
Figure 5.3: Testing BTglue cytotoxicity. Fibrous collagen scaffolds (CS) to which a single layer of BTglue (BG) was applied were neutralized with FBS/glycine solutions (+) or were used without neutralization (-) and were then seeded with fibroblasts.

The second group was treated with PBS for 26 hours at 37 ^{o}C as control. Rat dermal fibroblasts (50 x 10^3 cells per sample) were seeded on the scaffolds, cultured in DMEM/10% FBS media and MTS assay and Live/Dead performed 6 days after seeding. Number of living cells was calculated from MTS absorbance values (A490) from a calibration curve prepared with rat dermal fibroblasts cultured on standard culture plates.

5.2.2.5 *Cytotoxicity studies on PGG-treated and glued fibrous scaffolds*

Round fibrous scaffold coupons (3 cm^2) were prepared and 120 μl of BTglue (100 μl albumin followed by 20 μl glutaraldehyde) were applied on one surface and on only one half of the scaffold, leaving half of scaffold surface untreated with glue. Scaffolds were then treated with penta-galloyl-glucose (PGG) (0.1% and 0.15% PGG in 50 mM

phosphate buffer, pH 5.5 containing 20% isopropanol, n = 3 scaffolds per group) for 24 hours at 22°C.
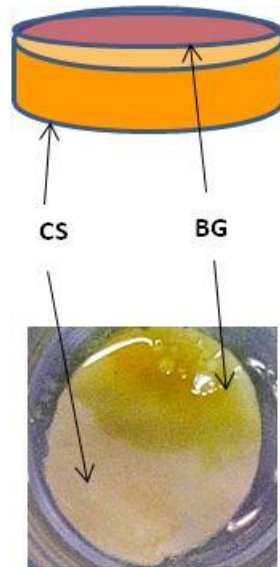

Figure 5.4: PGG toxicity testing. Fibrous collagen scaffolds (CS) to which a layer of BTglue (BG) was applied on ½ of the surface, were treated with PGG (0.1% and separately 0.15%), subjected to short wash and separately long wash procedures, neutralized with FBS/glycine and then seeded with fibroblasts.

Scaffolds not treated with PGG served as controls. Samples were also treated with 0.2% glutaraldehyde in PBS as positive cytotoxic controls. Scaffolds were then divided into two groups; one group was rinsed in sterile PBS containing 0.02% sodium azide for 20 minutes at room temperature under gentle agitation (short wash); the second group was rinsed in sterile PBS/azide for 5 days with daily changes at room temperature under gentle agitation (long wash). Scaffolds were rinsed, treated with FBS and glycine for neutralization (as above) and stored in sterile saline. Rat dermal fibroblasts ($1x10^5$ cells per scaffolds) were seeded on the scaffolds, cultured and MTS and Live/Dead assays

performed 5 days after seeding. Results are expressed as percentage viability relative to control samples (non-PGG treated group).

5.2.2.6 *Tri-layered scaffolds; stability and mechanical properties*

To test whether tri-layered scaffolds maintain stabilization properties, a layer of porous *spongiosa* scaffold was entrapped between two fibrous scaffold layers using BTglue as described above. The constructs were then subjected to 0.1% PGG for 24 hours, long wash protocol, neutralization as above and then exposed to collagenase (6.25 units/ml, 100 mM Tris buffer, 1 mM $CaCl_2$, 0.02% NaN_3, pH=7.8) for up to 20 days at 37ºC and resistance to enzyme measured by gravimetry.

5.2.2.7 *Shear properties*

To assess shear behavior of engineered tri-layered leaflets, 20 x 20 mm squares of fibrous scaffolds incorporating 10 x 10 mm of *spongiosa* layer were glued together using BTglue as described above. The two surfaces of glued engineered leaflets were mounted onto custom made plates using cyanoacrylate glue and mounted onto a micromechanical testing device (Mach-1 Micromechanical Systems, Biosyntech, MN) and sheared to mimic physiologic movements of valve leaflets. A deflection was applied by moving one of the shear plates with the linear positioner of the Mach-1. The shear angle was calculated by finding the arctangent of the ratio of deflection over tissue thickness. Shear force was recorded by the load cell and converted to shear stress by normalizing to the

area of specimen. Shear stress-shear angle relationships of tissues were then obtained and properties were compared to fresh valve cusps and glutaraldehyde-fixed valve cusps.

5.2.2.8 In vivo *evaluation of glued scaffolds*

Tri-layered constructs were prepared by gluing one 10 x 10 mm *spongiosa* scaffold between two fibrous layers cut between 10-15 x 10-15 mm using a 1-2 mm wide line of glue around the four sides. Samples were treated with 0.1% PGG, long wash procedure and neutralization and implanted subdermally (two implants per rat) in male juvenile Sprague-Dawley rats (n = 10) as described before [8]. High density polyethylene (HDPE) samples were also implanted as negative controls as per ISO-10993 standards (n = 3 rats) and sutured fibrous scaffolds served as controls.
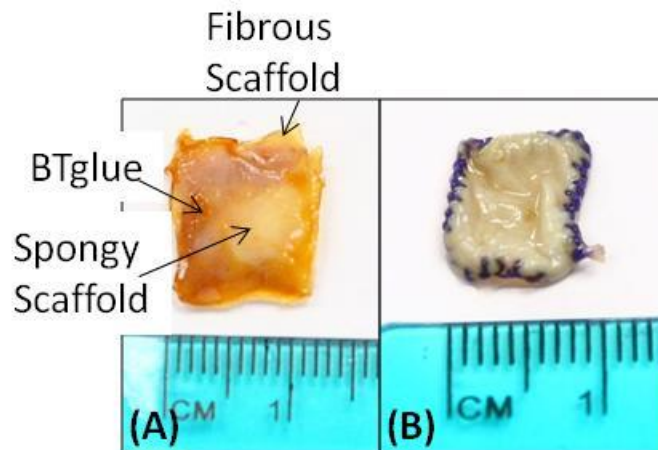

Figure 5.5: Scaffolds for implantation. (A) is a representative scaffold implanted showing the spongy scaffold between two layers of fibrous scaffold (spongy scaffold visualized due to the translucency of the fibrous scaffold. (B) shows the sutured scaffold that was implanted as a control.

The animal protocol was approved by the Animal Research Committee at Clemson University and NIH guidelines for the care and use of laboratory animals (NIH publication #86-23 Rev. 1996) were observed throughout the experiment. The rats were humanely euthanized at 5 weeks after surgery and samples retrieved for histology, calcium assay and matrix metalloproteinase (MMP) analysis [8]. To test for remote organ toxicity, liver, heart and kidney samples were collected from each animal.

For histology, paraffin sections were stained with Hematoxylin and Eosin, Masson's Trichrome and Alizarin Red stains. For identification of infiltrating cell types, immunohistochemistry was performed as described before [8] using mouse anti-rat monoclonal antibodies to macrophages (1:200 dilution, Chemicon, Temecula, CA), vimentin (1:500 dilution, Sigma, St. Louis, MO), type III collagen (1:200 dilution, Sigma, St. Louis, MO) and fibronectin (1:100 BD Labs) and sections were lightly counter-stained with Hematoxylin. As positive controls we used same antibodies to stain normal rat spleen (macrophage control) and rat skin (fibroblast control) in parallel with the explant sections.

Statistics

Results are represented as means ± the standard error of the mean (SEM). Statistical analysis was performed with one way Analysis of Variances (ANOVA) and results were considered significantly different at $p < 0.05$.

5.3   Results

5.3.1   Scaffold adhesive

Our novel scaffold adhesive (BTglue) showed good bonding strength when compared to other available medical grade glues (**Figure 5.6**) . BT-glue was five-fold stronger than fibrin glue and 20-plus stronger than silicon glue. When compared to Dermabond, a cyanoacrylate-based glue, BTglue was weaker; however, cyanoacrylates are not FDA-approved for internal use (**Figure 5.6**). Mechanical analysis revealed that the glued tri-layered leaflets were found to be stiffer than native porcine aortic leaflets but not different from glutaraldehyde-fixed porcine leaflets, and allowed shearing to lower angles (**Figure 5.7**).
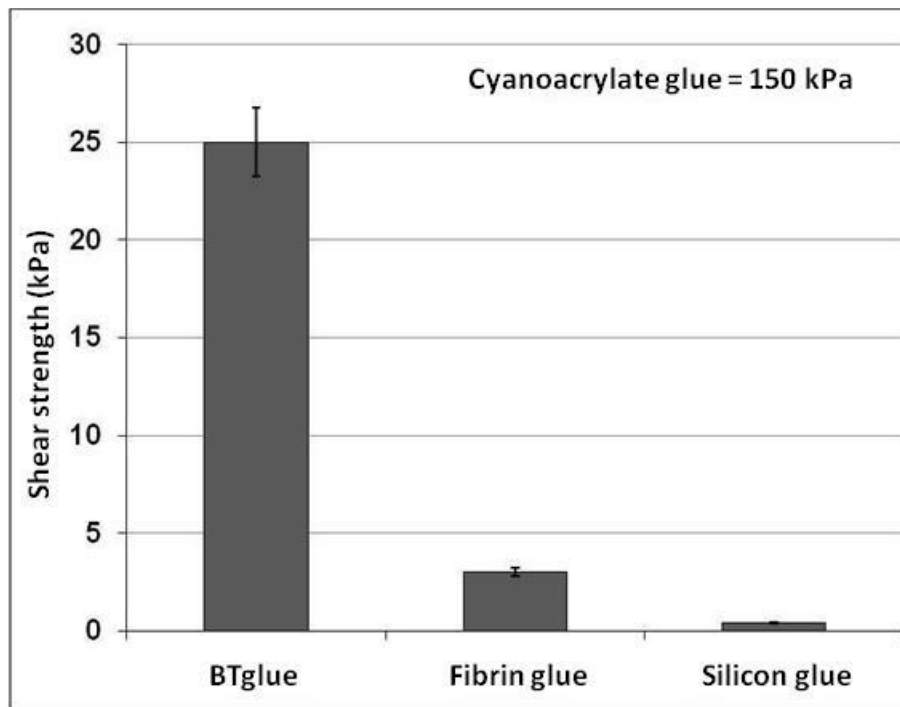

Figure 5.6: Testing of the scaffold adhesive. To test bond strength samples were glued by partial overlap subjected to pullout forces and shear strength calculated. Values are also shown for cyanoacrylate glue and fibrin glue.
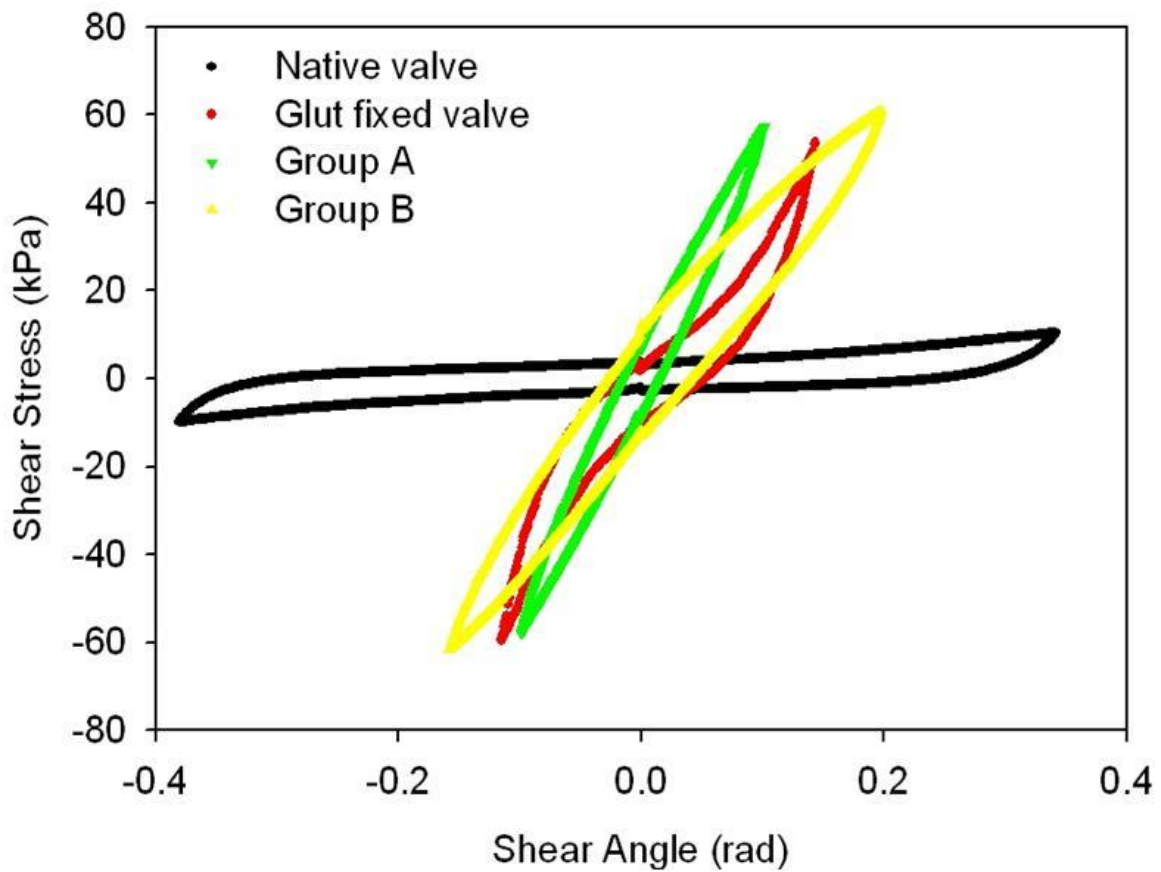
Figure 5.7. Testing of the scaffold adhesive. Test results showing shear stress-shear angle curves of the tri-layered construct; groups A and B are replicate experiments. Native porcine aortic valve leaflets and glutaraldehyde-fixed (Glut) leaflets were also plotted as a comparison (data provided by Jun Liao, University of Mississippi).

Additionally, trichrome evaluation of the samples prepared for lap shear showed glue infiltration into and between the collagen fibers of the fibrous scaffolds.
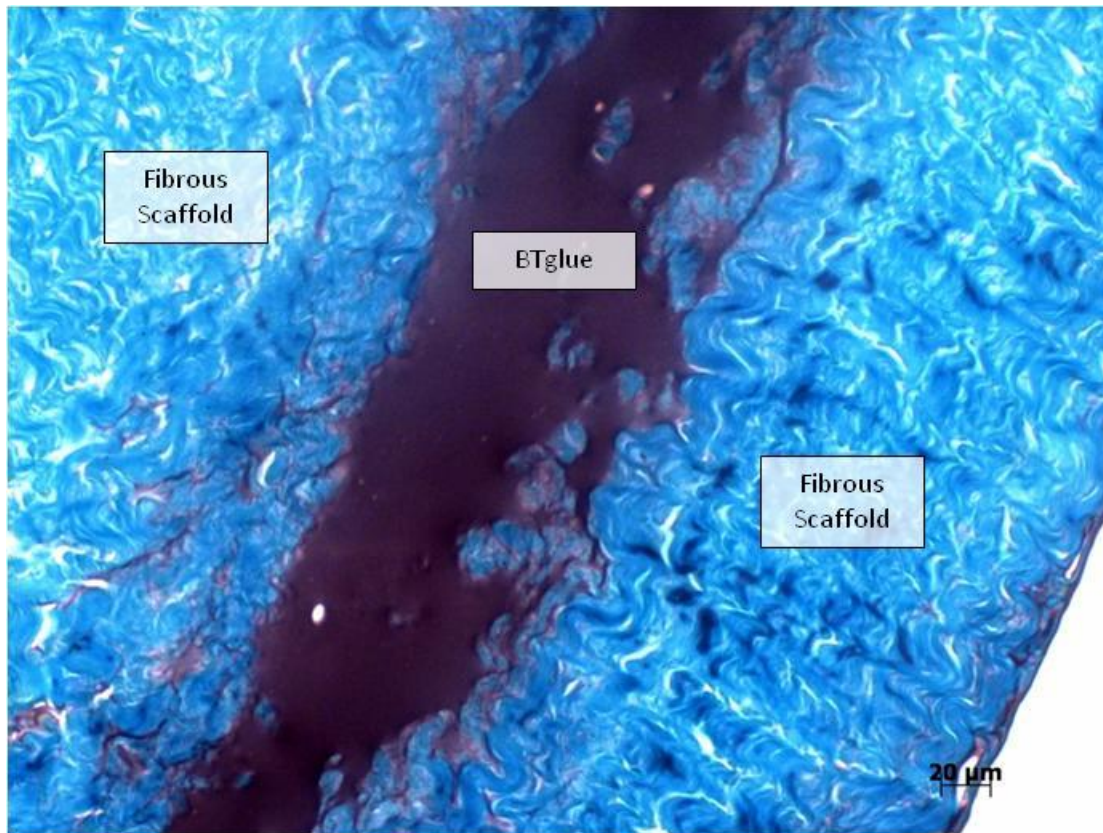
Figure 5.8: Testing of the scaffold adhesive. To test bond strength samples were glued by partial overlap subjected to pullout forces. Trichrome evaluation of these samples showed signification infiltration of the BTglue into the scaffolds and association with the collagen fibers.

BTglue was quite cytotoxic when left untreated, but was rendered very cell friendly and supported fibroblast proliferation after treatment with FBS and glycine to neutralize residual glutaraldehyde residues (**Figures 5.9, 5.10, 5.11**).
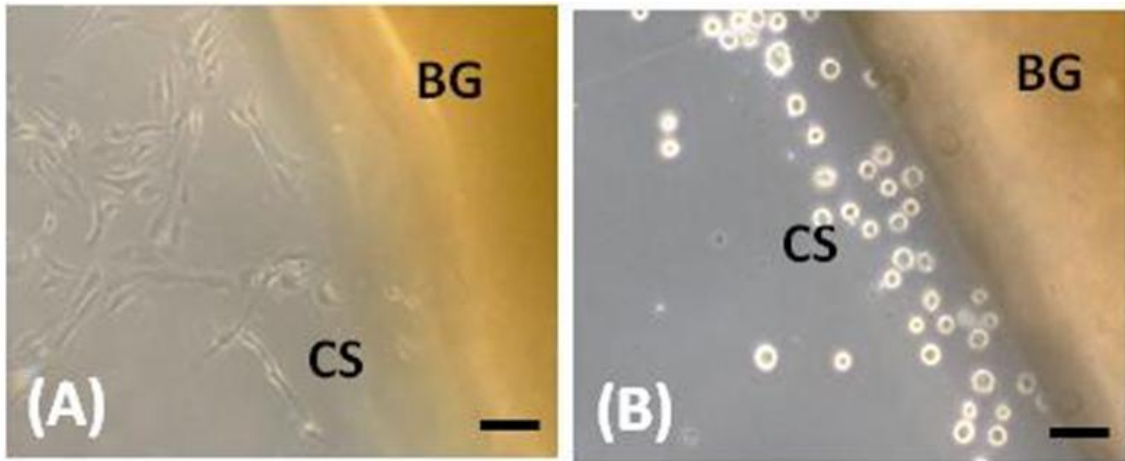
Figure 5.9: Cytotoxicity studies (A) Phase contrast image showing living cells. (B) Dead cells in glutaraldehyde-treated positive control sample. Bars are 100 μm.
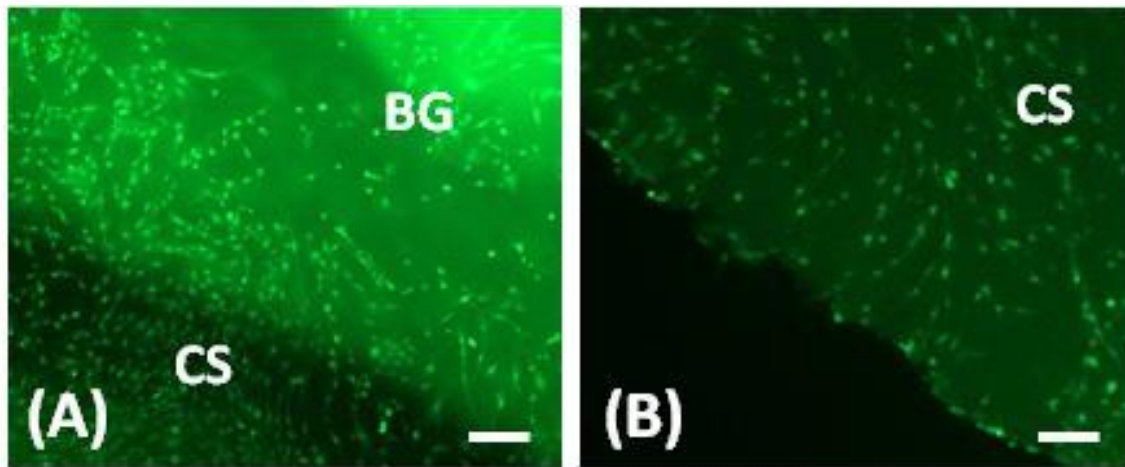
Figure 5.10: Cytotoxicity studies (A) Live cells covering both the glue and the scaffold surfaces. (B) Live cells covering the glue surface. Bars are 100 μm.
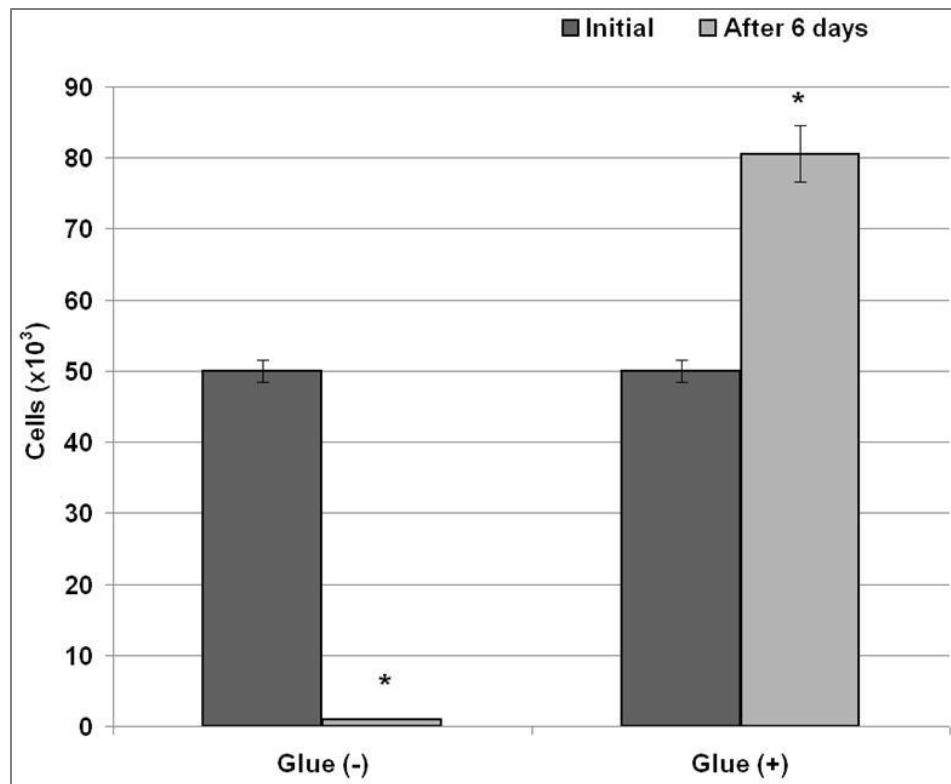
Figure 5.11: Testing BTglue cytotoxicity. Fibrous collagen scaffolds (CS) to which a single layer of BTglue (BG) was applied were neutralized with FBS/glycine solutions (+) or were used without neutralization (-) and were then seeded with fibroblasts. Cells numbers were measured at time zero and after 6 days using the MTS assay. *denotes statistical significance.

The glued pericardial constructs showed moderate resistance to collagenase (13%, 19% and 23% mass loss after 7, 14 and 20 days, respectively) possibly due to glutaraldehyde cross-linking of scaffold collagen in the gluing areas.

5.3.2 PGG cytotoxicity

To test toxicity of PGG-treated and glued samples, glued scaffolds were treated with increasing concentrations of PGG, rinsed shortly or for several days (long wash) and seeded with fibroblasts . MTS and Live/Dead results showed that long wash significantly improved cell viability as compared to the short wash protocol ($p < 0.05$) (**Figure 9,10, 12**).
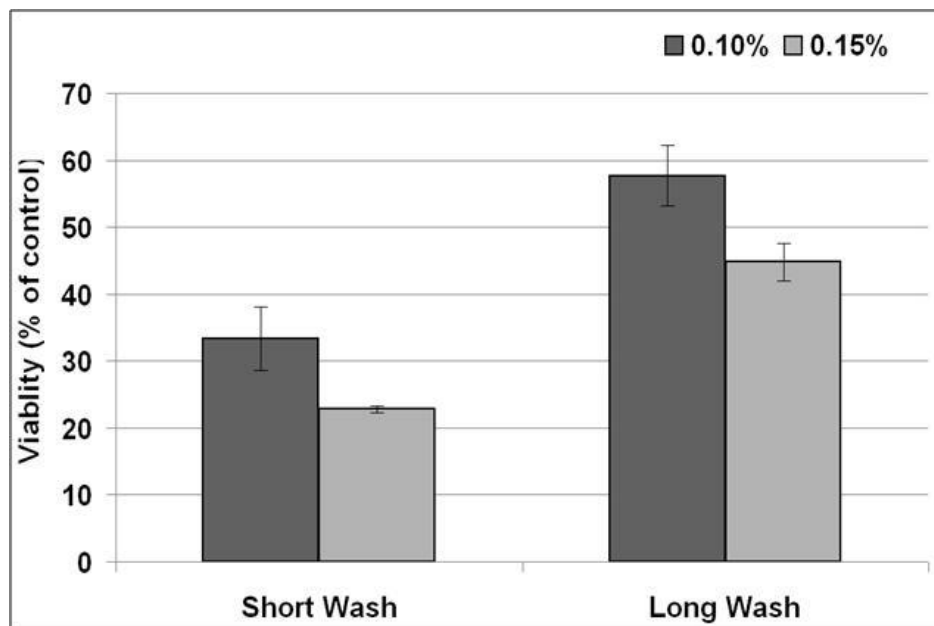
Figure 5.12: PGG toxicity testing. Fibrous collagen scaffolds (CS) to which a layer of BTglue (BG) was applied on ½ of the surface, were treated with PGG (0.1% and separately 0.15%), subjected to short wash and separately long wash procedures, neutralized with FBS/glycine and then seeded with fibroblasts. Cell numbers were measured after 5 days using the MTS assay. All values were statistically different ($p<0.05$).

Enzyme tests showed that neither treatments changed resistance to collagenase (data not shown), indicating that neutralization is not deleterious to scaffold stabilization.

5.3.3 *In vivo* studies

To evaluate biocompatibility of our tri-layered constructs we implanted samples subdermally in juvenile rats and analyzed them after 5 weeks. Animals exhibited similar weight gain ($p < 0.05$) indicating lack of systemic toxicity for all implants. In addition, histological analysis of liver, heart and kidney samples indicated lack of remote organ toxicity for all implants (data not shown). Implants were surrounded by a thin capsule and showed good integration into host subdermal tissues. As expected, negative control HDPE implants induced minimal host reactions which were limited to a very thin capsule.

Histological analysis of implanted tri-layered scaffolds revealed that scaffolds maintained their integrity and the glued areas did not separate or delaminate. The *spongiosa* scaffolds were found intact and no host cells were present inside the glued scaffold "pockets", indicating that the seal provided by the BTglue was not compromised. Host cells were present around the implants but not within the thickness of the acellular pericardium. Cells mostly associated with external collagen fibers which exhibited a "frayed" or unraveled aspect indicative of possible collagen degeneration (**Figure 5.13**). In many areas degraded collagen fibers were replaced by new matrix, as detected by Trichrome staining (**Figure 5.14**).

Figure 5.13. Implantation results. PGG-treated fibrous collagen scaffolds (CS) containing *spongiosa* scaffolds (SP) glued with BTglue (BG) were implanted subdermally and analyzed by histology after 5 weeks. (A-C) H&E stain of (A) unimplanted, and (B, C) implanted scaffolds.

Figure 5.14. Implantation results. PGG-treated fibrous collagen scaffolds (CS) containing *spongiosa* scaffolds (SP) glued with BTglue (BG) were implanted subdermally and analyzed by histology after 5 weeks. Trichrome stain (collagen blue, cells dark pink) of (D) unimplanted, and (E, F) implanted scaffolds.

Matrix metalloproteinase (MMP) activity was measured in explants from both groups using gelatin zymography (not shown); one major protease was identified in tissue extracts, namely MMP-2, migrating at around 65-80 kDa. These observations suggest that PGG-treated collagen scaffolds are not cytotoxic, are slowly degradable in vivo and may possibly support matrix remodeling. Immunohistochemistry revealed that the infiltrating cells were mainly macrophages and fibroblasts (**Figure 5.15**).
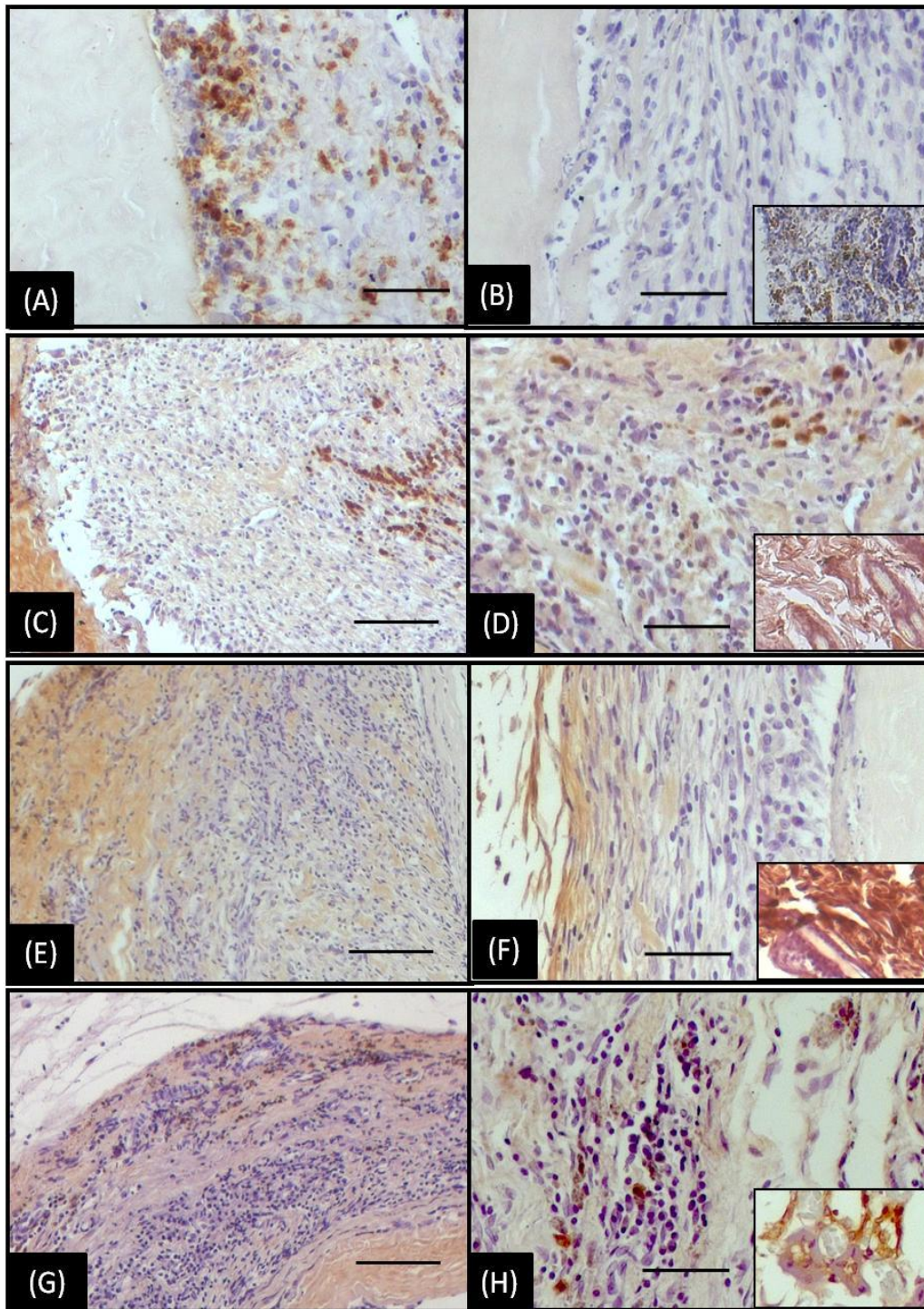
Figure 5.15: Implantation results: Immunohistochemical staining for (A,B and insert) macrophages, (C,D and insert) vimentin, (E,F and insert) collagen type III, fibronectin, (G,H and insert) showing positive results. (A,B,D,F H = 20X magnification)(C,E,G = 10x magnification)

Chemical analysis revealed a very low tendency towards calcification of our tri-layered glued constructs (5 ± 2 µg Ca/mg dry). Alizarin Red S staining confirmed these data and revealed calcium deposits in only 1 sample out of 6 analyzed (**Figure 5.16**). Calcium deposits appeared to associate with the glue and with the PGG-treated collagen scaffold in the vicinity of the BTglue suggesting that traces of glutaraldehyde may induce calcium deposition. Overall these observations support earlier data which showed that despite effective stabilization, PGG treatment does not induce collagen calcification [8].
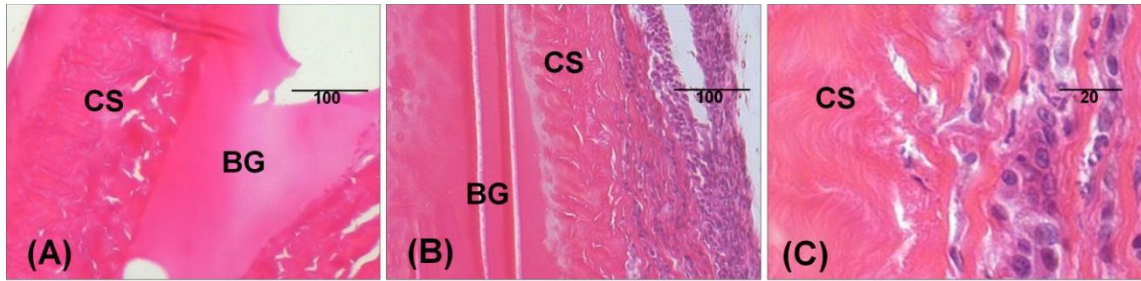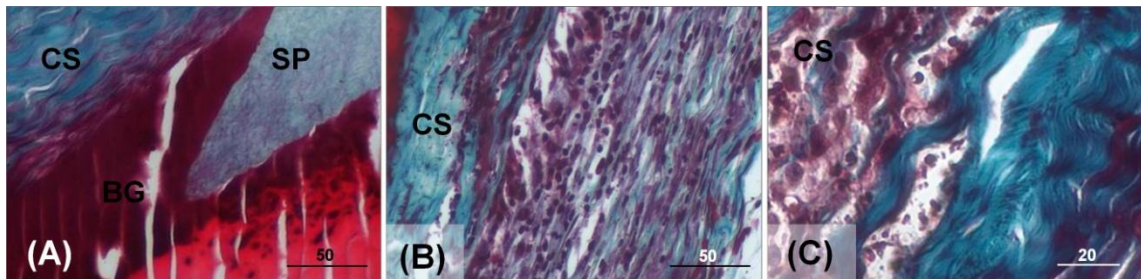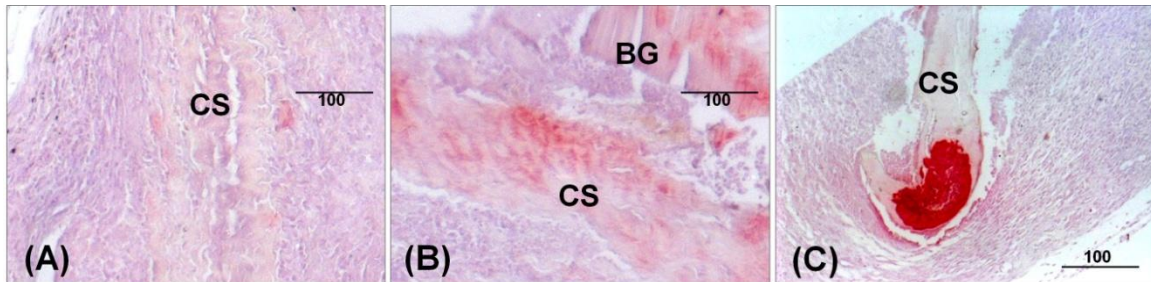

Figure 5.16: Implantation results. PGG-treated fibrous collagen scaffolds (CS) containing *spongiosa* scaffolds (SP) glued with BTglue (BG) were implanted subdermally and analyzed by histology after 5 weeks. Alizarin red stain for calcium deposits in the only sample (out of 6) which showed signs of calcification.

5.4   Discussion

For heart valve assembly, gluing techniques were developed and tested in vitro and in vivo. To our knowledge this is a first report on scaffold gluing techniques for heart valves tissue engineering. The albumin/glutaraldehyde glue has evolved conceptually from the very popular gelatin-resorcinol-formaldehyde (GRF), still in use throughout Europe and the USA [23]. Histology showed that application of the BTglue in two steps allowed albumin to first infiltrate several layers of collagen fibers within the scaffold

surfaces before application of the glutaraldehyde component. The bond strength of BTglue was found to be adequate for our applications and during shearing tests, bioreactor studies and subdermal implantation, the glue maintained its integrity, stability and an ability to seal. These tests, while elucidating the importance of a *spongiosa* layer and validating the effectiveness of the Bioglue, showed that adhering two pieces of pericardium together allowed for some shearing, revealing that the shear properties within our tissue engineered construct will rely heavily on the pulmonary artery scaffold, necessitating a tri-layered assembly. This is further substantiated by the fact that our test samples were adhered together at all edges completely by BTglue, with little spongiosa represented by the pulmonary artery scaffold. The BTglue in the shear stress-shear strain experiment represents the case by which all shearing is dependent on the amount of BTglue used, not the spongiosa. This scenario is a worst-case scenario, by which the glue makes the entire construct more stiff and influences the shear properties. This further highlights the need to perfect the glue-adherence points and amounts whereby the amount of glue and position of gluing will not have a deleterious effect on stiffness and ability of the layers to shear.

Scaffolds adhered with BTglue exhibited resistance to proteases and were easily rendered cytocompatible by neutralization. There is a possibility that the presence of glue between the *spongiosa* and *fibrosa/ventricularis* layers will inhibit homogeneous mesenchymal stem cell distribution in all three layers. To address this issue, we must optimize the assembly process to determine precise positioning of the gluing "points" and

the minimal amount of glue required to maintain integrity while allowing for cell migration within all three layers.

Upon sub-dermal implantation of the glued construct we observed one single area of calcification in close apposition with the glue, indicating that enhanced neutralization of aldehyde groups would be needed in the future. We have shown earlier that simple amines and diamines are capable of neutralizing effects of glutaraldehyde [24]. Perfecting the gluing application will also possibly alleviate this potential effect. The Glut-mediated calcification is further supported by the lack of cellular infiltration into the *spongiosa* layer. Lack of cellular infiltration can prove advantageous in future studies in which cell-seeded pulmonary artery scaffolds are inserted into the construct. The scaffold can thus serve as a immune privileged site, by which any type of cell can be seeded onto the scaffold.

In current study we used PGG as a stabilizer for the fibrous collagen scaffolds. The most effective method to create heart valve-shaped constructs from decellularized pericardium was treating dry scaffolds with PGG. In vitro studies showed that PGG, when used in concentrations higher than 0.15% could be cytotoxic [25]. To achieve an optimum balance of cell viability and scaffold stability, we chose to use 0.1% PGG followed by rinsing and neutralization. PGG treatment of the BTglue was not detrimental to gluing properties, confirming earlier studies which showed that use of glutaraldehyde in conjunction with PGG had a synergistic effect on tissue stabilization [26]. In vivo studies also showed that although most of the fibrous collagen scaffold was intact after 5 weeks implantation, there was some unraveling of the collagen fibers on the outside

edges of the implants associated with infiltration of macrophages, fibroblasts and signs of remodeling.

5.5 Conclusions

This study is a stepping stone towards development of a novel approach to heart valve tissue engineering. Recognizing the importance of each of the three layers in a native aortic heart valve, we have taken one step towards this goal by utilizing a bioadhesive that may hold the layers together. The BTglue was found to possess the mechanical properties necessary to maintain adhesion of the layers together while at the same time allowing cellular survival and growth on our glued scaffolds. This technique of adhering different scaffolds together to form a single tri-layered construct thus holds promise for applications in heart valve tissue engineering.

5.6 References

1.   Talman, E.A. and D.R. Boughner, *Glutaraldehyde fixation alters the internal shear properties of porcine aortic heart valve tissue.* Ann Thorac Surg, 1995. **60**(2 Suppl): p. S369-73.

2.   Talman, E.A. and D.R. Boughner, *Internal shear properties of fresh porcine aortic valve cusps: implications for normal valve function.* J Heart Valve Dis, 1996. **5**(2): p. 152-9.

3.   Schoen, F.J. and R.J. Levy, *Tissue heart valves: current challenges and future research perspectives.* J Biomed Mater Res, 1999. **47**(4): p. 439-65.

4.   Vesely, I., D. Boughner, and T. Song, *Tissue buckling as a mechanism of bioprosthetic valve failure.* Ann Thorac Surg, 1988. **46**(3): p. 302-8.

5.   Yacoub, M., *Viewpoint: Heart valve engineering. Interview by James Butcher.* Circulation, 2007. **116**(8): p. f44-6.

6. Sutherland, F.W., et al., *From stem cells to viable autologous semilunar heart valve.* Circulation, 2005. **111**(21): p. 2783-91.

7. Robinson, P.S., et al., *Functional tissue-engineered valves from cell-remodeled fibrin with commissural alignment of cell-produced collagen.* Tissue Eng Part A, 2008. **14**(1): p. 83-95.

8. Tedder, M.E., et al., *Stabilized collagen scaffolds for heart valve tissue engineering.* Tissue Eng Part A, 2009. **15**(6): p. 1257-68.

9. Liao, J., et al., *Molecular orientation of collagen in intact planar connective tissues under biaxial stretch.* Acta Biomater, 2005. **1**(1): p. 45-54.

10. Obermiller, J.F., et al., *A comparison of suture retention strengths for three biomaterials.* Med Sci Monit, 2004. **10**(1): p. PI1-5.

11. Oswal, D., et al., *Biomechanical characterization of decellularized and cross-linked bovine pericardium.* J Heart Valve Dis, 2007. **16**(2): p. 165-74.

12. Simionescu, D., A. Simionescu, and R. Deac, *Mapping of glutaraldehyde-treated bovine pericardium and tissue selection for bioprosthetic heart valves.* J Biomed Mater Res, 1993. **27**(6): p. 697-704.

13. Simionescu, D., R.V. Iozzo, and N.A. Kefalides, *Bovine pericardial proteoglycan: biochemical, immunochemical and ultrastructural studies.* Matrix, 1989. **9**(4): p. 301-10.

14. Simionescu, D.T. and N.A. Kefalides, *The biosynthesis of proteoglycans and interstitial collagens by bovine pericardial fibroblasts.* Exp Cell Res, 1991. **195**(1): p. 171-6.

15. Deac, R.F., D. Simionescu, and D. Deac, *New evolution in mitral physiology and surgery: mitral stentless pericardial valve.* Ann Thorac Surg, 1995. **60**(2 Suppl): p. S433-8.

16. Isenburg, J.C., et al., *Structural requirements for stabilization of vascular elastin by polyphenolic tannins.* Biomaterials, 2006. **27**(19): p. 3645-51.

17. Azimzadeh, A., et al., *Comparative study of target antigens for primate xenoreactive natural antibodies in pig and rat endothelial cells.* Transplantation, 1997. **64**(8): p. 1166-74.

18.   Strokan, V., et al., *Heterogeneous expression of Gal alpha1-3Gal xenoantigen in pig kidney: a lectin and immunogold electron microscopic study.* Transplantation, 1998. **66**(11): p. 1495-503.

19.   Daly, K.A., et al., *Effect of the alphaGal epitope on the response to small intestinal submucosa extracellular matrix in a nonhuman primate model.* Tissue Eng Part A, 2009. **15**(12): p. 3877-88.

20.   McPherson, T.B., et al., *Galalpha(1,3)Gal epitope in porcine small intestinal submucosa.* Tissue Eng, 2000. **6**(3): p. 233-9.

21.   Raeder, R.H., et al., *Natural anti-galactose alpha1,3 galactose antibodies delay, but do not prevent the acceptance of extracellular matrix xenografts.* Transpl Immunol, 2002. **10**(1): p. 15-24.

22.   Schoen, F.J., *Cardiac valves and valvular pathology - Update on function, disease, repair, and replacement.* Cardiovascular Pathology, 2005. **14**(4): p. 189-194.

23.   Chao, H.H. and D.F. Torchiana, *BioGlue: albumin/glutaraldehyde sealant in cardiac surgery.* J Card Surg, 2003. **18**(6): p. 500-3.

24.   Simionescu, A., D. Simionescu, and R. Deac, *Lysine-enhanced glutaraldehyde crosslinking of collagenous biomaterials.* J Biomed Mater Res, 1991. **25**(12): p. 1495-505.

25.   Isenburg, J.C., et al., *Elastin stabilization for treatment of abdominal aortic aneurysms.* Circulation, 2007. **115**(13): p. 1729-37.

26.   Isenburg, J.C., D.T. Simionescu, and N.R. Vyavahare, *Tannic acid treatment enhances biostability and reduces calcification of glutaraldehyde fixed aortic wall.* Biomaterials, 2005. **26**(11): p. 1237-45.

MOLDING, ASSEMBLY, AND BIOREACTOR TESTING OF TRI-LAYERED TISSUE ENGINEERED HEART VALVES
(AIM 3)

6.1   Introduction

Our novel strategy relies on use of stabilized collagen scaffolds that mimic the natural valve fibrous layers, based on decellularized porcine pericardium [8] and delicate, highly hydrated porous collagen scaffolds to be used as the middle *spongiosa* layer. Chemically stabilized pericardium has outstanding mechanical properties, a good record of implantation in humans as valves, and as reconstructive surgery biomaterial patches in other organs [9-15]. To reduce scaffold biodegradation, we have also investigated the use of penta-galloyl glucose (PGG), a naturally derived collagen-binding polyphenol [8, 16]. No reports to date have documented the use of PGG-stabilized acellular pericardium for construction of tissue engineered heart valves. Since the xenoantigen Galα1-3Gal (Galα), is responsible for rejection of vascularized organ transplants we are paying special attention to Galα detection in decellularized scaffolds [17-21].

Recognizing the outstanding mechanical performance of natural valve homografts, the vital importance of the three leaflet layers [22], and the need for reconstruction of the physiologic valve design, we developed five building blocks for this new approach: a) partially stabilized collagenous scaffolds which degrade slowly with time, b) anatomically analogous 3-D heart valve shapes made from solid molds, c) tri-layered constructs that mimic the native heart valve histo-architecture, d) autologous multipotent mesenchymal stem cells for repopulation and remodeling and e) mechanical

cues to induce stem cell differentiation into valvular cells capable of maintaining matrix homeostasis.

In current study we describe development of molds to be used as the forms on which to layer the 2 scaffolds we have developed and the utilization of our biological BTglue to assemble the tri-layered constructs.

6.2   **Materials/Methods**

6.2.1   **Materials**

High purity 1,2,3,4,6-Penta-O-galloyl-beta-D-glucose (penta-galloyl-glucose, PGG) was a generous gift from N.V. Ajinomoto OmniChem S.A., Wetteren, Belgium (www.omnichem.be). Silicone was obtained from Copy Flex Liquid Silicone, Cincinnati, OH (www.makeyourownmolds.com).

6.2.2   **Methods**

6.2.2.1 *Construction of molds for anatomically correct valves*

Whole porcine hearts collected at a local abattoir were brought to the lab on ice, rinsed with saline, and aortic and pulmonary valves dissected together with preservation of the entire anatomy of the cardiac base. Valves were then fixed for 48 hours in 0.6% glutaraldehyde (Glut) in 50 mM 4-(2-hydroxyethyl)-1-piperazineethanesulfonic acid buffered saline (pH=7.4) at 22ºC. At the onset of fixation the aortic heart valve cusps were lightly stuffed with Glut-imbibed cotton balls to maintain the valve in closed position. After removal of the cotton balls and rinsing, liquid Silicone (Copy Flex Liquid

Silicone, Cincinnati, OH) was poured into the aortic valve via the ascending aorta, while the coronaries were plugged to prevent leakage with pegs made from the silicone, and the silicone allowed to harden for 24 hours at room temperature. Final molds could easily be removed from the aorta.

After removal of the mold, a negative mold was formed in which the collagen scaffold could be pressed between to form the shape of the aortic valve. Briefly, the initial mold was coated with a silicone grease, to allow for easy removal) and placed into a specimen cup filled with approximately 80 mls of silicone. The silicone was allowed to harden for 24 hours at room temperature. Finally, the mold was easily extracted from the specimen cup leaving an exact negative mold of the molded aortic valve in the specimen cup. The specimen cup was then cut away from the negative mold.

6.2.2.2 *Construction of single layer, anatomically correct valves*

Fibrous collagen scaffolds prepared from porcine pericardium (see Chapter 4) were placed onto the molds, with the fibrous side of the pericardium in direct contact to the mold, and then the mold s pressed into the negative mold to ensure complete shaping of the collagen scaffold. After removal of the mold from the counter mold, the collagen scaffold was adhered to the counter mold with pins in the central gap, along the edges of the cusp, and along the base of the valve and air dried for 48 hours in a sterile bio-hood. The dried scaffold was then removed and fixed with 0.3% PGG for 24 hours. After fixation, the individual leaflets were separated by incisions to result in the 3 distinct leaflets. To test functionality of the heart valve-shaped fibrous scaffolds they were

148

mounted onto a silicone mock aorta support in a home-made pulse duplicator heart valve bioreactor tester system (described in detail in manuscript by Leslie Sierad et. al. accepted to Cardiovascular Engineering and Technology, May 2010). and cycled at about 1 Hz. Still frames were captured from digital movies using video editing software (VideoStudio 9, ULead Systems Inc., Torrance, CA).

6.2.2.3 *Construction of tri-layered, tissue engineered valves*

To test the association of the 3 layers and create layered constructs that resemble the valve histo-architecture, two sheets of fibrous pericardial scaffolds were superimposed and a small sheet of spongy scaffold was entrapped between the two fibrous scaffolds. The edges were then sealed by staples.

To create the histologically and anatomically correct scaffold constructs, molds formed above were used for the following purposes. Two fibrous collagen scaffolds prepared from porcine pericardium (described above) were placed onto negative molds (with fibrous sides placed together) and air dried for 48 hours in a sterile bio-hood. The scaffold was then separated and dissected at the level of the cusps. The two identical valve-shaped scaffolds were overlapped (with fibrous sides placed together again) and assembled by applying BTglue to the entire scaffold surface corresponding to the aorta and the sinuses, leaving the cusps un-attached. For bioreactor testing, the original porcine aortic root (from which the mold was cast) was rinsed in saline, the three native valve cusps excised by dissection and the assembled engineered valve was secured inside the aortic root using sutures and BTglue. To test functionality of the constructs they were

mounted onto our heart valve bioreactor. The device consists of a valve mounting ring assembly encased between a ventricular chamber and an aortic chamber filled with cell culture medium. The medium is pushed through the valve by a flexible silicone membrane diaphragm connected to an air pump. Extensive testing has shown that the bioreactor ensures comparable pumping functions to a living heart (data not shown-see A Pulsatile Bioreactor for Conditioning Tissue Engineered Heart Valves, MS Thesis by Leslie Sierad, Clemson University, May 2009). The tissue engineered valve was subjected to open-close cycles at 60 beats per minute, 40/20 mmHg, 10 mL stroke volume, at 37 ^{0}C, 5% CO_2 for 8 days. Cusp movements and still frames were captured with a Logitech webcam.

6.3   Results

6.3.1   *Construction of molds for anatomically correct valves*

The long term aim of our studies is to create anatomically correct scaffolds to be used as off-the-shelf constructs for heart valve tissue engineering. To create structures that mimic the heart valve anatomy, we used silicon molds from porcine heart valves.

Figure 6.1: Construction of molds for anatomically correct valves. Silicone molds were prepared from porcine heart valves.

Figure 6.2: Construction of molds for anatomically correct valves. Silicone molds were prepared from porcine heart valves seen in **Figure 6.1**. RC – right coronary; LC – left coronary; a, b, c – the three leaflets.

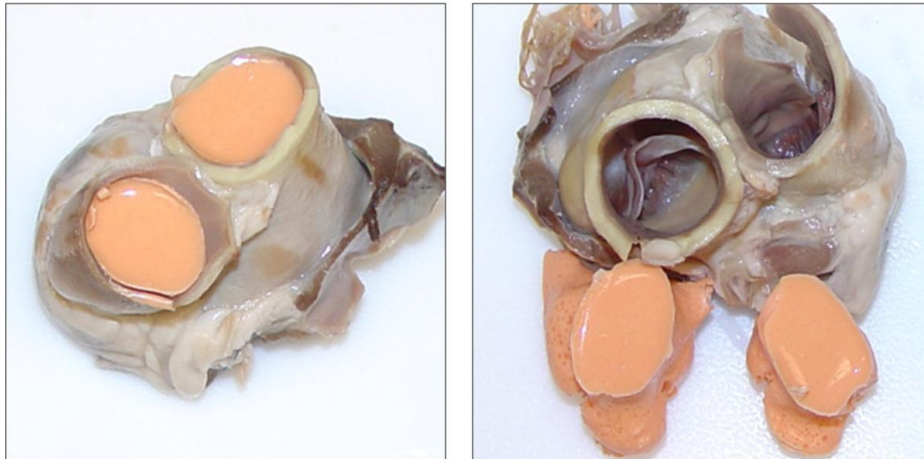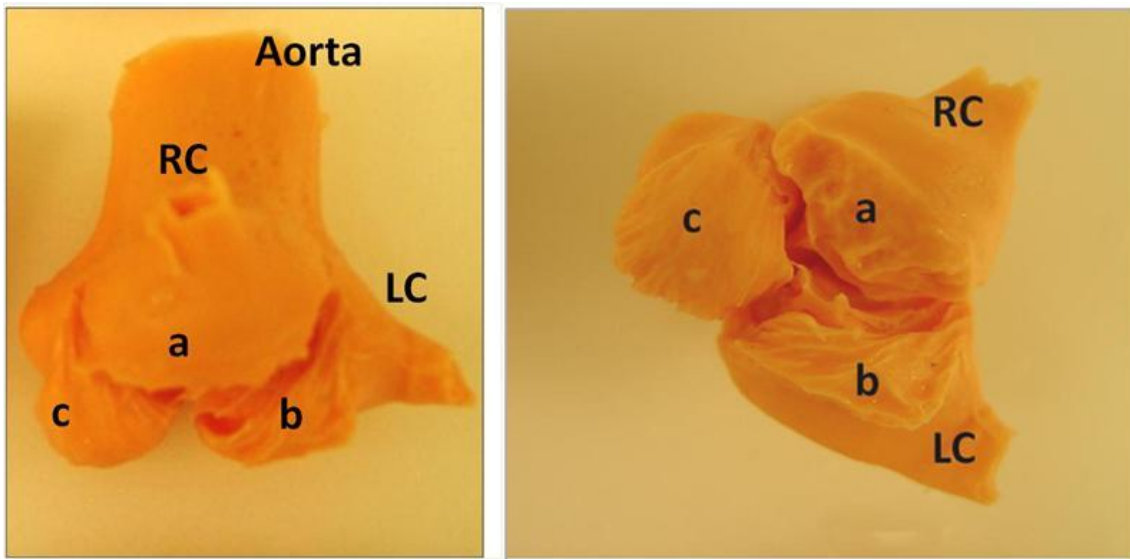The negative molds were then formed from the direct molds of the porcine aortic valves.
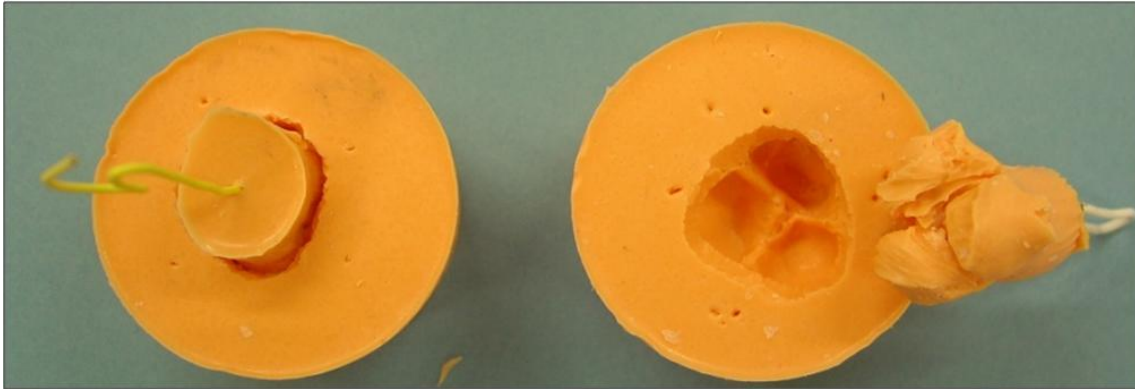
Figure 6.3: Construction of molds for anatomically correct valves. Silicone molds were prepared from porcine heart valves seen in **Figure 6.1** and negative molds were formed from the direct aortic valve molding.

6.3.2   *Construction of single layer, anatomically correct valves*

Scaffolds dried onto such molds adopted the valve structure down to very fine details (**Figure 6.4**). This shape was maintained after rehydration and PGG stabilization. The scaffold obtained a yellowish tint upon PGG fixation (**Figure 6.5**). The single-layer valve was then mounted in our custom made bioreactor (**Figure 6.6, 6.7**) and functioned acceptably in a pulse duplicator system (**Figure 6.8**).
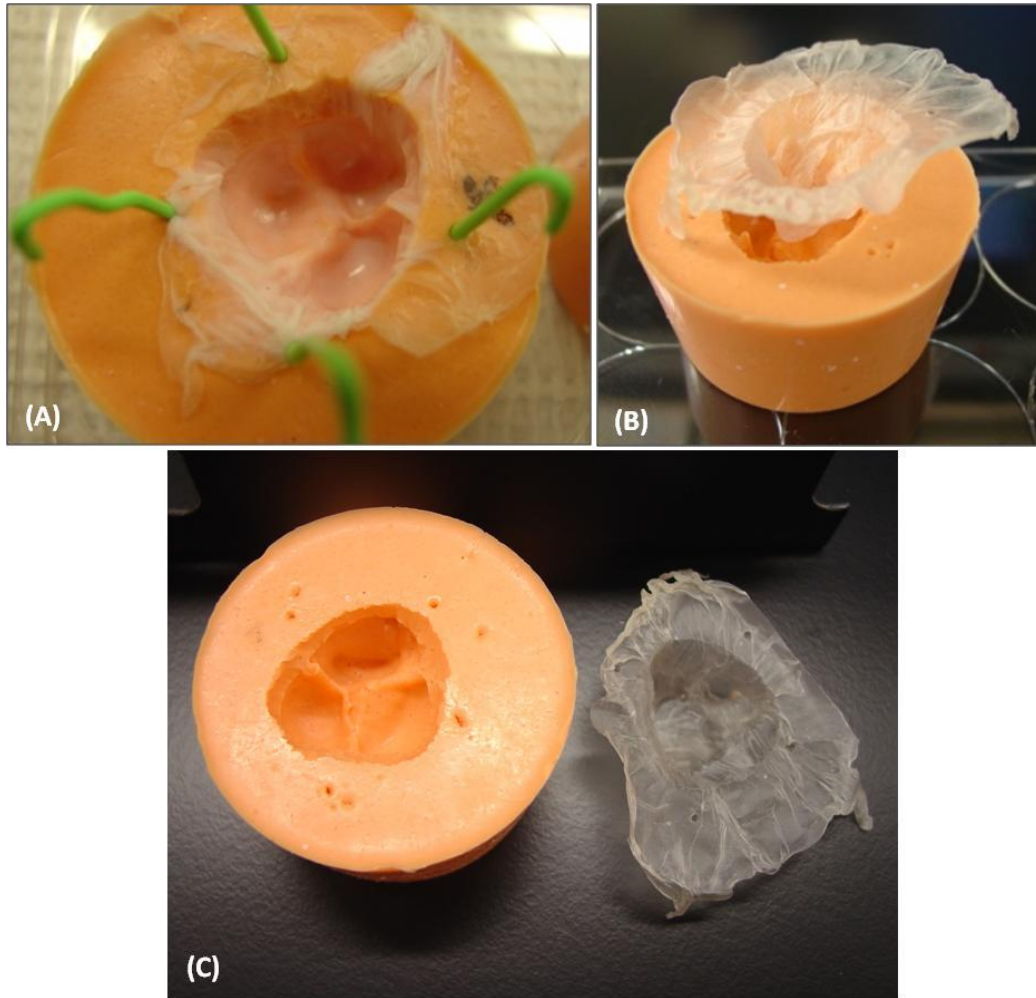
Figure 6.4: Construction of Single Layer, anatomically correct valves. Wet fibrous scaffolds (A) were dried onto molds. Upon removal, they retained the shape of the aortic valve, with the fine finistrations of the mold (B and C).
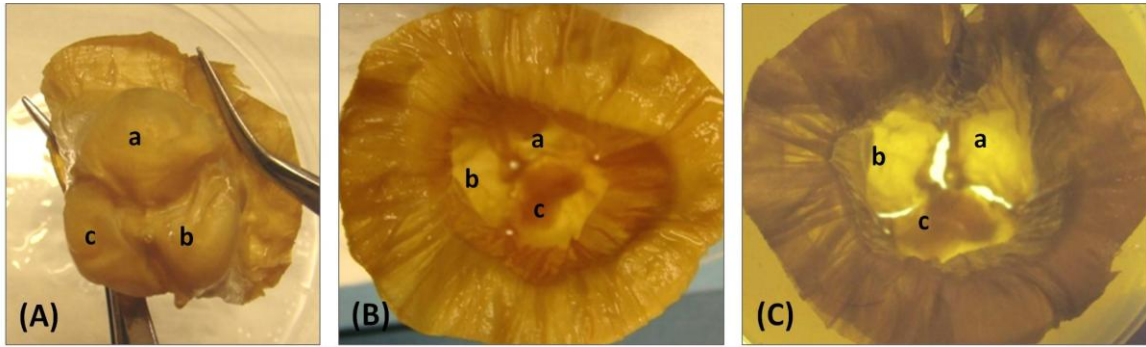
Figure 6.5: Construction of Single Layer, anatomically correct valves. Rehydrated/PGG fixed scaffold with the 3 leaflets dissected (C). (A) shows the ventricular side, while (B) shows the aortic side of the valve. RC – right coronary; LC – left coronary; a, b, c – the three leaflets.
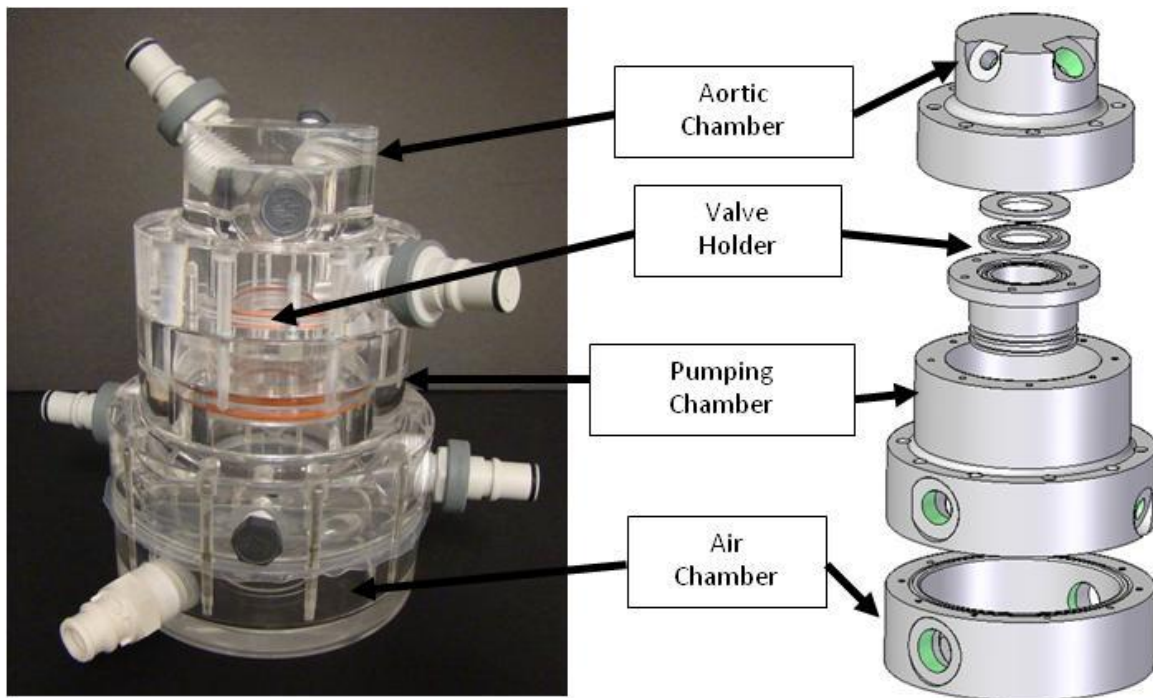
Figure 6.6: Picture and computer aided drafting representation of assembled bioreactor. (adapted from Leslie Sierad)
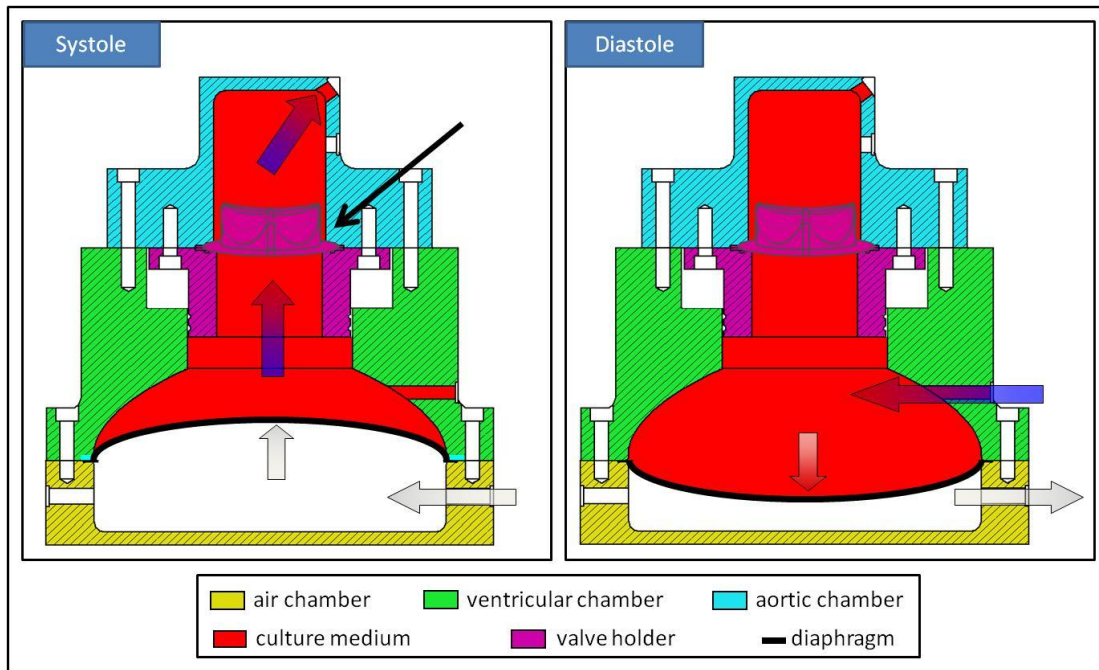
Figure 6.7: Cross-sectional view of the bioreactor demonstrating the pumping actions during systole and diastole. Black arrow signifies where the tissue engineered valve is mounted (Courtesy of Lee Sierad).
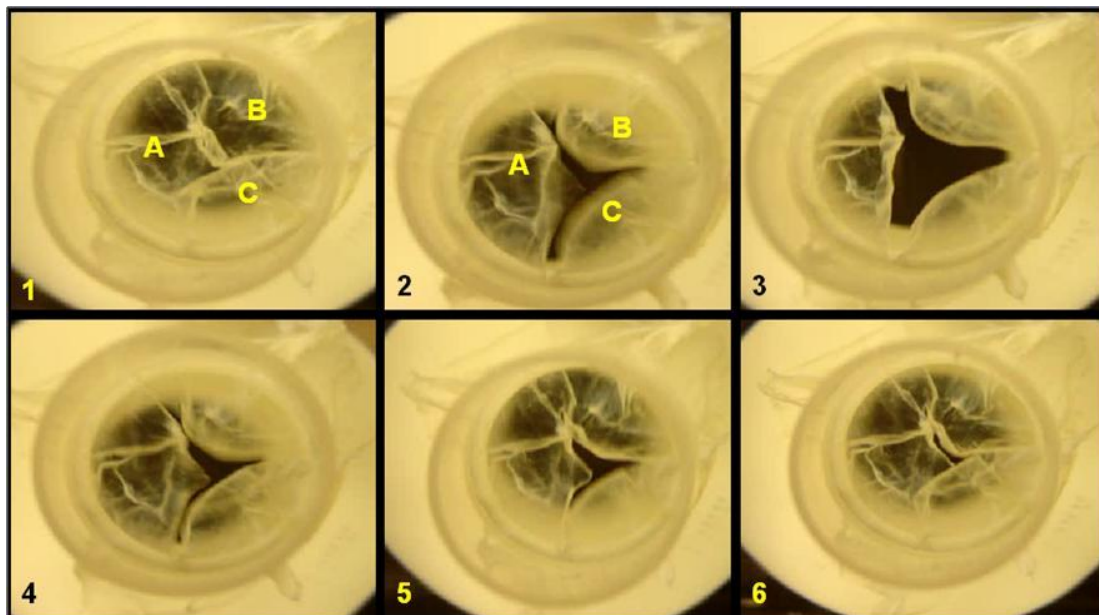
Figure 6.8: Still frames acquired from digital movies of a valve-shaped fibrous scaffold tested for functionality. The three leaflets are labeled A, B, and C.

6.3.3   *Construction of tri-layered, tissue engineered valves*

The long term aim of our studies is to build not only anatomically correct scaffolds but these scaffolds must be histologically correct structures for heart valves. To this end we have used different collagen scaffolds to form the 3 layers of the native aortic valve.

Histological analysis showed a unique tri-layered of the tri-layered structure resembling the heart valve histo-architecture (**Figure 6.9**) where a spongiosa layer (S) is entrapped between two fibrous layers (F).
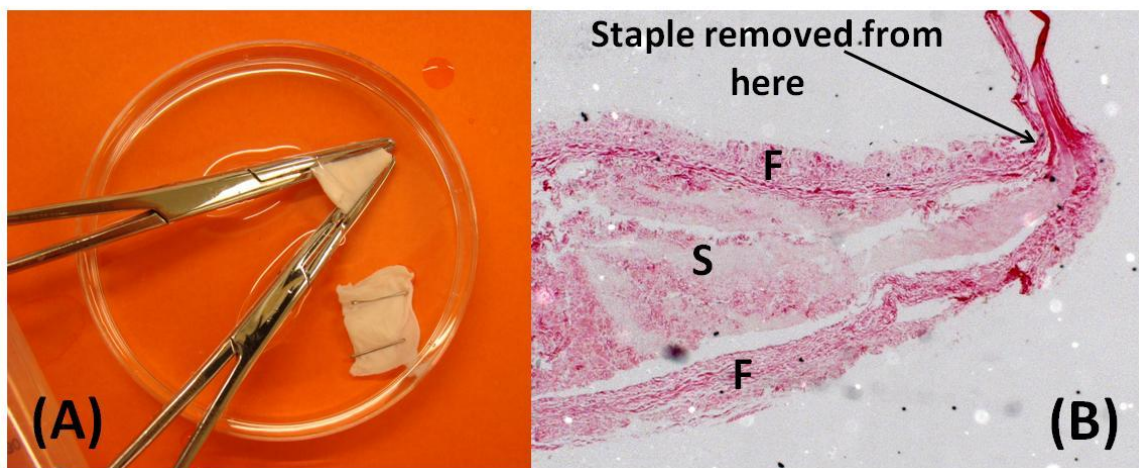
Figure 6.9: Tri-layered scaffolds made by entrapping a sheet of spongy (S) scaffold between two fibrous (F) scaffolds and edges sealed by staples (A). Histology and H&E stain (2.5 x) showed a fair resemblance to natural heart valve structure (B).

Thickness of fibrous scaffold is 0.125 +/- 0.005 mm (mean +/- SEM for n=40), and thus the total thickness of tri-layered scaffolds is expected to be less than 0.5 mm (3 x 0.124).

For making anatomically correct tri-layered constructs, after drying the two fibrous scaffolds on their molds, the scaffolds have acquired the shape of the aortic valve including the very delicate details of the 3D corrugations, which could then be preserved permanently by stabilization with PGG (see **Figure 6.4** and **6.5**). Two identical valve-shaped scaffolds were then overlapped and assembled using BTglue (**Figure 6.10**). The entire construct was then sutured into the aortic root from which the silicone mold shape was originally acquired. The reconstructed valve fit flawlessly within the natural root (**Figure 6.10** and **6.11**).

Functionality testing of the heart valve-shaped scaffolds showed good leaflet coaptation upon closure and adequate opening characteristics (**Figure 6.11**).
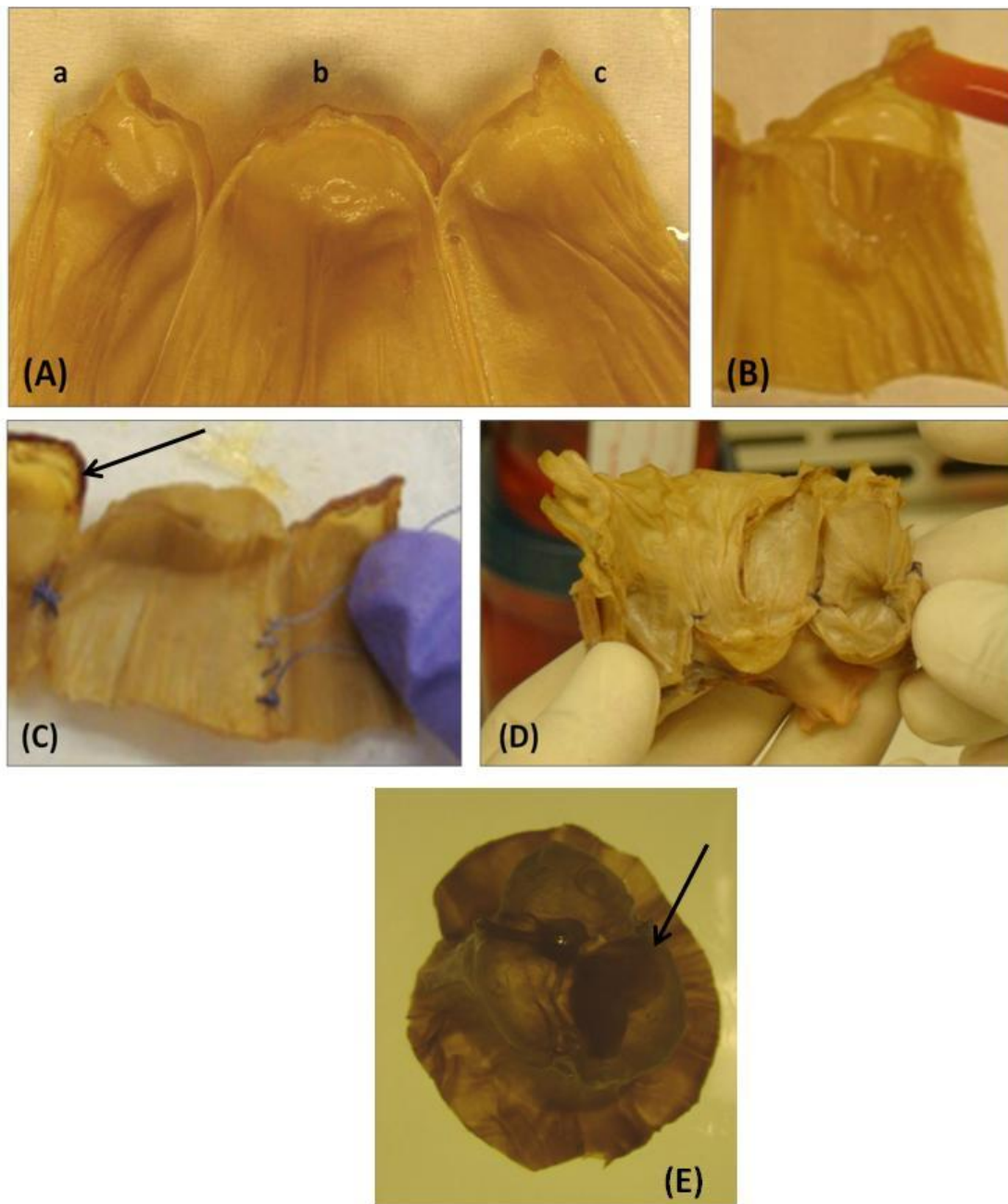
Figure 6.10: Valve-shape constructs were assembled by overlapping two identical fibrous scaffolds (A and B) and inserting a piece of spongy scaffold between the two layers (E, arrow shows spongy scaffold). BTglue was used at the open edges of the cusps (arrow in C) and both BTglue and sutures were placed at the level of valve wall, sinuses and cusp insertion points (D).
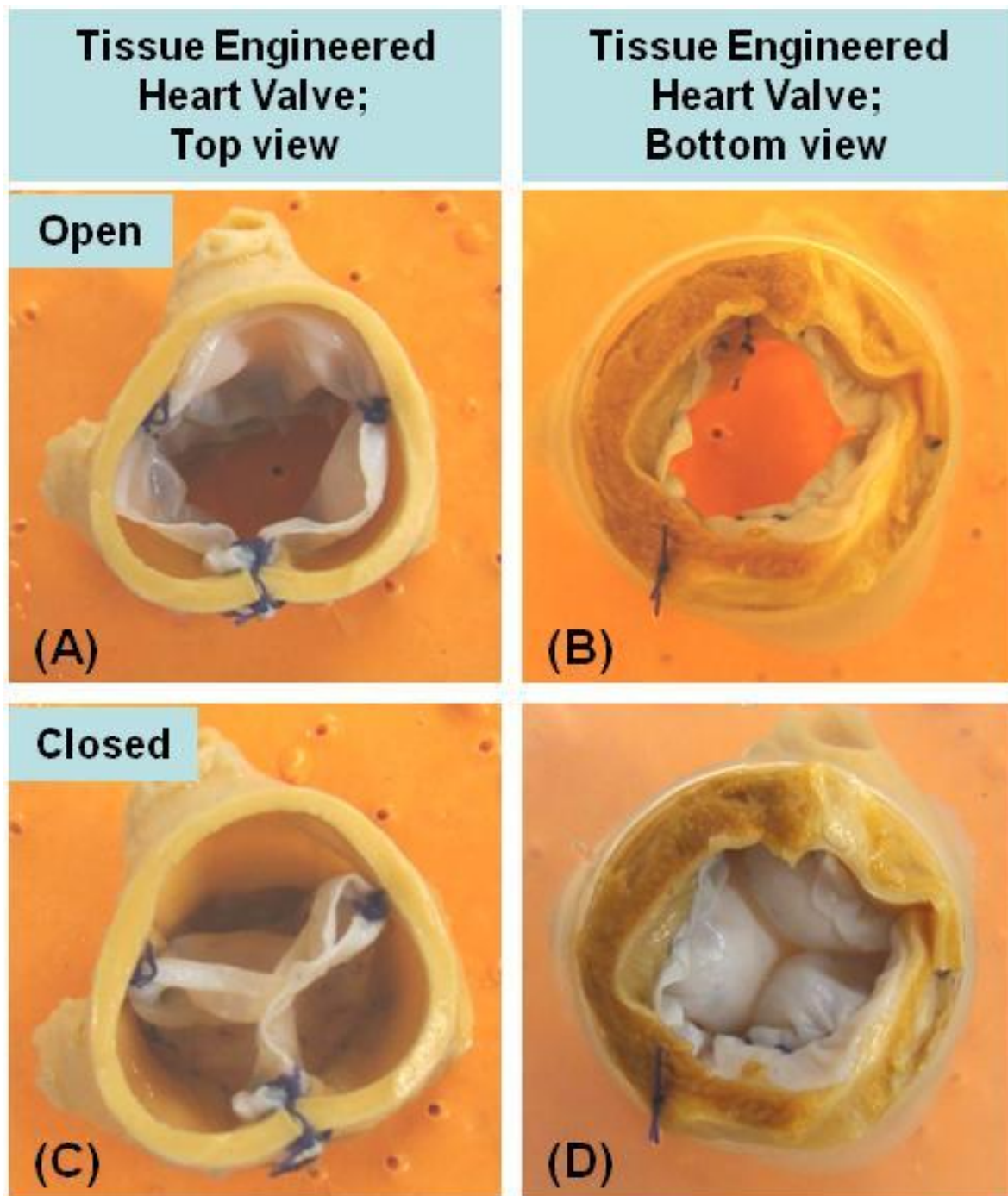
Figure 6.11: Tri-layered tissue engineered heart valve sutured inside a porcine aortic root.   (A,C) are top view and (B,D) are bottom view.
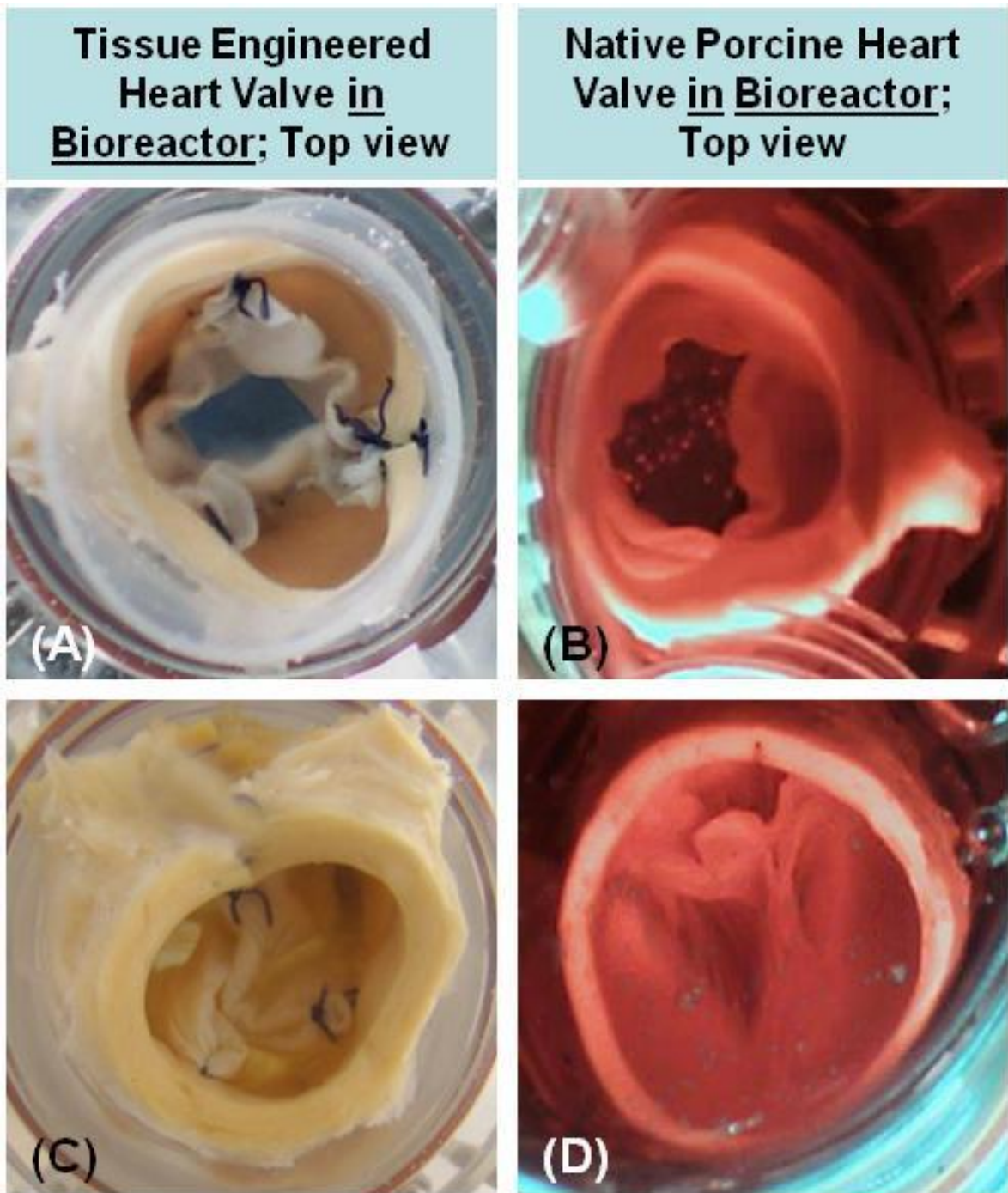
Figure 6.12: Bioreactor testing of the tissue engineered heart valve (A,C) showing comparable function to a living porcine aortic heart valve (B,D).

6.4   Discussion

The long term aim of our studies is to create anatomically correct scaffolds to be used as off-the-shelf constructs for heart valve tissue engineering. For this purpose we created silicone molds from porcine aortic heart valves and then modeled decellularized porcine pericardium into anatomically correct scaffolds. After drying them in their molds, the scaffolds have acquired the shape of the aortic valve including the very delicate details of the 3D corrugations, which could then be preserved by exposure to PGG. Two identical valve-shaped scaffolds were then overlapped and assembled using BTglue and sutured into the aortic root from which the silicone mold shape was originally acquired, to mimic a potential clinical scenario. Functionality testing of the heart valve-shaped scaffolds showed good leaflet coaptation upon closure and good opening characteristics . However, there is a possibility that the presence of glue between the spongiosa and fibrosa/ventricularis layers will inhibit homogeneous mesenchymal stem cell distribution in all three layers. To address this issue, we are currently optimizing the assembly process to determine precise positioning of the gluing "points" and the minimal amount of glue required to maintain integrity while allowing for cell migration within all three layers.

In an envisioned clinical scenario (see Project Rationale for complete details), imaging data obtained from the patient's valve would be translated into solid molds using a stereolithography system and the solid molds used for valve construction. Our current approach of using solid molds formed by pouring liquid silicone into an intact valve will obviously not be useful in a clinical setting, but our proof of concept work with the solid

molds demonstrates that our scaffolds can be fashioned into anatomically and histologically valve constructs comparable to the native aortic valve.

6.5   Conclusions

This study is a stepping stone towards development of a novel approach to heart valve tissue engineering. We utilized two types of acellular collagen scaffolds, a flat collagen sheet of high tensile strength and malleability and a highly hydrated scaffold that mimics valvular *spongiosa* layer. The scaffolds were assembled into anatomically analogous 3-D heart valve shapes using novel protein-based glue and tested in our custom-made bioreactor for functionality. While many aspects and details need to be optimized as far as scaffold assembly and animal testing are concerned, this approach appears promising for our envisioned translational scenario.

6.6   References

1.   Talman, E.A. and D.R. Boughner, *Glutaraldehyde fixation alters the internal shear properties of porcine aortic heart valve tissue.* Ann Thorac Surg, 1995. **60**(2 Suppl): p. S369-73.

2.   Talman, E.A. and D.R. Boughner, *Internal shear properties of fresh porcine aortic valve cusps: implications for normal valve function.* J Heart Valve Dis, 1996. **5**(2): p. 152-9.

3.   Schoen, F.J. and R.J. Levy, *Tissue heart valves: current challenges and future research perspectives.* J Biomed Mater Res, 1999. **47**(4): p. 439-65.

4.   Vesely, I., D. Boughner, and T. Song, *Tissue buckling as a mechanism of bioprosthetic valve failure.* Ann Thorac Surg, 1988. **46**(3): p. 302-8.

5.   Yacoub, M., *Viewpoint: Heart valve engineering. Interview by James Butcher.* Circulation, 2007. **116**(8): p. f44-6.

6.   Sutherland, F.W., et al., *From stem cells to viable autologous semilunar heart valve.* Circulation, 2005. **111**(21): p. 2783-91.

7.   Robinson, P.S., et al., *Functional tissue-engineered valves from cell-remodeled fibrin with commissural alignment of cell-produced collagen.* Tissue Eng Part A, 2008. **14**(1): p. 83-95.

8.   Tedder, M.E., et al., *Stabilized collagen scaffolds for heart valve tissue engineering.* Tissue Eng Part A, 2009. **15**(6): p. 1257-68.

9.   Liao, J., et al., *Molecular orientation of collagen in intact planar connective tissues under biaxial stretch.* Acta Biomater, 2005. **1**(1): p. 45-54.

10.   Obermiller, J.F., et al., *A comparison of suture retention strengths for three biomaterials.* Med Sci Monit, 2004. **10**(1): p. PI1-5.

11.   Oswal, D., et al., *Biomechanical characterization of decellularized and cross-linked bovine pericardium.* J Heart Valve Dis, 2007. **16**(2): p. 165-74.

12.   Simionescu, D., A. Simionescu, and R. Deac, *Mapping of glutaraldehyde-treated bovine pericardium and tissue selection for bioprosthetic heart valves.* J Biomed Mater Res, 1993. **27**(6): p. 697-704.

13.   Simionescu, D., R.V. Iozzo, and N.A. Kefalides, *Bovine pericardial proteoglycan: biochemical, immunochemical and ultrastructural studies.* Matrix, 1989. **9**(4): p. 301-10.

14.   Simionescu, D.T. and N.A. Kefalides, *The biosynthesis of proteoglycans and interstitial collagens by bovine pericardial fibroblasts.* Exp Cell Res, 1991. **195**(1): p. 171-6.

15.   Deac, R.F., D. Simionescu, and D. Deac, *New evolution in mitral physiology and surgery: mitral stentless pericardial valve.* Ann Thorac Surg, 1995. **60**(2 Suppl): p. S433-8.

16.   Isenburg, J.C., et al., *Structural requirements for stabilization of vascular elastin by polyphenolic tannins.* Biomaterials, 2006. **27**(19): p. 3645-51.

17.   Azimzadeh, A., et al., *Comparative study of target antigens for primate xenoreactive natural antibodies in pig and rat endothelial cells.* Transplantation, 1997. **64**(8): p. 1166-74.

18. Strokan, V., et al., *Heterogeneous expression of Gal alpha1-3Gal xenoantigen in pig kidney: a lectin and immunogold electron microscopic study.* Transplantation, 1998. **66**(11): p. 1495-503.

19. Daly, K.A., et al., *Effect of the alphaGal epitope on the response to small intestinal submucosa extracellular matrix in a nonhuman primate model.* Tissue Eng Part A, 2009. **15**(12): p. 3877-88.

20. McPherson, T.B., et al., *Galalpha(1,3)Gal epitope in porcine small intestinal submucosa.* Tissue Eng, 2000. **6**(3): p. 233-9.

21. Raeder, R.H., et al., *Natural anti-galactose alpha1,3 galactose antibodies delay, but do not prevent the acceptance of extracellular matrix xenografts.* Transpl Immunol, 2002. **10**(1): p. 15-24.

22. Schoen, F.J., *Cardiac valves and valvular pathology - Update on function, disease, repair, and replacement.* Cardiovascular Pathology, 2005. **14**(4): p. 189-194.

CHAPTER 7

STEM CELL DIFFERENTIATION WITHIN TRI-LAYERED TISSUE ENGINEERED HEART VALVES
(AIM 4)

7.1   Introduction

The predominant cell populations in heart valves, valvular interstitial cells (VICs), continuously secrete matrix components such as collagen, GAGs and as well as matrix degrading enzymes such as matrix metalloproteinases (MMPs) and other matrix degrading enzymes such as GAG-degrading enzymes that mediate remodeling that mediate remodeling [1-3]. VICs exhibit a dynamic phenotypic spectrum ranging from quiescent fibroblast-like cells (characterized by expression of vimentin, fibroblast surface antigen and low expression of alpha-smooth muscle cell actin and MMP-13), to activated VICs, assimilated as myofibroblasts (characterized by proliferation, migration and high expression of alpha-smooth muscle cell actin) [4-8]. Overall, permanent interactions between mechanical forces, valvular cells and the matrix dictate adaptability and durability of heart valves. Duplication of these structures and interactions in a man-made device is truly the bioengineers' dream and has the potential to provide tremendous clinical benefits.

Cell sourcing for seeding heart valve scaffolds includes differentiated cells (smooth muscle cells, fibroblasts) and mesenchymal or embryonic stem cells [9, 10]. Other cell sources include peripheral blood and human umbilical cord blood [11]. Upon biochemical and/or mechanical stimulation, most of these cells express markers of quiescent VICs such as vimentin, among others [12].

165

As stated before, our approach aims to combine partially stabilized collagen scaffolds that can be formed into anatomically analogous tri-layered, 3-D heart valve shapes made from solid molds that mimic the native heart valve histo-architecture. Also, we aim to use autologous multipotent mesenchymal stem cells for repopulation and remodeling and mechanical cues to induce stem cell differentiation into valvular-like cells capable of maintaining matrix homeostasis. To assemble the 3D heart valve structures we developed and implemented use of biological adhesives in tissue engineering, as discussed in Chapter 5. We have reported on extensive characterization of the acellular fibrous pericardial scaffolds used to mimic the fibrosa and ventricularis layers [13]. In current study we describe the use of our novel scaffolds to be used as the spongiosa layer that can be seeded with adult stem cells. We also show that bioreactor conditioning of stem cell-seeded tri-layered valves induced differentiation into VIC-like cells.

7.2   <u>Materials and Methods</u>

7.2.1   Materials

High purity 1,2,3,4,6-Penta-O-galloyl-beta-D-glucose (penta-galloyl-glucose, PGG) was a generous gift from N.V. Ajinomoto OmniChem S.A., Wetteren, Belgium (www.omnichem.be). Human bone marrow derived stem cells (hBMSCs) were obtained from Cell Applications, Inc. San Diego, CA) and all other chemicals were of highest purity available from Sigma Aldrich, St. Louis, MO.

7.2.2 Methods

7.2.2.1 *Cell seeding of spongy scaffolds*

Sterile *spongiosa* scaffolds were seeded with 5 x 10^4 cells/cm^2 human bone marrow derived stem cells (hBMSCs) by direct drop wise pipetting of cell suspensions onto scaffolds and culturing for 2 days before being inserted into the fibrous scaffold construct (described fully in Chapter 6). Briefly, two identical valve-shaped scaffolds were overlapped and assembled by applying BTglue to the entire scaffold surface corresponding to the aorta and the sinuses, leaving the cusps un-attached. For bioreactor testing, the original porcine aortic root (from which the mold was cast) was rinsed in saline, the three native valve cusps excised by dissection and the assembled engineered valve was secured inside the aortic root using sutures and BTglue. The entire construct was then rinsed and neutralized with 50% FBS and glycine (as described in Chapter 6). To finalize assembly, stem cell-seeded *spongiosa* (see below) was inserted between the two cusp-shaped scaffolds and the free cusp edges sealed with a thin line of BTglue. The edges of the cusps were rapidly neutralized by dipping in glycine.

7.2.2.2 *Cell seeded tri-layered construct bioreactor conditioning*

To test functionality of the constructs they were mounted onto our heart valve bioreactor (described in detail in manuscript accepted to Cardiovascular Engineering and Technology, May 2010). The device consists of a valve mounting ring assembly encased between a ventricular chamber and an aortic chamber filled with cell culture medium. The medium is pushed through the valve by a flexible silicone membrane diaphragm

connected to an air pump. Extensive testing has shown that the bioreactor ensures comparable pumping functions to a living heart (data not shown-see A Pulsatile Bioreactor for Conditioning Tissue Engineered Heart Valves, Thesis by Leslie Sierad, May 2009). The stem cell-seeded tissue engineered valve was subjected to open-close cycles at 60 beats per minute, 40/20 mmHg, 10 mL stroke volume, at 37 ^{0}C, 5% CO_2 for 8 days. Cell viability after 8 days of bioreactor conditioning was performed by Live/Dead stain. Cells were also stained with mouse anti-human vimentin and separately with anti alpha-smooth muscle cell actin (1:200 dilutions) and AlexaFluor-594 (Molecular Probes, Eugene, OR) tagged secondary antibody for immunofluorescence detection. Porcine valvular interstitial cells (VICs) were also stained for comparison.

7.3   Results

7.3.1   *Cell seeding of Spongy Scaffolds*

The overall goal of this project is to assemble a tri-layered construct to mimic the ultrastructure of the native heart valve. The viability and adaptability of the tri-layered construct is contingent on the viability of the cells incorporated into the construct (see **Figure 7.1**). Therefore, we tested several methods of introducing stem cells into the spongiosa layer. The first of which, injection of hBMSCs into the spongiosa layer after the spongy scaffold has been inserted between the fibrous scaffolds, yielded few viable cells upon removal of the spongiosa layer after 24 hour dynamic functionality testing of the entire construct and evaluation by Live/Dead (data not shown).
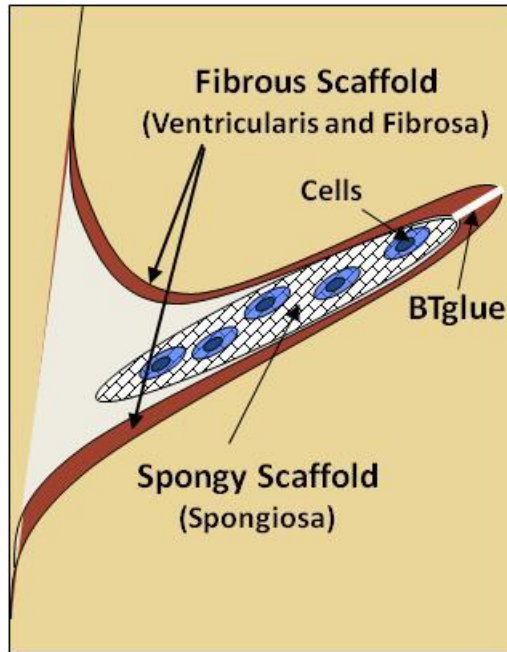
Figure 7.1: Schematic of the tri-layered construct with location of introduced stem cells.

The second method of cell seeding involved the pre-incubation of the spongy scaffolds with hBMSCs and inserting of the pre-seeded spongy scaffold between the two fibrous scaffolds. This yielded more viable cells (see section 7.3.2 below for cell viability results) and is thus the method that was chosen.

To summarize the procedure of valve assembly and spongiosa insertion, fibrous scaffolds were dried onto molds and PGG treated. The valve-shape constructs were then assembled by overlapping two identical fibrous scaffolds using BTglue and sutures placed at the level of valve wall, sinuses and cusp insertion points. Stem cell-seeded spongiosa scaffolds (arrow in Figure 7.2c) were inserted between the fibrous scaffolds inside the cusp structure and edges sealed with BTglue. Finally, the entire construct was sutured inside the original aortic root from which the mold was cast.

Figure 7.2: Valve-shape constructs (a, b, c in (A) denotes individual leaflets) were assembled by overlapping two identical fibrous scaffolds (B) using BTglue and sutures placed at the level of valve wall, sinuses and cusp insertion points (C). Stem cell-seeded spongiosa scaffolds (E-arrow) were inserted between the fibrous scaffolds inside the cusp structure and edges sealed with BTglue. (F) The construct was sutured inside the original aortic root from which the mold was cast (G).
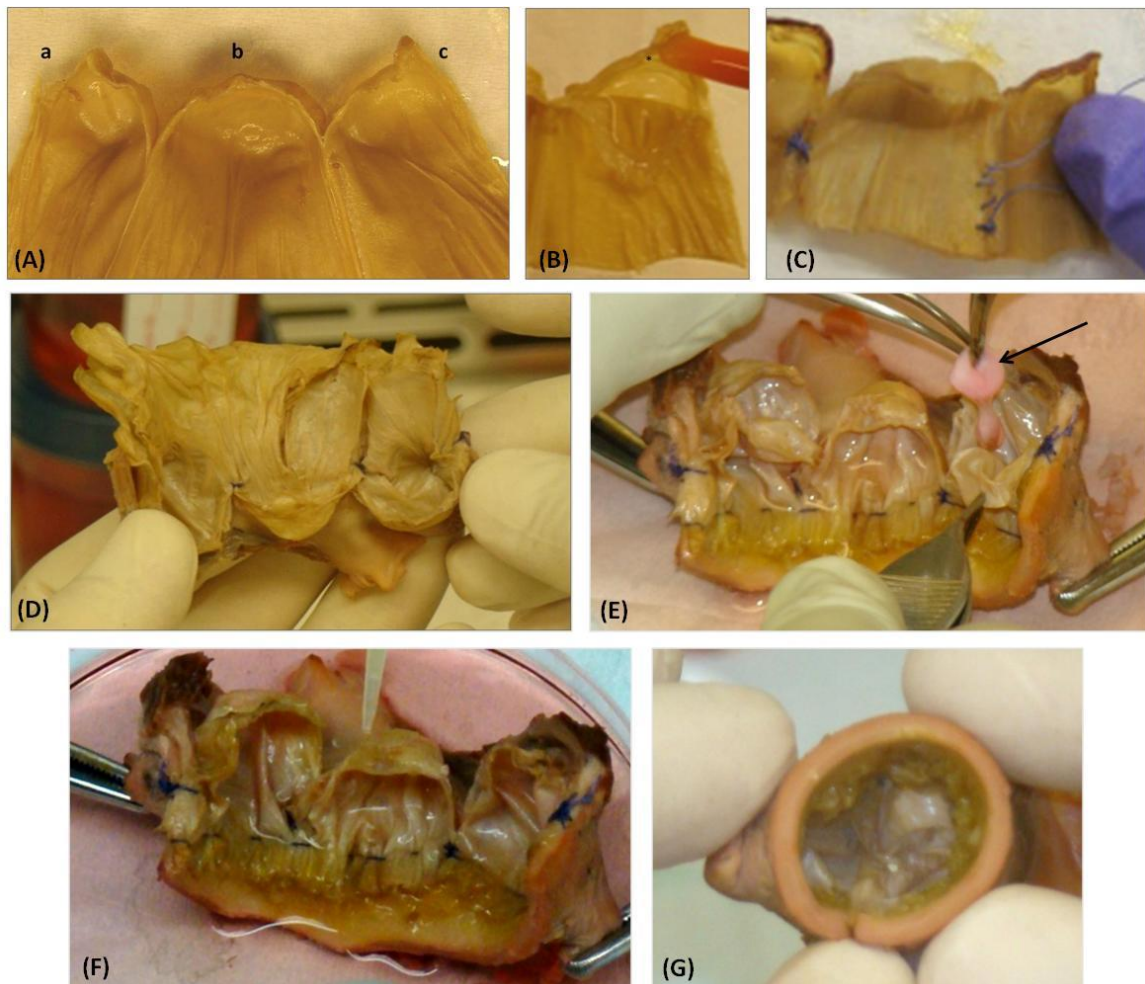
Functionality testing of the tri-layered construct yielded fair results. After 2 days of conditioning in sterile culture media, one cusp (a) had to be excised due to a superfluous amount of tissue that impeded the opening and closing of the construct (**Figure 7.3,C**), after which the bi-leaflet construct opened and closed more normally. **This highlights the need for more investigation into the assembly process (see Recommendations for Future Work)**.
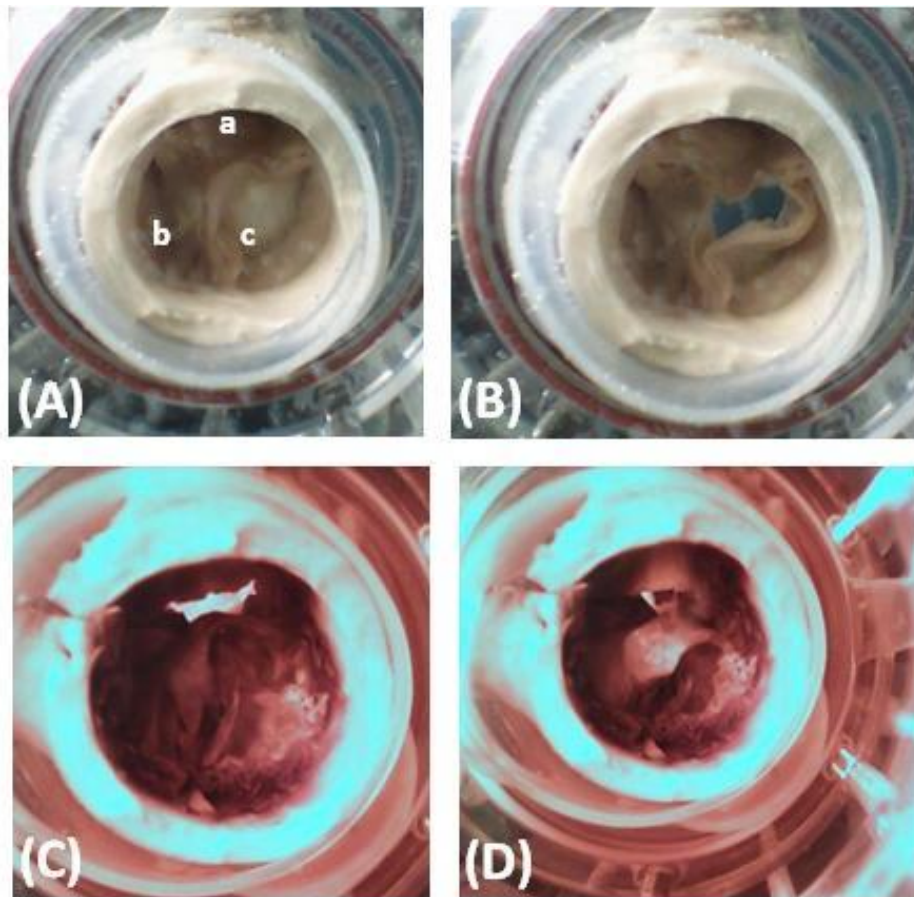

Figure 7.3: Initial functionality testing of the valves in a pulsatile bioreactor; aortic view (A and B), with   a, b, c – the three leaflets. Stem cell-seeded tissue engineered valve being subjected to bioreactor conditioning in sterile cell culture media (red) (C and D). External diameter of the porcine valve used in this study was about 23 mm.

7.3.2 *Cell seeded tri-layered construct bioreactor conditioning*

A short-term bioreactor study, in which the pulmonary artery scaffolds were seeded with hBMSCs, revealed that the seeding procedure for the spongiosa and subsequent insertion into a "sandwich" construct did not affect cell survival after 3 days while supported signs of stem cell differentiation (data not shown) . After 8 days in the heart valve bioreactor, cell viability was maintained at more than 90% and hBMSCs elongated significantly and stained positive for vimentin, but very weak for alpha-smooth muscle cell actin. Although absolute clear markers for VICs are still a matter of debate, this staining pattern is indicative of non-activated, quiescent VICs [8] (Figure . Static controls were also alive, but cells did not elongate and stained very weakly for vimentin and actin (Figure 7 9).
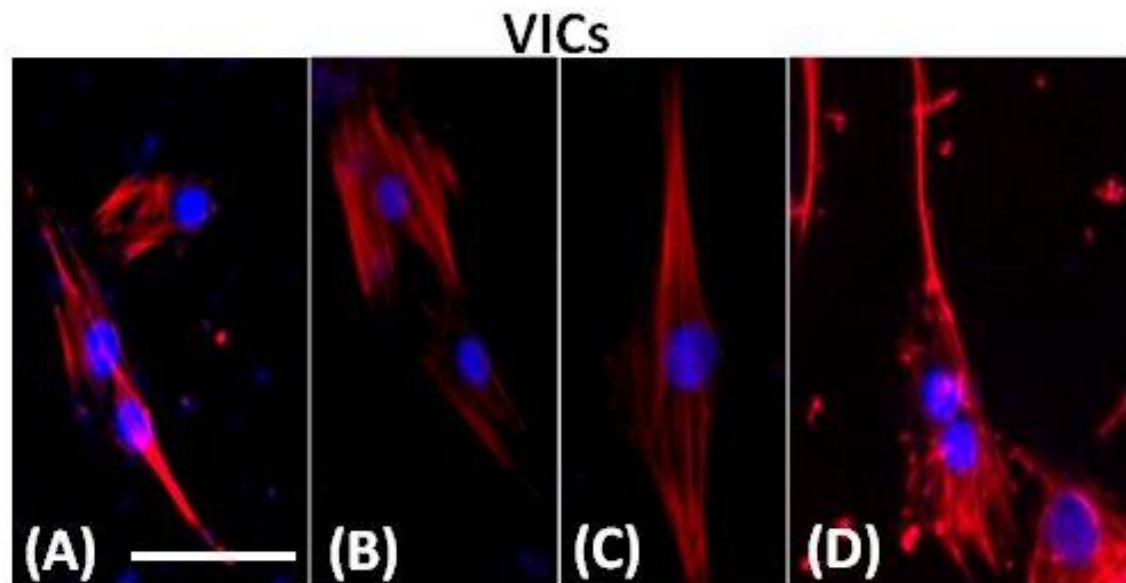
Figure 7.4 Control VICs stained for actin (A-C) and vimentin (D) (both red, with overlapped DAPI blue nuclear stain). Bar are 100 μm.

Stem cells retrieved from the bioreactor shared similarities to native VICs, indicating that physiologic mechanical stimuli offered by our 3D tissue engineered heart valve constructs and the bioreactor encouraged differentiation of stem cells into VIC-like cells, a much sought-after outcome of valvular tissue engineering. Moreover, these results were
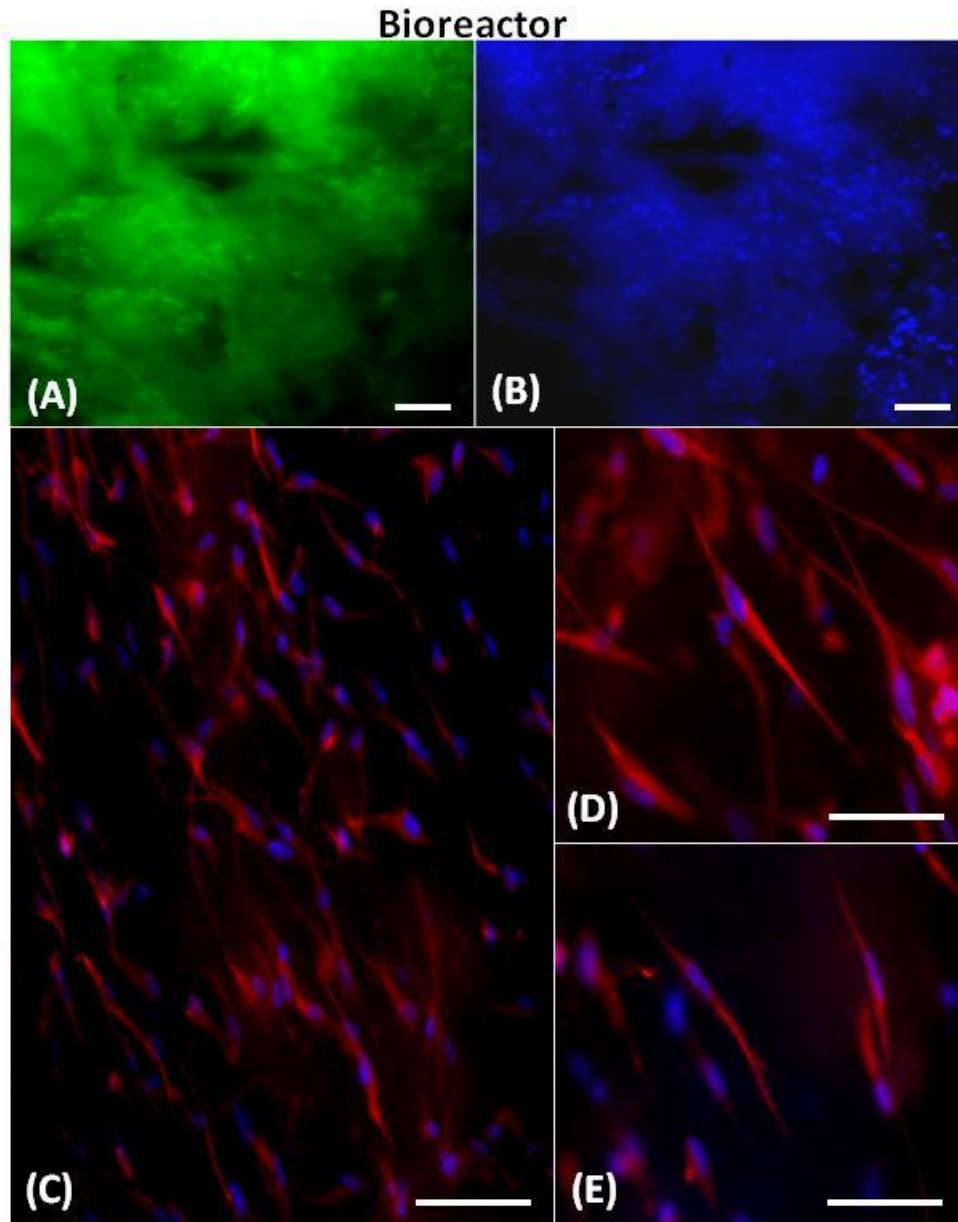
Figure 7.5 Bioreactor results with stem cell-seeded valves after 8 days. Cell viability was confirmed using Live/Dead stain (live cells green, dead cells red) in(A). (B) shows DAPI nuclear staining confirming presence of cells. (C-D) show immunofluorescence staining (red, with overlapped DAPI blue nuclear stain) showing elongated, vimentin positive cells. Bars are 100 μm.

obtained within constructs made from collagen scaffolds that would resist physiologic

pressure immediately after implantation.
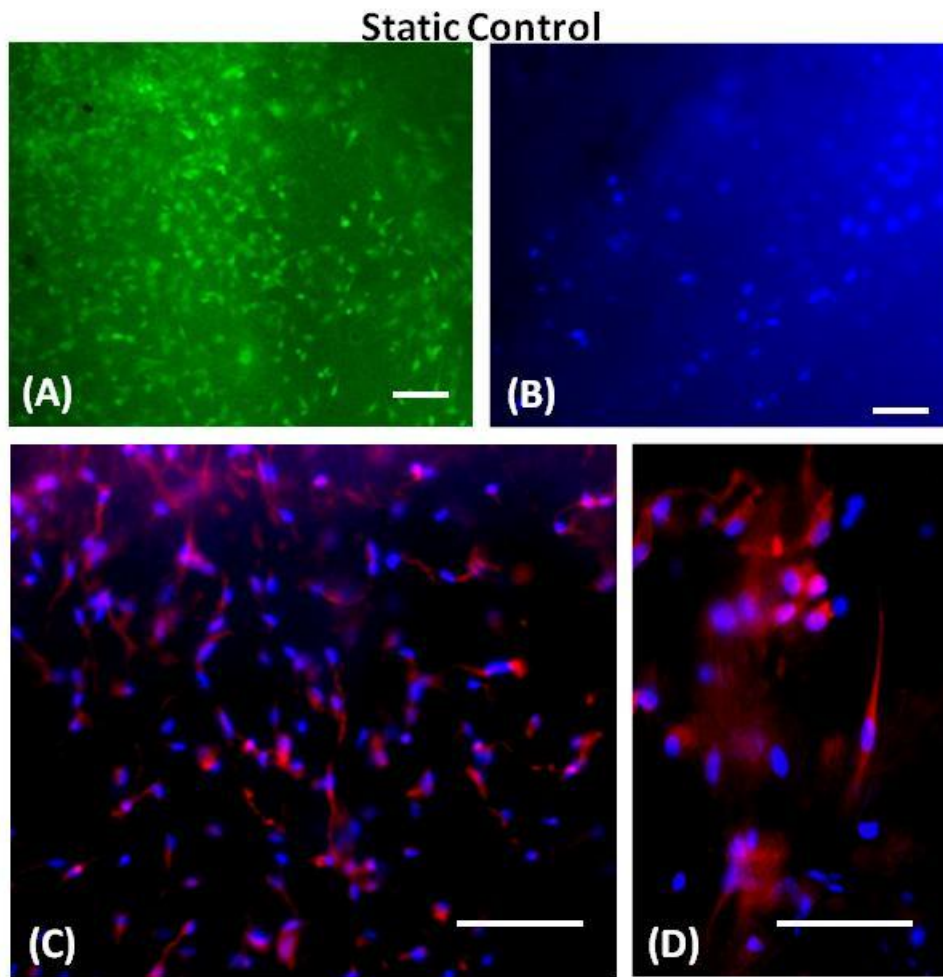
Figure 7.6 Cell viability (A) and DAPI staining (B) in static controls. Immunofluorescence staining showing very few vimentin-positive cells (C and D). Bars are 100 μm.

7.4   **Discussion**

Our vision of a potential translational scenario using stabilized collagen scaffolds and autologous stem cells involves the following steps. After initial diagnosis and collection of mesenchymal stem cells from the patient, imaging of the diseased heart valve would provide anatomical coordinates for reconstruction of the heart valve geometry into solid molds using appropriate software and hardware. Concomitant with stem cell isolation, valves will be made from decellularized collagen scaffolds by assembly into tri-layered constructs and then cusps seeded with autologous stem cells as described in the current study. After conditioning in bioreactors for 1-2 weeks for stem cell pre-differentiation into VIC-like cells, the patient-tailored engineered heart valve would be surgically implanted.

Our working premise is that the extracellular matrix of cardiovascular tissues provides ideal scaffolds for valvular tissue engineering. Previously we described development of collagen scaffolds to be used as the fibrous layers of the heart valve cusps [14] and a scaffold to be used as a spongiosa layer for heart valve tissue engineering. When the spongy scaffold is seeded with cells and conditioned in bioreactors, such scaffold-enclosed "cell pockets" maintained cell viability and allowed transmission of mechanical cues to induce stem cells differentiation into VIC-like cells. However, with differentiation of the stem cells into VIC-like cells, and remodeling of the scaffold, the problem of overproduction and continued growth of the valve is possible [15]. The patient would have to be monitored for valve hypertrophy, whereas to mitigate this occurrence, growth factors may need to be incorporated into the scaffold, with the

dosage, release, and duration optimized for a balance between tissue growth and remodeling. To ascertain the extent of valve growth, accelerated aging tests must be preformed, whereby *in vitro* bioreactor studies in conjunction with growth factor studies could elucidate how the valve will remodel and possibly grow as it ages.

7.5 <u>Conclusions</u>

This study is a stepping stone towards development of a novel approach to heart valve tissue engineering. The scaffolds we have previously developed were assembled into anatomically analogous 3-D heart valve shapes using novel protein-based glue, seeded with stem cells and conditioned in bioreactors to induce stem cell differentiation. It can be concluded that histiologically similar mechanical stimuli offered by our TEHV encourages differentiation of stem cells into activated valvular interstitial cells.

While many aspects and details need to be optimized as far as scaffold assembly and animal testing are concerned, this approach appears promising for our envisioned translational scenario.

7.6 <u>References</u>

1.   Simionescu, D.T., J.J. Lovekamp, and N.R. Vyavahare, *Degeneration of bioprosthetic heart valve cusp and wall tissues is initiated during tissue preparation: an ultrastructural study.* J Heart Valve Dis, 2003. **12**(2): p. 226-34.

2.   Simionescu, D.T., J.J. Lovekamp, and N.R. Vyavahare, *Extracellular matrix degrading enzymes are active in porcine stentless aortic bioprosthetic heart valves.* J Biomed Mater Res A, 2003. **66**(4): p. 755-63.

3.   Simionescu, D.T., J.J. Lovekamp, and N.R. Vyavahare, *Glycosaminoglycan-degrading enzymes in porcine aortic heart valves: implications for bioprosthetic heart valve degeneration.* J Heart Valve Dis, 2003. **12**(2): p. 217-25.

4.   Mendelson, K. and F.J. Schoen, *Heart valve tissue engineering: concepts, approaches, progress, and challenges.* Ann Biomed Eng, 2006. **34**(12): p. 1799-819.

5.   Latif, N., et al., *Characterization of structural and signaling molecules by human valve interstitial cells and comparison to human mesenchymal stem cells.* J Heart Valve Dis, 2007. **16**(1): p. 56-66.

6.   Ku, C.H., et al., *Collagen synthesis by mesenchymal stem cells and aortic valve interstitial cells in response to mechanical stretch.* Cardiovasc Res, 2006. **71**(3): p. 548-56.

7.   Taylor, P.M., et al., *The cardiac valve interstitial cell.* Int J Biochem Cell Biol, 2003. **35**(2): p. 113-8.

8.   Liu, A.C., V.R. Joag, and A.I. Gotlieb, *The emerging role of valve interstitial cell phenotypes in regulating heart valve pathobiology.* Am J Pathol, 2007. **171**(5): p. 1407-18.

9.   Fang, N.T., et al., *Construction of tissue-engineered heart valves by using decellularized scaffolds and endothelial progenitor cells.* Chin Med J (Engl), 2007. **120**(8): p. 696-702.

10.   Visconti, R.P., et al., *An in vivo analysis of hematopoietic stem cell potential: hematopoietic origin of cardiac valve interstitial cells.* Circ Res, 2006. **98**(5): p. 690-6.

11.   Schmidt, D., et al., *Engineering of biologically active living heart valve leaflets using human umbilical cord-derived progenitor cells.* Tissue Eng, 2006. **12**(11): p. 3223-32.

12.   Fraser, J.K., et al., *Fat tissue: an underappreciated source of stem cells for biotechnology.* Trends Biotechnol, 2006. **24**(4): p. 150-4.

13.   Tedder, M.E., et al., *Stabilized collagen scaffolds for heart valve tissue engineering.* Tissue Eng Part A, 2009. **15**(6): p. 1257-68.

14.   Tedder, M.E., et al., *Stabilized Collagen Scaffolds for Heart Valve Tissue Engineering.* Tissue Eng Part A, 2008.

15.	Neuenschwander, S. and S.P. Hoerstrup, *Heart valve tissue engineering.* Transpl Immunol, 2004. **12**(3-4): p. 359-65.

CHAPTER 8

CONCLUSIONS AND RECOMMENDATIONS FOR FUTURE WORK

8.1   Conclusions

Tissue engineering, the emerging science of combining scaffolds, cells and specific mechanical and biochemical signals is feasible and holds great promise for treatment of heart valve disease [1, 2]. Recognizing the vital importance of the three leaflet layers [3], the outstanding hemodynamics of natural valve homografts [4] and the need for reconstruction of the physiologic valve design, we hypothesize that combination of four elements can be utilized for tissue engineering of the "ideal" aortic heart valve: A) Constructs made from partially stabilized collagenous scaffolds, B) Anatomically analogous 3-D heart valve shapes made from tri-layered structures that mimic the native heart valve histo-architecture, C) Autologous multipotent bone marrow derived stem cells for repopulation and remodeling. These ideas were tested in the work presented here, allowing us to draw the following conclusions:

- We could successfully decellularize pericardium and pulmonary arteries to yield pure, porous, collagenous scaffolds

- Scaffold fixation with PGG:

  - Partially stabilized the fibrous collagen scaffolds

  - Allowed for cell infiltration *in vivo*

- Scaffold adherence with BTglue showed that:

  - Our novel glue was able to adhere the scaffold together

- o Was non toxic to cells

- Molding of native aortic heart valves with liquid silicone was:

  - o Able to duplicate the shape and fine corrugations of the individual leaflets

  - o Served as a platform on which the collagenous scaffolds could be molded

  - o The formed collagenous scaffolds could be combined to form a tri-layered construct that mimics the native histo-architecture of an aortic heart valve

  - o The formed valve construct functioned comparably to a native aortic valve during bioreactor testing

- Bioreactor testing of stem cell-seeded tri-layered scaffolds

  - o Supported cell growth and survival

  - o May possibly support stem cell differentiation into valvular interstitial-like cells

Therefore, our tissue engineered heart valve replacement approaches hold promise to create a living heart valve that can potentially grow with the patient.

8.2   <u>Recommendations for Future Work</u>

As this project is still in its early stages, there is much work to be done to optimize the entire process. At each step in the process there are aspects that must be investigated in order to make this a viable process that may be utilized in a clinical setting.

1) The use of a fibrous scaffold with elastin (not removing the elastin from the pericardium during the scaffold preparation process is one possibility) can be investigated for the use of the *ventricularis*.

2) The glycosaminoglycan (GAG) content should be evaluated in the fibrous scaffolds.

3) The GAG content in the *sponsiosa* must be augmented to better approximate the GAG content in the native aortic valve.

4) In terms of the fixation process, a better balance must be established between cell toxicity, stability, and degradation afforded by PGG cross-linking.

   a) In addition, another cross-linking chemical should be evaluated (such as N-(3-dimethylaminopropyl)-Nethylcarbodiimide (EDC)) to augment PGG and aid in better establishing this balance

5) In terms of gluing:

   a) Alternative polymerizing agents (other than Glut) can be investigated that could minimize the deleterious effects of Glut.

   b) If Glut is still utilized, the neutralization process should be improved to minimize the calcification caused by Glut.

   c) The elasticity of the glue should be increased to better match the scaffold properties and thus decrease stresses placed of the scaffold due to the glue.

6) In terms of the molding and assembly process:

   a) A computer aided system should be utilized to form the 3-D rendering of the aortic valve that may be used for molding of the tissue scaffolds

b) A rapid prototyping interface should be implemented to process the solid molds (this will replace the silicone molding, that cannot be utilized in a clinical setting)

c) How the valve is assembled, considering how much tissue is used for the leaflets must be addressed.

d) Dr. Ivan Vesely maintains that a precise central gap is key to valve function [5], therefore amount of tissue used, suture positions, glue amounts, and leaflet orientation is key.

e) Optimizing BTglue adhering locations must also be evaluated and perfected, by assessing how much BTglue to use, where it should be applied (at edges of cusps, at junction of leaflet and aortic arch), and application procedures (when in the assembly process to apply BTglue).

f) Once the valve leaflets are constructed, a mechanism by which the valve construct can be mounted must be tested and perfected, by which either mounting rings, stents, or direct mounting either with sutures, BTglue, or a combination of the two should be evaluated.

7) For stem cell seeding and differentiation,

a) Different sources for stem cells should be investigated (such as adipose-derived stem cells)

b) Biochemical and further mechanical factors should be implemented that influence differentiation

c) Fundamental studies on native VICs should be performed to establish a standard by which the cells we use for seeding should be compared.

8) In further bioreactor studies,

   a) Long-term   bioreactor experiments should be performed to evaluate the mechanics of the valve over time, as well as stem cell differentiation and remodeling potential of our scaffolds

   b) The interface between the surface of the scaffold and blood should be addressed, whereby the physical and chemical structure of the surface is ascertained via atomic force microscopy(AFM) studies, and bioreactor functionality studies whereby the fluid environment around the construct is more closely representative of the in vivo environment in which it will be implanted to assess hemolysis and thrombogenicity

   c) The valve must be endothelialized, to mimic the surface characteristics of a native valve and potentially alleviate hemolytic and thrombogenic problems associated with blood/biomaterial interactions

9) Once these points are addressed, large animal studies (preferably primate implantation) should be performed that follows our proposed translational clinical scenario:
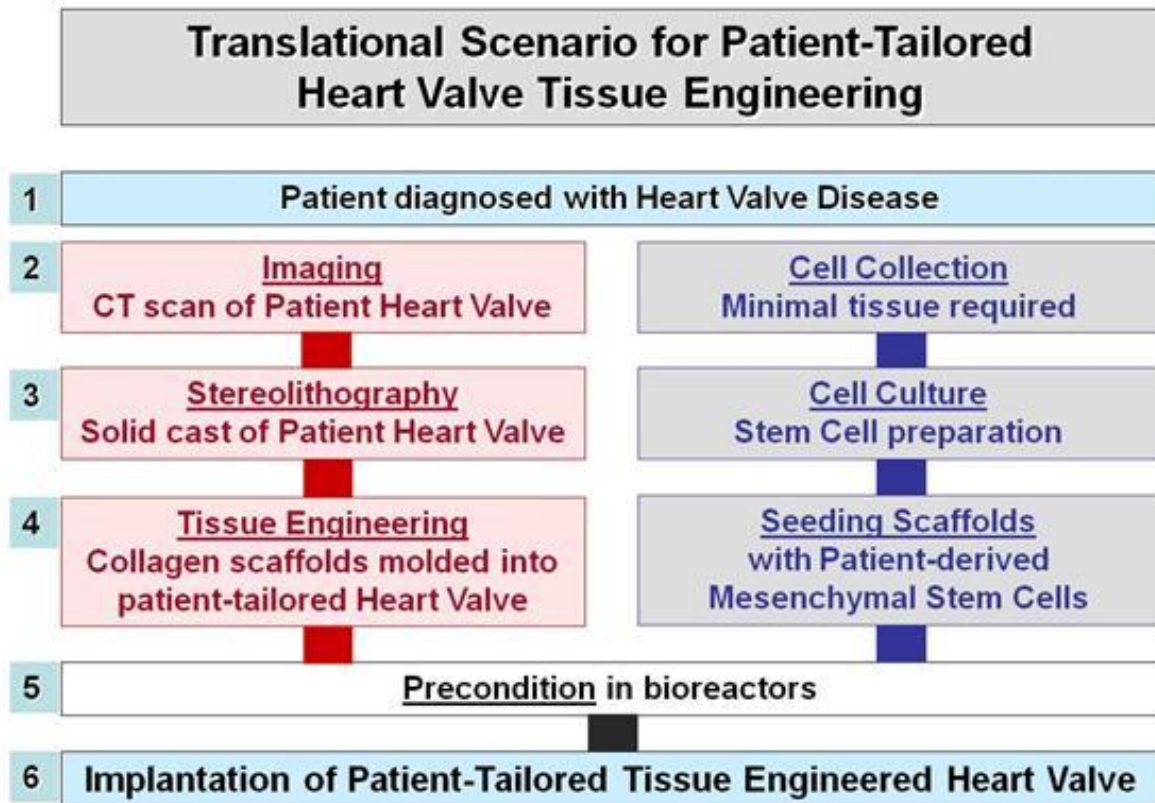
Translational Scenario for Patient-Tailored Heart Valve Tissue Engineering

1	Patient diagnosed with Heart Valve Disease	
2	**Imaging** CT scan of Patient Heart Valve	**Cell Collection** Minimal tissue required
3	**Stereolithography** Solid cast of Patient Heart Valve	**Cell Culture** Stem Cell preparation
4	**Tissue Engineering** Collagen scaffolds molded into patient-tailored Heart Valve	**Seeding Scaffolds** with Patient-derived Mesenchymal Stem Cells
5	Precondition in bioreactors	
6	Implantation of Patient-Tailored Tissue Engineered Heart Valve	

Figure 8.1: Translational Scenario for Patient-Tailored Heart Valve Tissue Engineering

Overall, this translational scenario will cost no more than the currently available bioprosthetic heart valve, which currently range from anywhere between $5,000 and $20,000 [6]. High initial costs will include the imaging software and the rapid prototyping machine for steriolithography for actual manufacturing. The highest recurring costs for each patient will be the CT scans for imaging, but even current patients receiving a valve replacement necessitate scans. All other aspects of the process will incur will monetary requirements, while the benefits of receiving a patient-tailored valve will be innumerable.

8.3 <u>References</u>

1. Mendelson, K. and F.J. Schoen, *Heart valve tissue engineering: concepts, approaches, progress, and challenges.* Ann Biomed Eng, 2006. **34**(12): p. 1799-819.

2. Butcher, J., *Viewpoint: Heart valve engineering.* Circulation, 2007. **116**(8): p. F44-F46.

3. Schoen, F.J., *Cardiac valves and valvular pathology - Update on function, disease, repair, and replacement.* Cardiovascular Pathology, 2005. **14**(4): p. 189-194.

4. Sodian, R., et al., *Application of stereolithography for scaffold fabrication for tissue engineered heart valves.* Asaio Journal, 2002. **48**(1): p. 12-16.

5. Vesely, I., *Heart valve tissue engineering.* Circ Res, 2005. **97**(8): p. 743-55.

6. Pick, A. *How much do Heart Valve Replacements Cost?* 2010 [cited 2010 October 14]; Available from: http://www.heart-valve-surgery.com/heart-surgery.